ROLE OF AGGREGATION CONDITIONS AND PRESENCE OF SMALL HEAT SHOCK PROTEINS ON Aβ STRUCTURE, STABILITY AND TOXICITY

A Dissertation

by

SUNG MUN LEE

Submitted to the Office of Graduate Studies of
Texas A&M University
in partial fulfillment of the requirements for the degree of

DOCTOR OF PHILOSOPHY

May 2005

Major Subject: Chemical Engineering

ROLE OF AGGREGATION CONDITIONS AND PRESENCE OF SMALL HEAT SHOCK PROTEINS ON Aβ STRUCTURE, STABILITY AND TOXICITY

A Dissertation

by

SUNG MUN LEE

Submitted to Texas A&M University
in partial fulfillment of the requirements
for the degree of

DOCTOR OF PHILOSOPHY

Approved as to style and content by:

Theresa A. Good (Co-Chair of Committee)	Daniel F. Shantz (Co-Chair of Committee)
Eva M. Sevick-Muraca (Member)	William H. Griffith (Member)
	Kenneth R. Hall (Head of Department)

May 2005

Major Subject: Chemical Engineering

ABSTRACT

Role of Aggregation Conditions and Presence of Small Heat Shock Proteins on Aβ Structure, Stability and Toxicity. (May 2005)

Sung Mun Lee,

B.S., Korea University;

M.S., Seoul National University

Co-Chairs of Advisory Committee: Dr. Theresa A. Good
Dr. Daniel F. Shantz

Alzheimer's disease (AD) is a neurodegenerative disorder that is one of such diseases associated with protein aggregation. Aβ is the main protein component of senile plaques in AD, and is neurotoxic when aggregated. In particular, soluble oligomeric forms of Aβ are closely related to neurotoxicity. In this dissertation, we examine the differences in Aβ aggregation intermediates, and final structures formed when only a simple modification in Aβ aggregation conditions is made, the presence or absence of mixing during aggregation. We show that intermediates in the aggregation pathway show significantly different structural rearrangements. The protein stabilities of Aβ species show that spherical aggregates corresponding to the most toxic Aβ species change their structure the most rapidly in denaturant, and that in general, increased toxicity correlated with decreased aggregate stability.

In Alzheimer's disease, even delaying Aβ aggregation onset or slowing its progression might be therapeutically useful, as disease onset is late in life. Small heat

shock proteins (sHsps) may be useful for prevention of Aβ aggregation, since sHsps can interact with partly folded intermediate states of proteins to prevent incorrect folding and aggregation. In this research, several small heat shock proteins (sHsps) are tested to prevent Aβ aggregation and toxicity. sHsps used in this research are Hsp17.7, Hsp27, and Hsp20. All types of Hsp20, Hsp20-MBP, His-Hsp20 and His-Hsp20 without 11 residues in C-terminus, can prevent Aβ1-40 aggregation. Hsp20 also prevents Aβ toxicity in the same concentration ranges of it aggregation prevention activity. Hsp17.7 and Hsp27, however, can inhibit Aβ1-40 aggregation but not toxicity. A number of experiments to examine the mechanism of Hsp20 suggest that multivalent binding of sHsp to Aβ is necessary for the toxicity prevention activity.

Conclusively, different Aβ incubation conditions *in vitro* can affect the rate of Aβ fibril formation, the morphology, the toxicity and the conformation of intermediates in the aggregation pathway. Hsp20 rather than other sHsps may be a useful molecular model for the drug design of the next generation of Aβ aggregation inhibitors to be used in the treatment of AD.

ACKNOWLEDGEMENTS

First, I would like to express my gratitude to my advisor, Dr. Theresa Good, for her support, encouragement, and concern throughout my graduate studies. I would never have been able to finish truly challenging works without her help.

I'll give a thank to Dr. Erik Fernandez, a professor of the chemical engineering department, University of Virginia for invaluable comments to guide me to a deeper understanding of knowledge works.

I am grateful to Dr. Allison Rich-Ficht and Kenneth Carson, a professor and a graduate student of medical biochemistry and genetics, Texas A&M University for a fruitful collaboration.

I am fortunate to have Dr. Daniel Shantz as a co-chair, Dr. Eva Sevick-Muraca and Dr. William Griffith as committee members.

I thank my colleagues at the department of chemical engineering, Texas A&M University and the department of chemical and biochemical engineering, University of Baltimore, Baltimore County for providing a good working atmosphere.

I also thank my friends in Korea for helping me out of trouble all the times.

Finally, I'm very grateful to my parents, my parents-in-law, my sisters, my sisters-in-law, and my brothers-in-law for supporting me. I give a special thanks to my wife for encouraging and inspiring me to be a better person and lightening up my life.

TABLE OF CONTENTS

CHAPTER Page

LIST OF FIGURES

FIGURE Page

LIST OF TABLES

CHAPTER I

INTRODUCTION

Due to the passing of the former U.S. president, Ronald Reagan, last year, Alzheimer's disease (AD) is once again in the limelight. Currently, over 4.5 million people in United States suffer with AD and about 360,000 new cases occur each year. (Brookmeyer et al. 1998; Hebert et al. 2003) Alzheimer's disease (AD) is defined as a neurodegenerative disease that causes dementia and gradual loss of brain cells. AD is an age dependent disease. Scientists estimate that more than 10% of Americans over the age of 65 and half of those over the age 85 are afflicted by AD. (Jorm et al. 1987; Evans et al. 1989) The dramatically longer life span of people during the 20th century has resulted in a much greater number of individuals suffering from neurodegenerative disorders that are common in the elderly.

AD is a disease associated with protein aggregation. The two hallmarks of AD are neuritic plaques and neurofibrillary tangles. These hallmarks result from the deposition of sticky β-amyloid (Aβ) and the aggregation of hyperphosphorylated tau proteins respectively. What causes AD is still mystery. However, increasing evidence shows that aggregated Aβ causes toxicity to neuron cells *in vitro*. (Lambert et al. 1998; Walsh et al. 1999; Ward et al. 2000; Klein et al. 2001; Walsh et al. 2002; Chromy et al. 2003) Many believe that aggregation of Aβ is one of the initiating factors in AD. Aβ is produced by

---

This dissertation follows the style of *Protein Science*.

APP (β-Amyloid Precursor Protein) as a proteolytic cleavage product with 39-43 residues. (Joachim et al. 1989; Rogers et al. 1992) The 40- and 42-residue Aβ are the main components of senile or neuritic plaques found in AD. The highly hydrophobic Aβ1-42 is implicated in amyloid fibril nucleation, while the more soluble Aβ1-40 is the main form circulating in normal plasma and cerebrospinal fluid. (Seubert et al. 1992; Shoji et al. 1992) Accumulating data show that while Aβ aggregates readily into amyloid fibrils, the Aβ species in soluble oligomeric forms rather than fibrils are closely associated with the neurotoxicity *in vivo* and *in vitro*. (Dahlgren et al. 2002) Toxicity has been attributed to Aβ-derived diffusible ligands (ADDLs) composed of Aβ1-42, with molecular weights between 17 to 42kDa (Lambert et al. 1998; Klein et al. 2001) and heterogeneous globular species (also described as ADDLs) with hydrodynamic radii between 3 to 8nm (Chromy et al. 2003). Spherical aggregates, not described at ADDLs, with radii over 15 nm have also been reported to be toxic (Hoshi et al. 2003). Toxic protofibrils of Aβ1-40 have been described with hydrodynamic radii ranging from 9 nm to over 300 nm (Walsh et al. 1999; Ward et al. 2000; Wang et al. 2002). Understanding the relationship between Aβ features such as structure that are associated with toxicity will be essential if we hope to develop new strategies to prevent the formation of Aβ toxic species. An improved understanding of structure function relationships in Aβ may provide cues to the mechanism of action of Aβ in the central nervous system.

Prevailing thought over the past several decades has been that Aβ aggregation is associated with toxicity, therefore much research has gone into understanding the mechanism of Aβ aggregation. Several studies show that Aβ forms fibrils via a

conformational transition from α-helix/random coil to β-sheet.(Walsh et al. 1997; Walsh et al. 1999) The secondary structure and fibril elongation of Aβ depends on multiple factors, such as pH, temperature, peptide concentration, and ionic strengtḥ.α-helical and/or random coil content has been shown to be coincident with high solubility and protease susceptibility whereas a β-sheet content has been shown to be correlated with poor solubility and resistance to proteolysis. (Barrow and Zagorski 1991; Barrow et al. 1992; Snyder et al. 1994; Shen and Murphy 1995; Soto and Castano 1996; Fezoui and Teplow 2002; Kawooya et al. 2003; Stine et al. 2003; Manning and Colon 2004) Aβ fibril formation is basically self-initiated because no other chemicals or side reactions are involved. Much research has been performed to elucidate how Aβ monomers are converted to fibrils. One probable mechanism is a nucleation-dependent model. (Lomakin et al. 1997; Serio et al. 2000) In the nucleation-dependent model, the initial aggregation rate is very slow until a critical size called nuclei is reached. Once the nucleus is formed, rapid aggregation proceeds by addition of monomers. Any agents which could prevent nuclei formation and eliminate Aβ nuclei from solution once formed may be very useful as an Aβ aggregation (and toxicity) inhibitor.

In this dissertation, we examined several questions associated with understanding the mechanism of Aβ aggregation under different conditions, the relationship between structure, toxicity, and stability of different aggregation species, and investigated a class of small heat shock proteins as a means to alter that Aβ aggregation pathway. We examined the differences in Aβ aggregation intermediates, and final structures formed when only a simple modification in Aβ aggregation conditions was made, the presence

of absence of mixing during aggregation. We show, that while the final structures in the Aβ aggregation pathway are comparable by measures such as electron microscopy, the toxicity of fibrils formed are significantly different. In addition, intermediates in the aggregation pathway show significantly different structural rearrangements. We examined the stabilities of the different Aβ species formed during aggregation using change in conformation in the denaturants, urea and guanidine hydrochloride (GuHCl). The changes in structure of Aβ species upon exposure to denaturants were monitored by circular dichroism (CD) at 220nm. When guanidine hydrochloride unfolding was used as a simple measure of stability of different aggregated species, the structures that changed conformation at the lowest concentrations of guanidine hydrochloride were also the most toxic structures. In urea, the stabilities were expressed as free energy differences between native and unfolded states of Aβ as a function of urea concentration and in pure water. The trends in stabilities of Aβ aggregation species upon exposure to urea were similar to that observed in GuHCl, although the differences in urea were not drastic in GuHCl. Spherical aggregates, corresponding to the most toxic Aβ species examined, changed structure at the lowest urea concentrations (which would correspond to the greatest instability). These results suggest that other characteristics besides tertiary structure as can be measured by electron micrograph are more indicative of toxicity of Aβ species.

Small heat shock proteins (sHsps) are expressed in almost all organisms when cells get stressed in unfavorable environments. They exist as large oligomeric complexes of 300-800kDa with monomeric molecular mass of 15-43kDa. (van den et al. 1999; Clark

and Muchowski 2000; MacRae 2000) Important roles of sHsps are to stabilize other proteins during stress conditions and to protect them from aggregation. (van den et al. 1999; Bruey et al. 2000) A novel small heat shock protein, Hsp20, isolated from the bovine erythrocyte parasite *Babesia bovis* has chaperone like properties. Preliminary results showed that this novel protein inhibited the aggregation of denatured alcohol dehydrogenase (ADH). Thus, Hsp20 was examined for its ability to prevent aggregation and toxicity of Aβ.

Using three different Hsp20 constructs, a maltose binding protein fusion (Hsp20-MBP), a polyhistidine fusion (His-Hsp20) and His-Hsp20 without 11 residues in C-terminus, we showed that all types of Hsp20 prevented aggregation of Aβ and Aβ toxicity. Hsp20 was able to prevent amyloid formation of Aβ with optimal activites at molar ratios of Hsp20 to Aβ of 1:1000 as indicated by Congo red binding. Hsp20 attenuated the toxicity of Aβ in SH-SY5Y and PC12 neuronal cells at analogous molar ratios. His-Hsp20 was more active than Hsp20-MBP, but His-Hsp20s showed almost the same activities regardless of the existence of 11 residues in the C-terminus which appear to play a role in the self assembly of Hsp20. Hsp20 seems to be able to prevent Aβ aggregation via a stoichiometric binding or a novel mechanism. Hsp20 prevents Aβ aggregation at much lower concentrations than have been observed with other Aβ aggregation inhibitors. Other types of sHsps such as Hsp17.7 from carrot, and human recombinant Hsp27 were also tested in Aβ aggregation and toxicity assays. Both carrot and human sHsps inhibited Aβ1-40 aggregation but did not prevent toxicity. Conclusively, Hsp20 may be a useful molecular model for the design of the next

generation of Aβ aggregation inhibitors to be used in the treatment of AD.

This body of work adds to our understanding of how Aβ aggregates, how novel proteins interact with Aβ to prevent its aggregation, and how Aβ aggregation, structure, and stability is related to Aβ toxicity.

CHAPTER II

LITERATURE REVIEW

AMYLOIDOSES - DISEASE RELATED TO PROTEIN AGGREGATION

Proteins are synthesized on ribosomes from mRNA carrying genetic information of DNA. Proteins have only biological activity when they are correctly folded. However, the mechanism of folding of polypeptides into specific three-dimensional structures has been a mystery. Proteins are susceptible to environmental changes such as temperature, pH, pressure, and denaturants. (Creighton 1993) Unfolded proteins could be formed by unfavorable environments, or misfolded or mutated proteins could be produced associated with mutations in genes (DNA), or problems in transcription (mRNA), translation (ribosome), or in chaperones or other folding machinery in the cell. The unfolded, misfolded or mutated proteins are targeted for degradation. (Dobson 2003; Goldberg 2003; Sitia and Braakman 2003) Those proteins are refolded by chaperone proteins or degraded by the ubiquitin-proteasome pathway.(Goldberg 2003) The misfolded or unfolded proteins are prone to form aggregates via inappropriate interaction with other proteins because hydrophobic regions are exposed to the hydrophilic cell environment. (Fig. 2.1)

The aggregates can damage or kill cells through mechanisms that are under investigation. A variety of unrelated diseases have common pathological features associated with aggregated protein deposits. In all of these diseases, proteins that are

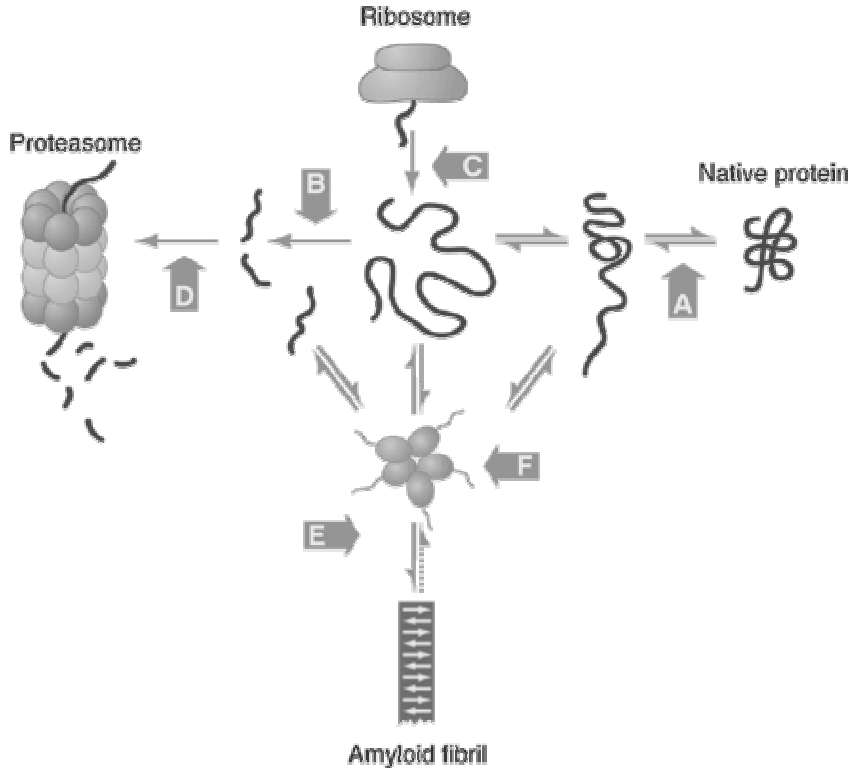

Figure 2. 1. The conversion of normal soluble proteins into insoluble aggregates. (A) stabilizing native protein, (B) Inhibiting the protein from aggregation by enzyme degradation, (C) Protein synthesis, (D) Clearance of misfolded protein, (E) Formation of fibril, (F) Accumulation of fibril precursor. (Dobson 2003)

normally soluble convert into insoluble aggregates that form toxic deposits. Amyloidosis is the extracellular deposition of insoluble protein fibrils leading to tissue damage and disease. (Serpell 2000) More than 20 unique proteins such as β-amyloid (Aβ), α-synuclein, calcitonin, transthyretin, and β_2-macroglobulin are involved in amyloidoses. (Tan and Pepys 1994; Carrell and Gooptu 1998; Kelly 1998) Neurodegenerative diseases such as Alzheimer's disease, Parkinson's disease, Huntington's disease, amyotrophic lateral sclerosis, and prion disease are caused by aggregation of such proteins. (Taylor et al. 2002; Ross and Poirier 2004) (Table 2. 1) While the precursor proteins from which the aggregated proteins associated with disease listed in Table 2. 1 all differ from each other in biological function, primary sequences, and morphologies (from intact globular proteins to unstructured peptide molecules), the protein aggregates that form during amyloidosis share many common features such as relative insolubility, protease resistance, specific optical behavior (e.g. birefringence) with certain dye molecules like Congo red and characteristic cross-β pattern in X-ray diffraction. (Sipe 1992; 1994; Taubes 1996; Lansbury 1999) The aggregates of those proteins also form similar macroscopic structures characterized by long straight and unbranched fibrils.(Serpell 2000; Serpell et al. 2000; Smith et al. 2003; Jansen et al. 2004) Because of the insolubility and the inability of the amyloids to be crystallized, the structure of aggregates at a molecular and nano scale is still under veil, but the structure is slowly being uncovered with the help of some techniques such as X-ray diffraction and solid NMR. (Petkova et al. 2002; Thompson 2003) In this dissertation, β-amyloid (Aβ) related to Alzheimer's disease will be discussed.

Table 2. 1 Diseases related to aggregation and deposition of abnormal protein. (Tan and Pepys 1994; Carrell and Gooptu 1998; Kelly 1998; Taylor et al. 2002; Ross and Poirier 2004)

Disease	Toxic Proteins Involved
Alzheimer's disease	Aβ and tau
Parkinson's disease	α-Synuclein
Huntington's disease	Huntingtin
Prion disease	PrP^{Sc}
Tauopathy	tau
Familial amyotrophic lateral sclerosis	SOD1
Other polyglutamine disease (DRPLA, SAC1-3, etc., SBMA)	Atrophin-1, ataxins or AR
Fronto-temporal dementia with Parkinsonism	tau
Primary Systemic Amyloidosis	Immunoglobulin Light Chain
Senile Systemic Amyloidosis	WT Transthyretin (TTR)
Familial Amyloid Polyneuropathy I	Variant Transthyretin (TTR)
Familial Mediterranean Fever	Serum Amyloid A
Secondary Systemic Amyloidosis	Serum Amyloid A
Hereditary (Icelandic) Cerebral Angiopathy	Cystatin C
Familial Amyloid Polyneuropathy (III)	Apolipoprotein A1
Hemodialysis Amyloidosis	β_2-Microglobulin
Finish Hereditary Systemic Amyloidosis	Gelsolin
Type II Diabetes	Islet Amyloid Polypeptide (IAPP)
Medullary Carcinoma of the Thyroid	Calcitonin
Hereditary Renal Amyloidosis	Fibrinogen
Injection-Localized Amyloidosis	Insulin
Atrial Amyloidosis	Atrial Natriuretic Factor (ANF)
Autosomal Dominant Hereditary Amyloidosis	Variant Lysozyme
Familial Visceral Amyloidosis	Lysozyme

ALZHEIMER'S DISEASE

Alzheimer's disease (AD) is a neurodegenerative disorder that causes progressive memory loss and severe dementia in the late stage of AD. Many of the symptoms resulting from brain cell death keep patients from having appropriate social relationships with others. The common symptoms of AD are dementia, a gradual loss of memory, problems with reasoning or judgment, disorientation, difficulty in learning, loss of language skills, and decline in the ability to perform routine tasks. According to statistics from the Alzheimer's Association, approximately 4.5 million Americans have AD and 13.2 million Americans will have AD by the middle of this century (2050) unless appropriate drugs are developed to prevent the disease. (Hebert et al. 2003) The increasing numbers of patients with AD are in part a result of the longer life expectancy of people in this century, as the greatest risk factor for AD is age. One in 10 people over 65 and nearly half of those over 85 have AD. (Jorm et al. 1987; Evans et al. 1989) U.S. society spends at least $100 billion a year on AD. (Meek et al. 1998)

The majority of AD cases are sporadic forms of the disease. Only 5–10% of AD patients have familial Alzheimer's disease (FAD) with a defined inheritance pattern. (van Duijn et al. 1991; Barinaga 1995; Hutton et al. 1996) There are two abnormal structures in the brain associated with AD. As shown if Fig. 2.2, the two hallmarks of Alzheimer's disease are amyloid plaques, which are clumps of protein fragments (β-amyloid) that accumulate outside of cells, and neurofibrillary tangles, which are clumps of altered protein (tau) inside cells. (Selkoe 2001) Besides these two main proteins (β-amyloid and tau), many other factors are related to AD. (Farlow 1998; Selkoe 2001;

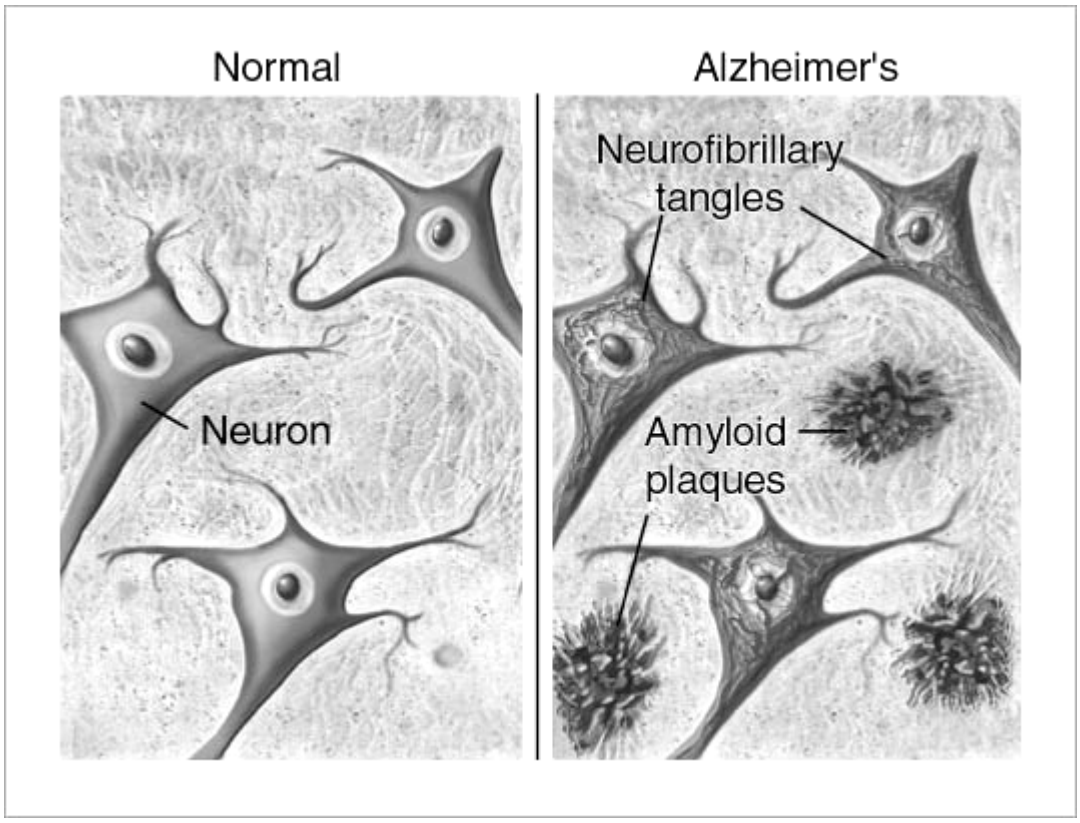

Figure 2. 2. Neuritic plaques and neurofibrillary tangles in Alzheimer's disease. (from American Health Assistance Foundation - http://www.ahaf.org/alzdis/about/Amyloid Plaques .htm, Accessed on March 30, 2005)

Butterfield et al. 2002; Poirier 2003)

Risk Factors in Alzheimer's Disease

The major genes related to AD are those for the amyloid precursor protein (APP), presenilins 1 and 2 and ApoE. Genetic factors (APP, Presenilin 1 and 2) are associated with familial Alzheimer's disease (FAD) or early onset of AD,(Tanzi et al. 1996; Lippa 1999) whereas other factors such as oxidative stress, cholesterol, and inflammation are related to sporadic AD. (Farlow 1998; Butterfield et al. 2002; Poirier 2003)

GENETIC FACTORS

APP (β-Amyloid Precursor Protein): The APP gene is on chromosome 21. (Goate et al. 1991; Selkoe 2001) APP contains the Aβ sequence at the C terminus as shown in Fig.2.3. (Neve et al. 2000; Selkoe 2001) Mutations in APP or alterations of its normal function may cause AD. (Tanzi et al. 1992; Campion et al. 1996) A high proportion of people with Down syndrome, who inherit an extra copy of chromosome 21, develop AD at an early age. (Tanzi 1996; Petronis 1999; Lott and Head 2001; Head and Lott 2004) These facts suggest that mutations in APP or extra copies of chromosome 21 are strongly linked to AD. APP is an integral plasma membrane protein. It is thought to mediate the transduction of extracellular signals into the cell via its C-terminal tail. (Neve et al. 2001) APP is normally cleaved endoproteolytically at the cell surface within the Aβ sequence by an α-secretase such as TACE (tumor necrosis factor alpha converting enzyme, also referred to ADAM17) and ADAM10 (a disintegrin and metalloprotease

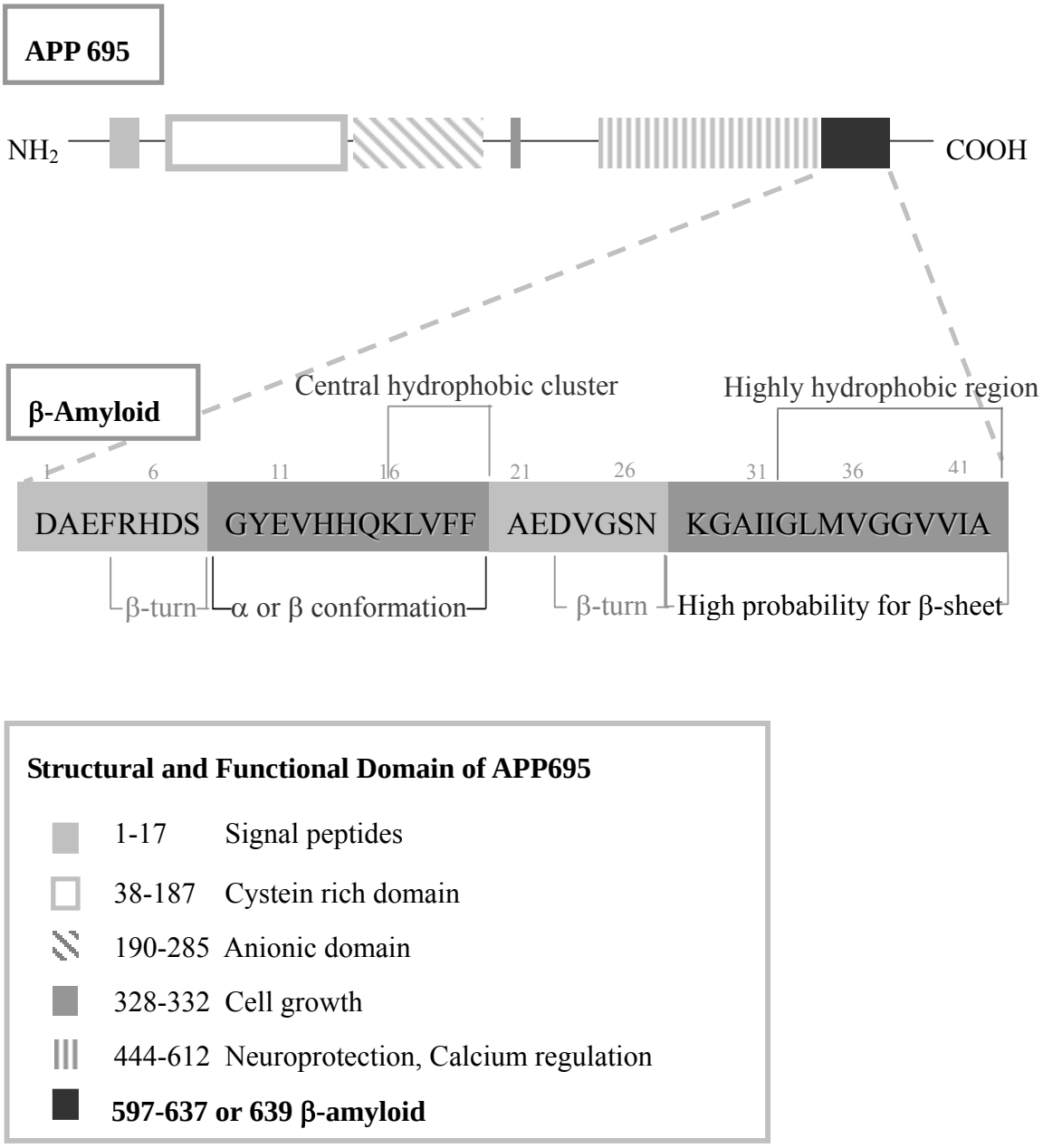

Figure 2. 3. Schematic figure of structural and functional domain of APP695. (Neve et al. 2000) and the primary and secondary structure of Aβ (Serpell 2000)

domain 10). (Allinson et al. 2003; Allinson et al. 2004) The α-secretase produces two soluble fragments: one is the neuroprotective secreted amyloid precursor protein (APPsα) and the other is nonamyloidogenic 3kDa Aβ secreted products. (Neve et al. 2000) β–secretase and γ– secretase cleave APP at the N-terminus and C-terminus of the Aβ protein sequence. (Sinha and Lieberburg 1999) The principal β–secretase in neurons is the aspartic protease BACE1 (β-site APP cleaving enzyme 1).(Vassar 2004) The γ– secretase is a high molecular weight complex composed of Presenilin 1 (PS1), mature Nicastrin, APH-1, and Pen-2. (Kimberly et al. 2003) Mutations in both APP and presenilins (PS) increase overall secretion of Aβ or secretion of the long (42~43 amino acid) form of Aβ (Aβ1-42) relative to the shorter 40 amino acid form. (Borchelt et al. 1996; Mehta et al. 1998; Neve et al. 2000; Selkoe 2001)

Presenilin: Presenilins 1 (PS1) and 2 (PS2) genes which are linked to early onset AD, are on the chromosomes 14 and 1, respectively. (Levy-Lahad et al. 1995; Hardy 1997; Rohan de Silva and Patel 1997; Selkoe 2001) Presenilin knock-out mice show the normal levels of APP protein expression as well as normal secretory derivatives from the α- and β-secretase cleavages but have abnormal γ-secretase function. (Czech et al. 2000; Fraser et al. 2000; Zimmer 2000) The mutations of these genes can increase the production of longer form of Aβ1-42 rather than relatively short form of Aβ1-40. (Borchelt et al. 1996; Czech et al. 2000; Fraser et al. 2000; Zimmer 2000) Presenilins could interact with glycogen synthase kinase 3β (GSK-3β) which is one of the kinases related to phosphorylation of tau protein. (Ishiguro et al. 1992; Mandelkow et al. 1993) Mutation of PS1 in some FAD cases appear to increase the interaction between PS1 and

GSK-3β, which also increase phosphorylation of tau. (Irving and Miller 1997; Gantier et al. 2000) Conclusively, hyperphosphorylated tau proteins lose their ability to associate with the cytoskeleton and form paired helical filaments. There are a number of tau-pathies that lead to neurodegeneration unrelated to Alzheimer's disease.

ApoE4 (Apolipoprotein E4): The apolipoprotein E (ApoE) gene is located on chromosome 19. (Saunders 2001; Sorbi et al. 2001) ApoE is responsible for moving fats between cells and absorbing cholesterol from food in the intestine. The ApoE gene has three alleles, ε2, ε3, and ε4. ε2 allele protects the cell and reduces the risk of developing AD but it is rare. (Aleshkov et al. 1997; Manelli et al. 2004) The most prevalent form, the ε4 allele of ApoE, is a major risk factor for late onset AD. (Neve et al. 2000; Selkoe 2001; Combarros et al. 2002) ApoE4 enhances the deposition of Aβ peptides in both the cerebral cortex and microvasculature. (Holtzman et al. 2000) ApoE4 also increases the steady state Aβ level in brain by inhibiting its degradation. (Rebeck et al. 2001)

NON GENETIC FACTORS RELATED TO SPORADIC ALZHEIMER'S DISEASE

Oxidative Stress: Several studies show that oxidative stress is one of major pathological mechanism in AD. (Good et al. 1996; Mark et al. 1996) Oxidative stress refers to the state in which oxidant agents (free radicals) are overproduced and exceed the antioxidant capacities. Aβ peptide has been reported to produce hydrogen peroxide (H_2O_2) through metal ion reduction, resulting in the formation of hydroxy free radical. (Zimmer 2000) Free radicals peroxidize membrane lipids and oxidize proteins producing a variety of catostrophic cellular damages. (Schubert et al. 1995; Aksenov et

al. 2001) As such, there is increasing interest in the protective role of different antioxidants in AD such as vitamin E, glutathione, ascorbate, catalase, melatonin and estrogen because antioxidants are known to be free radical scavengers. (Miranda et al. 2000) Reactive astrocytes and microglial cells around neuritic plaques are common in the pathology of AD. These activated glia overexpress a number of proteins that may propagate inflammatory and oxidative stress responses that may contribute to the disease. (Dandrea et al. 2001)

Inflammation: Inflammation is a normal immune response to injury or disease. Chronic inflammation can itself cause damage to tissues. Inflammation in the brain may, therefore, contribute to nerve damage. Two facts strongly suggest the involvement of inflammation in AD. First, inflammatory proteins such as amyloid P (McGeer et al. 2001) and α1-antichymotrypsin (Aisen 1996) have been observed in brain regions affected by AD. The other fact is that nonsteroidal anti-inflammatory drugs (NSAIDs) are associated with a reduced risk of developing AD. (Hoozemans et al. 2003; Minghetti 2004) Many believe that inflammation is strongly related to Aβ. (Butterfield et al. 2002; Barger 2004; Broytman and Malter 2004; Zhang et al. 2004)

Cholesterol: High blood cholesterol levels may be one risk factor for AD, possibly because high cholesterol enhances Aβ production. (Marx 2001) The high cholesterol level in the cell membrane also increases the Aβ toxicity to neurons. The role of cholesterol in AD is still under research. (Hartmann 2001; Simons and Ehehalt 2002) However, there is growing evidence that cholesterol plays an important role in regulation of α- and β-secretase. (Simons et al. 2001) Recent research shows that α-secretase

(ADAM10) cleavage of APP is favored over other secretase cleavage when cholesterol lowering agents such as methyl-β-cyclodextrin are used. (Kojro et al. 2001) When elevated cholesterol levels are delivered to the central nervous system (CNS) by ε4 allele of ApoE, it could result in changes in the membrane fluidity and the composition of lipid rafts. (Simons and Ehehalt 2002) Cholesterol concentration at the cellular level is controlled by transcriptional regulation (Simons and Ikonen 2000) because of its toxicity, but elevated dietary cholesterol uptake can increase the level of Aβ through promoting β-secretase activity.

Other Factors: Metals such as aluminum, zinc and copper are suspected to be associated with AD. (Gouras and Beal 2001; Becaria et al. 2002) Traces of aluminum are found in the brain of Alzheimer's patients. (Basun et al. 1991) However the role of aluminum in risk for AD is uncertain. Zinc and copper ions are believed to accelerate the Aβ aggregation and have been proposed as important in AD. (Miura et al. 2000; Huang et al. 2004) Other factors under investigation as risk factors in AD include head injury,(Hinkebein et al. 2003) infectious organisms (e.g. herpesvirus (HSV) 1 (Dobson and Itzhaki 1999)), depression,(Sheline et al. 2002), and ethnicity and/or race.(Tang et al. 1996)

PROTEINS INVOLVED IN ALZHEIMER'S DISEASE

Protein tau: Neurofibrillary tangles contain insoluble paired helical filaments (PHFs) consisting of a ropelike section composed of 2 fibers twisted around each other. (Friedhoff et al. 2000; Iqbal et al. 2003) PHF are mainly composed of the abnormal

hyperphosphorylated microtubule-associated protein (MAP) tau. (Selkoe 2001; Iqbal et al. 2003) From the results of electrophoresis, tau proteins in AD have a higher molecular weight than normal proteins. The slower migration was shown to result from increased phosphorylation of tau. (Greenberg and Davies 1990; Iqbal et al. 1991) Tau, multifunctional MAP, plays roles in the organization of microtubules via stabilizing the microtubules against instability, and bridging these polymers with other cytoskeletal filaments. (Kosik et al. 1986; Cross et al. 1993; Maccioni and Cambiazo 1995; Mandelkow et al. 1995; Saragoni et al. 2000) The most relevant protein kinases involved in tau phosphorylation are GSK-3β (Ishiguro et al. 1992; Takashima et al. 1993; Imahori and Uchida 1997) and Cyclin-dependent kinase 5 (Cdk5) (Tsai et al. 1994; Michel et al. 1998; Alvarez et al. 1999; Patrick et al. 1999)

β-Amyloid (Aβ): Aβ is produced by the cleavage of APP in the activity of β- and γ-secretase. (Sinha and Lieberburg 1999) One of the most plausible hypotheses in AD is Aβ hypothesis. In this hypothesis, Aβ initiates the pathological cascade that leads to amyloid plaques, neuronal dysfunction, and the complex symptoms related to AD. (Hardy 1997; Selkoe 1999) The Aβ hypothesis has been strengthened by research that indicates that aggregates of Aβ show toxicity in *in vitro* experiments, and that most risk factors in AD are related to Aβ. (Hensley et al. 1994; Festy et al. 2001) Strong evidence comes from the studies that overexpression of mutant APP, mutant presenilin 1 (γ-secretase) and 2 result in age-dependent Aβ plaque formation that is related to the cognitive impairment. (Neve et al. 2000) Interestingly, many people with Down syndrome develop AD at an early age. (Petronis 1999; Lott and Head 2001; Head and

Lott 2004) Mutations of the tau gene cause a spectrum of neurodegenerative disease, but not AD. (Murrell et al. 1999; Nacharaju et al. 1999; Sahara et al. 2000; Rosso et al. 2002; van Herpen et al. 2003) This series of these facts indicate that Aβ is a key factor in AD. However, a drawback of this hypothesis is that amyloid deposits are not precisely colocated with neuronal dysfunction. (Lee et al. 2004) Many transgenic mice model show some discrepancies between amyloid deposits and neurodegeneration. (Price et al. 1998) Although some important pieces in the puzzle are still missing, e.g. the relationship between Aβ and tau proteins and between Aβ and neurodegeneration *in vivo*, many researchers believe that AD can be stopped or delayed if Aβ aggregation is blocked or reduced. Therefore, it is very important to investigate the properties of β-amyloid and its aggregation in order to understand AD. In this dissertation, we will focus on understanding the relationship between Aβ aggregation and toxicity, and the prevention of Aβ aggregation and toxicity by using various small heat shock proteins.

β-Amyloid (Aβ) Protein in Alzheimer's Disease

THE STRUCTURE OF Aβ AS A MAJOR FACTOR IN AD

A number of studies show that Aβ is found in the cerebrospinal fluid of AD patient and at comparable concentrations in age-matched control patients. Aβ is also found in the plasma of healthy individuals. This shows that Aβ is normally produced and is soluble under certain conditions. (Seubert et al. 1992; Shoji et al. 1992; Gursky and Aleshkov 2000) Aβ is produced from APP with isoforms of 39-43 residues, (Bayer et al. 2001; Turner et al. 2003) but the 40- and 42-residue amyloid β-peptides are the main

components of neuritic plaques in AD The highly hydrophobic Aβ1-42 is implicated in amyloid fibril nucleation and plaque formation, while the more soluble Aβ1-40 is the main form circulating in normal plasma and cerebrospinal fluid. (Seubert et al. 1992; Shoji et al. 1992)

As seen in Fig. 2.3, the sequence of the amyloid peptides can be split into four clusters, two hydrophilic segments from 1-16 and 22-28 and two hydrophobic segments from17-21 and 29-42. Two β-turns are predicted between residues 6 and 8, and residue 23 and 27. (Kowalewski and Holtzman 1999; Lynn and Meredith 2000; Serpell et al. 2000) Residues 1-10 that have the negative charge are involved in electrostatic interactions. N terminal truncated peptides of Aβ have been used to demonstrate that residues 1-9 were not necessary for fibril formation. But the N terminus is thought to be important for initiating the α-β conformational switching and possibly in copper binding. Residues 29-42 are critical for amyloid aggregation and fibril stabilization. The C terminus from residue 28 shows a high probability for β-sheet structure. Fragments of 10-23 and 29-42 amino acid residues were both found to form β-sheet structure by FTIR, but 29-42 is less soluble and formed only very short fibrils, whereas 14-23 formed long fibrils. Residues 17-21 are hydrophobic and a crucial fragment for the fibril formation, but at least 10 residues, 14-23, is necessary for the long fibril formation. (Tjernberg et al. 1999)

α-helical and/or random coil content has been shown to be associated with high solubility and protease susceptibility whereas a β-sheet content has been shown to be associated with poor solubility and resistance to proteolysis. (Jacchieri 1998) The

transformation of Aβ from α-helix to β-sheet triggers aggregation and fibril formation. (Otvos et al. 1993; Roher et al. 2000) One cause of protein misfolding and aggregation is thought to be the exposure of the hydrophobic region of such unstably folded proteins to an aqueous environment. (Dobson 2003; Goldberg 2003) The secondary structure and fibril elongation of Aβ depends on multiple factors, such as pH, temperature, peptides concentration, and ionic strength. (Barrow and Zagorski 1991; Barrow et al. 1992; Snyder et al. 1994; Shen and Murphy 1995; Fezoui and Teplow 2002; Kawooya et al. 2003; Stine et al. 2003) Aβ has different secondary structures in different solvents. Some organic solvents that dissolve Aβ are generally used in *in vitro* experiments because Aβ is hard to dissolve in the aqueous solvent. Aβ has no detectable β-sheet content in pure Dimethylsulfoxide (DMSO), one third β-sheet in 0.1% trifluoroacetate (TFA), and two third β-sheet in 35% acetonitrile/0.1% TFA. (Shen and Murphy 1995) Recent studies found that higher Aβ concentration and stronger ionic strength increase the Aβ fibril elongation. Higher contents of β-sheet and longer fibrils are induced at 37^{o}C rather than 0^{o}C and pH 5.8 rather than pH 7.4. (Fraser et al. 1991; Barrow et al. 1992; Shen and Murphy 1995; Wood et al. 1996; Harper et al. 1999; Szabo et al. 1999; Gursky and Aleshkov 2000)

Aβ is known to be toxic when Aβ monomers aggregate to form small oligomers, protofibrils, and fibrils. (Lambert et al. 1998; Ward et al. 2000) Toxicity has been attributed to Aβ-derived diffusible ligands (ADDLs) composed of Aβ1-42, with molecular weights between 17 to 42kDa (Lambert et al. 1998; Klein et al. 2001) and heterogeneous globular species (also described as ADDLs) with hydrodynamic radii

between 3 to 8nm. (Chromy et al. 2003) Spherical aggregates, not described at ADDLs, with radii over 15 nm have also been reported to be toxic. (Hoshi et al. 2003) Toxic protofibrils of Aβ1-40 have been described with hydrodynamic radii ranging from 9 nm to over 300 nm. (Walsh et al. 1999; Ward et al. 2000; Wang et al. 2002) When investigators have compared toxicity of fibril and oligomer Aβ species, they have found that the oligomeric species were more toxic. (Dahlgren et al. 2002)

FIBRIL FORMATION MECHANISMS OF Aβ

Aβ monomers undergo a conformational transformation from α-helix to β-sheet aggregate to form fibrils. (Jacchieri 1998; Koteiche and McHaourab 1999; Takahashi et al. 2000a; Takahashi et al. 2000b) General Aβ aggregates are 6-10nm in diameter, nonbranching fibrils, with three to six laterally associated filaments. (Fraser et al. 1991; Stine et al. 1996; Harper et al. 1997; Walsh et al. 1997; Serpell 2000) A great deal of research has been performed in order to elucidate how small peptides- Aβ monomers are converted to fibrils. Aβ fibril formation is self-initiated because no other chemicals are involved. Thoughts about the mechanism of fibril formation can be classified into three classes; one is a nucleation-dependent model, another is a template-assisted model, and the final one is a micelle-formation model.

In the nucleation-dependent model, the initial aggregation rate is very slow until a critically sized nuclei is reached. The kinetic barrier to ordered aggregation results from the thermodynamically unfavorable assembly of the nucleus. Once the nucleus is formed, rapid aggregation by addition of monomers follows. (Jarrett et al. 1993; Gorman

and Chakrabartty 2001; Pallitto and Murphy 2001; Murphy 2002; Souillac et al. 2002) This model was proposed from the results of turbidity measurements. Turbidity changes during Aβ fibril formation indicate that a lag phase exists in the beginning of incubation or aggregation, followed by a rapid increase in turbidity associated with fibril growth. In the template-assisted model, the conformational change of Aβ from non β-sheet to β-sheet is catalyzed by the presence of preformed aggregates. β-sheet conformation monomers are added to form longer fibrils. (Tomski and Murphy 1992; Inouye and Kirschner 1998) In the micelle-formation model, above the critical micelle concentration (CMC), Aβ monomers form a micelle before they form nuclei. The equilibrium between the monomer and micelles occurs rapidly. Fibrils are grown by the addition of monomers. (Lomakin et al. 1997; Murphy and Pallitto 2000)

Trends in Drug Developments for AD

DRUGS APPROVED BY FOOD & DRUG ADMINISTRATION (FDA) FOR AD

Until now, five drugs for AD have been approved by FDA. One of them – memantine, an N-methyl-D-asparate (NMDA) antagonist - is thought to work by blocking the action of the neurotransmitter glutamate.(Religa and Winblad 2003; Farlow 2004) Glutamate is used in areas of the brain affected by AD, and excess glutamate is toxic to neurons. Memantine is for the treatment of moderate to severe AD, (Religa and Winblad 2003) whereas the other drugs approved are for mild to moderate AD. (Birks et al. 2000; Doody 2003) Four drugs - tacrine, (Kurz 1998; Qizilbash et al. 2000) donepezil, (Birks and Harvey 2003; Smith Doody 2003; Roman and Rogers 2004)

rivastigmine, (Farlow 2003; Gabelli 2003) and galantamine (Olin and Schneider 2002; Loy and Schneider 2004) - inhibit the breakdown of acetylcholine, a neurotansmitter which is important in cognitive function in areas of the brain affected by AD.

CHEMICALS OR PROTEINS TO PREVENT Aβ AGGREGATION & TOXICITY

Based on the Aβ aggregation hypothesis, many research groups have focused on finding agents that prevent or reduce Aβ aggregation and toxicity. (Ghanta et al. 1996; Lansbury 1997; Pallitto et al. 1999; Cairo et al. 2002) Some chemicals such as polyphenol (Choi et al. 2001; Ono et al. 2004), apomorphine (Lashuel et al. 2002) and hexadecyl-*N*-methylpiperidinium (HMP) bromide (Wood et al. 1996) are reported to prevent Aβ aggregation and toxicity. Congo red and Chrysamine G, a more lipophilic variant of Congo red, disrupt Aβ aggregation and toxicity. (Lorenzo and Yankner 1994; Kisilevsky et al. 1995; Klunk et al. 1998) Daunomycin, rifampicin, and benzofurans can also interfere with Aβ aggregation and toxicity (Tomiyama et al. 1996; Howlett et al. 1999). Pentamer peptides, KLVFF (Tjernberg et al. 1996; Pallitto et al. 1999), LPFFD (Soto et al. 1998), GVVIN, and RVVIA (Hetenyi et al. 2002) have been used to prevent Aβ aggregation. All of these compounds are used at fairly high levels suggesting that they interact with a monomer of Aβ, and that high levels would have to be administered for *in vivo* treatment.

ENZYMES INVOLVED IN Aβ DEGRADATION AND ANTIBODY FOR Aβ

In a physiological system, excessive Aβ proteins can be cleared by several degrading enzymes such as insulin-degrading enzyme, neprilysin and plasmin. (Carson

and Turner 2002; Turner et al. 2004) The research into enzymatic Aβ degradation could be good target for drug development for AD and might lead to improved understanding of Aβ aggregation *in vivo*. (Saito et al. 2003) A new immunotherapeutic approach has been developed which is based on vaccination with Aβ1-42. Immunization of APP-transgenic mice showed significant reduction of Aβ and cognitive improvement. (Schenk 2002; Robinson et al. 2004) However, Aβ vaccines are still controversial because of safety concerns associated with inflammation in the brain. (Munch and Robinson 2002; Mathews and Nixon 2003; Orgogozo et al. 2003)

SMALL HEAT SHOCK PROTEIN IN Aβ AGGREGATION & TOXICITY

Small heat shock proteins (sHsp) which have chaperone like activity have also been investigated to prevent Aβ aggregation or toxicity. Human sHsp27 inhibited Aβ1-42 fibril formation (Kudva et al. 1997). αB-crystallin, one of α–crystallin subunits prevented Aβ fibril formation *in vitro*, but increased the toxicity of Aβ1-40 (Stege et al. 1999).

Protein Stability Based on Two Transition States

While many biophysical tools have been used to study Aβ structure and aggregation, there have been no reports of measurements of protein stability using structure change in denaturants to study properties of Aβ and its aggregated species.

The free energy for the stability of any protein in urea can be obtained by the assumption that protein is in equilibrium of two states, folded or native state (N) and completely unfolded state (U) with no partially unfolded intermediates. (Pace 1990)

$$N \leftrightarrow U \tag{2-1}$$

Based upon the equilibrium of two states, the fraction of unfolded state can be calculated by

$$f_U = \frac{y_N - y_{obs}}{y_N - y_U} \tag{2-2}$$

where f_U is the fraction of unfolded state, y_{obs} is the observed variable, and y_N, and y_U are linear characteristics of native and unfolded states. The equilibrium constant for the transition between native and unfolded states can be expressed by the fraction of unfolded protein and the characteristics of native and unfolded states

$$K = \frac{[U]}{[N]} = \frac{f_U}{1 - f_U} = \frac{y_N - y_{obs}}{y_{obs} - y_u} \tag{2-3}$$

where K is equilibrium constant between N and U, [U] and [N] are the concentration of unfolded and native states. The free energy difference, ΔG, between native and unfolded states can be obtained by the thermodynamic relationship between Gibbs free energy and equilibrium constant.

$$\Delta G = - R T \ln K = - R T \ln \frac{y_N - y_{obs}}{y_{obs} - y_u} \tag{2-4}$$

where ΔG is the free energy difference between unfolding and native states, R is gas constant and T is the absolute temperature. The free energy change upon unfolding can be determined experimentally and denaturant concentration is generally linearly relationship with the free energy change. (Pace and Shaw 2000)

$$\Delta G = \Delta G_{H2O} - m[\text{Urea}] \tag{2-5}$$

where [Urea] is the concentration of urea, m is the slope of this equation, and ΔG_{H2O} is the free energy change in the environment without urea. ΔG_{H2O} refers to the

conformational stability of the protein without denaturant and m denotes the difference in accessible hydrophobic surface area in native and unfolded states. (Tanford 1970; Myers et al. 1995; Spudich and Marqusee 2000)

We believe that application of the analysis of stability to Aβ may be useful in understanding properties of Aβ aggregates and their toxicity.

SMALL HEAT SHOCK PROTEINS (sHsps)

General Characteristics of Small Heat Shock Proteins (sHsps)

Molecular chaperones interact with partly folded intermediate states of proteins to prevent incorrect folding and aggregation. (Ehrnsperger et al. 1997; Kudva et al. 1997; Clark and Muchowski 2000; Hatters et al. 2001; Hartl and Hayer-Hartl 2002; Muchowski 2002) The first identified chaperone was a heat shock protein, since the protein was induced by elevated temperature. Small heat shock proteins (sHsps) are expressed in almost all organisms when cells become stressed during unfavorable environmental conditions. They exist as large oligomeric complexes of 300-800kDa with monomeric molecular mass of 15-43kDa. (van den et al. 1999; Clark and Muchowski 2000; MacRae 2000) Important roles of sHsps are to stabilize other proteins under the stressed condition and protect them from aggregation. (van den et al. 1999; Bruey et al. 2000) sHsps prevent the aggregation of substrate proteins in an ATP independent manner. (Ganea 2001; Narberhaus 2002) sHsps are composed of three parts in the primary sequence, the N-terminal domain, the α-crystallin domain, and the C-termial extension. α-crystallin domains, highly conserved 80-100 amino acid sequences

located in the C-terminal regions, are very important for the self assembly of sHsps and the binding of sHsps to their substrates. (Fig. 2.4) (de Jong et al. 1993; Caspers et al. 1995; Koteiche and McHaourab 1999; Clark and Muchowski 2000) Mutations of various substrate binding sites suggest that sHsps bind substrate proteins through multiple contacts within the α-crystallin domain. N-terminal domain has variable sequence and length. This domain is responsible for sHsp assembly, which results in polydisperse sHsp. The C-terminal extension shares no homologous sequence, but this domain has common polar and flexible properties which are probably related to protein solubility. sHsps protect substrate proteins from unfolding when they are under unfavorable environments such as higher temperature, denaturants, and UV. (Ganea 2001)

Small Heat Shock Proteins - Hsp20 (Novel α-Crystallin), Hsp17.7, and Hsp27

α-crystallin is 12~43kDa member of the small heat-shock protein family that is able to prevents irreversible aggregation. In the lens, α-crystallin contributes to lens transparency and has chaperone like activity. (Horwitz 1992; 2000) There are two oligomeric subunits, A and B. Outside the lens, only αB-crystallin is induced in response to stress. (Stege et al. 1999; Liang 2000; Abgar et al. 2001)

A novel protein (Hsp20) was isolated from the erythrocyte parasite *Babesia bovis*. (Dr. Allison C. Rice-Ficht, Department of Medical Biochemistry and Genetics, Texas A&M University, College Station, Texas). (Brown et al. 2001) According to the sequence homology (BLAST search of the NCBI), the sequence of this protein is similar

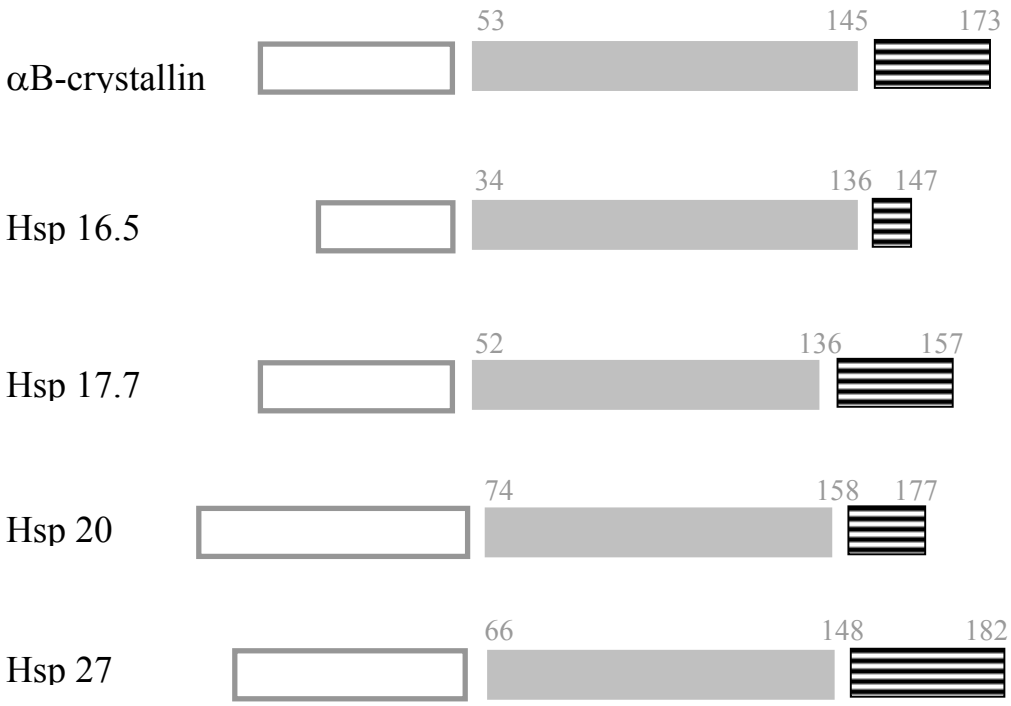

Figure 2. 4. Schematic drawing of three domains in small heat shock proteins. (□ N-terminus, ▒ α-crystallin domain, and ▤ C-termial extension) αB-crystallin and Hsp16.5 are from (Salerno et al. 2003), and Hsp17.7 (carrot), Hsp20 (*B. Bovis*), and Hsp27 (human) are obtained by BLAST in the NIH web server.

to that of the plant sHsp, α-crystallins, and *Toxoplasma gondii* hsp30/bag1. This novel protein has shown α-crystallin activity in *in vitro* studies. Alcohol dehydrogenase (ADH), when heat denatured, aggregates and shows increased turbidity with time. However the addition of the novel protein (Hsp20) at the beginning of ADH incubation can reduce the turbidity of the ADH. The novel protein is known to form oligomers in solution, but the structure and the form of this protein at various solvents are under research.

Hsp17.7 isolated from carrot can protect the carrot from thermal stress. (Dr. Lynn Zimmerman, Department of Biological Science, University of Maryland Baltimore County, Baltimore, Maryland) It suggests that Hsp17.7 has chaperone like activity. (Malik et al. 1999) Many small heat shock proteins such as Hsp16.5 act as chaperones when unfolded proteins are generated. However, some proteins such as Hsp12.6 do not have any molecular chaperone function.

Hsp 27 purified from human has more than 80% sequence homology with Hsp25 from mouse. Hsp27 is expressed in variety of cells such as muscle, skin, motor, and sensory neurons. In AD, increased expression of αB-crystallin and Hsp27 was found. Hsp27 prevents Aβ1-42 aggregation *in vitro*, although it has less activity to inhibit preformed amyloid. (Kudva et al. 1997)

Because small heat shock proteins are known to prevent protein aggregation, it is possible that they may be useful in preventing aggregation and toxicity of Aβ. All small heat shock proteins used in this research have chaperone like properties and an α-crystallin domain in common.

In summary, while much has been learned concerning Aβ and the role of Aβ aggregation in toxicity associated with AD, there is still much to learn. There is still no clear understanding of the relationship between Aβ size, structure, and toxicity and how aggregated Aβ leads to toxicity. Mechanisms of Aβ aggregation are still spectulative. While agents have been developed which reduce Aβ aggregation, none are useful at low concentrations that might be accessible therapeutically. New tools, new approaches and new compounds are needed in research into the role of Aβ aggregataion and toxicity.

CHAPTER III

ROLE OF AGGREGATION CONDITIONS IN STRUCTURE, STABILITY AND TOXICITY OF INTERMEDIATES IN THE Aβ FIBRIL FORMATION PATHWAY

OVERVIEW

β-amyloid peptide (Aβ) is among the main protein components of senile plaques that are one of the histopathological hallmarks in Alzheimer's disease (AD). Aβ readily forms fibrils that have high β-sheet content, and it is this fibril or aggregated structure of Aβ that is associated with senile plaques in AD. From recent studies, it is known that Aβ is toxic when aggregated. In particular, soluble oligomers have comparable neurotoxicity. However, the relationship between neurotoxicity and the size of Aβ aggregates or oligomers is still under investigation. Here, I show that different Aβ incubation conditions *in vitro* can affect both the rate of Aβ fibril formation and the conformation of intermediates in the aggregation pathway. When mixed, Aβ aggregates faster than non-mixed Aβ as determined by Congo red binding, however, the morphology of fibrils formed at the end of aggregation with or without mixing, as observed in electron micrographs, are comparable. Interestingly, intermediates formed during Aβ aggregation as examined via circular dichroism spectroscopy, size exclusion chromatography, and electron microscopy, differ greatly under mixing and non-mixing conditions. Data

suggest that without mixing, Aβ undergoes a significant conformational change upon aggregation to a fibril form that is not seen when Aβ is mixed during aggregation. Unfolding studies in guanidine hydrochloride indicate that fibrils formed without mixing are more stable to unfolding in detergent than aggregation intermediates or Aβ fibrils formed with mixing. In addition, Aβ fibrils formed without mixing were less toxic to differentiated SH-SY5Y cells than the Aβ aggregation intermediates of fibrils formed with mixing. These results suggest that it is not the tertiary structure alone of Aβ that correlates with its toxicity, but possibly other characteristics such as stability to unfolding in detergent that influence the toxic properties of Aβ. Given that aggregation of Aβ *in vivo* may differ significantly from *in vitro* aggregation conditions, understanding the other factors that influence toxicity outside of tertiary structure may help guide development of agents to prevent Aβ toxicity associated with Alzheimer's disease.

INTRODUCTION

Alzheimer's disease (AD) is a progressive, neurodegenerative disease of the central nervous system and the leading cause of dementia in aging population. One of the histopathological hallmarks of AD is the formation of neuritic plaques, the major protein component of which is β-amyloid peptide (Aβ). Two variants of Aβ, Aβ1-40 and Aβ1-42, are the most abundant forms found in AD. (Bayer et al. 2001; Turner et al. 2003)

Accumulating data show that while Aβ aggregates readily into amyloid fibrils, the Aβ species in soluble oligomeric forms rather than fibrils are closely associated with the

neurotoxicity *in vivo* and *in vitro*. Toxicity has been attributed to Aβ-derived diffusible ligands (ADDLs) composed of Aβ1-42, with molecular weights between 17 to 42kDa (Lambert et al. 1998; Klein et al. 2001) and heterogeneous globular species (also described as ADDLs) with hydrodynamic radii between 3 to 8nm. (Chromy et al. 2003) Spherical aggregates, not described at ADDLs, with radii over 15 nm have also been reported to be toxic. (Hoshi et al. 2003) Toxic protofibrils of Aβ1-40 have been described with hydrodynamic radii ranging from 9 nm to over 300 nm. (Walsh et al. 1999; Ward et al. 2000; Wang et al. 2002) When investigators have compared toxicity of fibril and oligomer Aβ species, they have found that the oligomeric species were more toxic. (Dahlgren et al. 2002) While some investigators in general believe that there is a common structure associated with amyloid toxicity, (Kayed et al. 2003) a careful characterization of such a common structure is still not available.

Part of the challenge in elucidating the relationship between Aβ structure and toxicity are the numerous environmental factors such as solvents, pH, temperature, and ionic strength that are associated with how investigators aggregate Aβ *in vitro* that affect Aβ structure. (Barrow and Zagorski 1991; Barrow et al. 1992; Snyder et al. 1994; Shen and Murphy 1995; Fezoui and Teplow 2002; Kawooya et al. 2003; Stine et al. 2003)

In work presented here, I examined the differences in Aβ aggregation intermediates, and final structures formed when only a simple modification in Aβ aggregation conditions was made, the presence of absence of mixing during aggregation. I show, that while the final structures in the Aβ aggregation pathway are comparable by measures such as electron microscopy, the toxicity of fibrils formed are significantly

different. In addition, intermediates in the aggregation pathway show significantly different structural rearrangements. When guanidine hydrochloride unfolding was used as a simple measure of stability of different aggregated species, the structures that changed conformation at the lowest concentrations of guanidine hydrochloride were also the most toxic structures. Thus it appears that other characteristics besides tertiary structure as can be measured by electron microscopy are more indicative of toxicity of Aβ species.

MATERIALS AND METHODS

Materials

β-Amyloid (Aβ)–(1-40) was purchased from AnaSpec (San Jose, CA). Human neuroblastoma SH-SY5Y cells (ATCC number: CRL-2266) were purchased from ATCC (Manassas, VA). Cell culture reagents were purchased from Invitrogen Life Technologies (Carlsbad, CA). Superose6 HR 10/30 Column was purchased from Amersham Pharmacia Biotech. (Piscataway, NJ). All other disposable supplies for FPLC were purchased from Amersham Pharmacia Biotech. Congo red was purchased from Fisher Chemicals. (Pittsburgh, PA). All other chemicals, unless otherwise specified were obtained from Sigma-Aldrich Co..

Protein Sample Preparation

Aβ1-40 was dissolved in 0.1% (v/v) Trifluoroacetic acid (TFA) solvent at the concentration of 10mg/ml. This solution was incubated at room temperature for 20~30

minutes in order to completely dissolve the Aβ. Filtered phosphate-buffered saline (PBS, 4.3 mM Na_2HPO_4, 137 mM NaCl, 2.7 mM KCl and 1.4 mM KH_2PO_4, pH 7.4) was added to the Aβ solution to make the final concentrations used in experiments. For cell viability assays, MEM medium was used instead of PBS buffer. For aggregation with mixing, Aβ samples were mixed on the rotator at 18 rpm and 37°C, and samples were taken out with time. For aggregation without mixing, Aβ samples were incubated without disturbance in a 37°C incubator.

Congo Red Binding

Congo red was dissolved in PBS at the concentration of 120μM and syringe filtered. The Congo red solution was mixed with protein samples at 1:9 ratios to make the final concentration of Congo red 12μM. After a short vortex, the mixtures were incubated at room temperature for 30~40 minutes. Absorbance measurements from 400nm to 700nm (UV-Vis spectrometer model UV2101, Shimadzu Corp.; Kyoto, Japan). Alternatively, Congo red absorbance was read at 405 nm and 540 nm using an Emax Microplate Reader (Molecular Devices, Sunnyvale, CA). In both cases, PBS buffer was used as blank control. The concentration of Aβ fibrils was estimated from Congo red binding via equation 3-1:

$$[A\beta_{FIB}] = ({}^{541}A_t/4780) - ({}^{403}A_t/6830) - ({}^{403}A_{CR}/8620) \qquad (3\text{-}1)$$

where ${}^{541}A_t$ and ${}^{403}A_t$ are the absorbances of the Congo red-Aβ mixtures at 541 nm and 403 nm, respectively, and ${}^{403}A_{CR}$ is the absorbance of Congo red alone in phosphate

buffer. (Klunk et al. 1999) In the Microplate reader, absorbances at 405nm and 540nm were assumed to be same as those at 403nm and 541nm.

Size Exclusion Chromatography (SEC)

A Superose6 HR 10/30 Column attached to FPLC (Fast Performance Liquid Chromatography) (Pharmacia; Piscataway, NJ) was used to determine the molecular size of Aβ species. PBS buffer was used as a mobile phase with flow rate of 0.5mL/min. A 100μL sample loop was used. For Aβ samples where aggregation with mixing occured, 100μL of the Aβ samples were centrifuged at 7,000rpm for 3 minutes prior to SEC analysis. For the aggregation without mixing samples (non-mixed), samples were centrifuged at 7,000rpm and 30 seconds. Supernatants of centrifuged samples were loaded in the 100μL loop and injected into the column. Aβ species were detected by UV detector at 254nm. The following proteins were used for calibration standards: ribonuclease (13.7kDa), chymotrypsin (25kDa), ovalbumin (43kDa), and albumin (67kDa), aldolase (158kDa), catalase (232kDa), ferritin (440kDa), thyroglobulin (660kDa), and BD 2000 (2,000kDa). To calculate relative areas of Aβ in peaks from the SEC chromatograms, first the total area of a 100 μM Aβ sample was obtained from a chromatogram obtained without a column in the FPLC system. On the basis of this total area, relative areas from the SEC spectrum was calculated

Circular Dichroism (CD)

Secondary structure of Aβ was measured using a PiStar-180 Circular Dichroism

Spectrometer (Applied Photophysics; Leatherhead, United Kingdom)**.** CD spectra in the far UV range (190~260nm) were obtained using a 1 cm quartz cell, at 37^{o}C, using a Xe lamp as a light source, a 1.0nm bandwidth, 1.0nm step interval, and 1.5 second/nm scanning speed. The spectrometer was purged with nitrogen gas during measurement. PBS buffer was used for the calibration.

Electron Micrograph (EM)

200μl of Aβ peptide solution, prepared as described above, was mixed, placed on glow discharged grids, and then negatively stained with 1% aqueous ammonium molybdate (pH 7.0). Grids were examined in a Zeiss 10C transmission electron microscope at an accelerating voltage of 80 kV. Calibration of magnification was done with a 2,160 lines/mm crossed line grating replica (Electron Microscopy Sciences, Fort Washington, PA).

Aβ Stability with Guanidine Hydrochloride (GuHCl)

100μM Aβ samples were prepared as described in the protein sample preparation. Aβ samples at 37^{o}C incubator were taken out in 0 (fresh Aβ), and 24 hours for mixed samples and 4, 8, and 72 hours for non-mixed samples. GuHCl was dissolved in PBS buffer and prepared in different concentrations. Aβ samples were mixed with GuHCl solution at the ratio of 1:9. The final Aβ concentration in each sample was 10μM. The final GuHCl concentrations varied from 0.5M to 7M. Aβ samples in different GuHCl concentrations were incubated at 37^{o}C for 2 hours such that the protein could come to

equilibrium with the GuHCl. CD spectra were taken of the incubated Aβ-GuHCl samples and each were calibrated against a solutions of GuHCl at the same concentration in PBS buffer. CD intensity at 220 nm is typically a minimum for β-sheet structures such as would be found in aggregated Aβ, and thus was used as an indicator of change in protein structure with detergent addition.

Cell Culture

SH-SY5Y cells were grown in Minimum Essential Medium (MEM) supplemented with 10% (v/v) Fetal Bovine Serum (FBS), 25mM Sodium bicarbonate, 100units/ml penicillin, and 100mg/ml streptomycin. Cells were cultured in a 5% (v/v) CO2 environment at 37^{o}C incubator. Low passage number cells were used (<p20) in all experiments to reduce instability of cell line.

Biological Activity Assay

For biological activity tests, SH-SY5Y cells at a density of 1x10^{5}cells/well were grown in 96 well plates. Cells were fully differentiated by addition of 20ng/mL NGF for 8 days. Aβ samples in MEM medium were added to the differentiated SH-SY5Y cells and the cells were incubated with Aβ samples at 37^{o}C for 2 hours. Negative controls (cells in medium with no Aβ) and positive controls (cells treated with 800μM H_2O_2 in 50% (v/v) medium for 2 hours) were also prepared. At least 3 wells were prepared for each Aβ treatment, and each positive and negative control.

Cell viability was determined by using 2 fluorescent dyes, Annexin V-PE and 7-

Amino-actinomycin (7-AAD). Annexin V-PE is a Ca^{2+} dependent phospholipid binding protein that has high binding affinity for phosphatidylserine on apoptotic cells. 7-AAD is taken up by necrotic or damaged cells, whereas live cells exclude 7-ADD. In this experiment, cells unstained for both Annexin V-PE and 7-AAD were taken as live cells. In order to stain the dead cells, Aβ treated cells were washed with PBS 1~2 times and 1x binding buffer was added to the cells. (1x binding buffer: 10mM Hepes/NaOH (pH 7.4), 140mM NaCl, 2.5mM $CaCl_2$) 5μL of Annexin V-PE and 5μL of 7-AAD were added to the cells and cells were incubated for 15~20 minutes at room temperature in the dark room. 150μL of 2x binding buffer was added to the cells, and cells were collected using a scrapper. Stained cells in 96 well plates were loaded in the FACS array (BD FACSArray, BD Bioscience; San Jose, CA) and fluorescence histograms for cells were obtained. To set up compensation and gates for the cell viability assays, 3 sets of staining controls were prepared, unstained cells, cells stained with Annexin V-PE alone, and cells stained with 7-AAD alone. Cells not stained with either dye (population with low fluorescence intensities for Annexin V-PE and 7-AAD) were taken as live cells, and the relative cell viabilities were calculated using equation 3-2.

$$\text{Relative Cell Viability}\,(\%) = \frac{(\text{L.C.}_{\cdot\text{sample}} - \text{L.C.}_{\cdot\text{H2O2}})}{(\text{L.C.}_{\cdot\text{NControl}} - \text{L.C.}_{\cdot\text{H2O2}})} \text{ x } 100 \qquad (3\text{-}2)$$

where $\text{L.C.}_{\cdot\text{sample}}$ is live cells (%) of Aβ treatment, $\text{L.C.}_{\cdot\text{Ncontrol}}$ is live cells (%) of negative control, and $\text{L.C.}_{\cdot\text{H2O2}}$ is live cells (%) of H_2O_2 treatment (positive control).

Statistical Analysis

For each experiment, at least three independent determinations were made.

Significance of results was determined via the paired t test with $p<0.05$ (95% confidence interval) unless otherwise indicated. Data are plotted as the mean plus or minus the standard error of the measurement.

RESULTS

Kinetics of Aβ Aggregation with and without Mixing

We examined the structure of 100μM Aβ samples when aggregated with mixing and without mixing. Congo red binding was used as an indicator of extended β-sheet structure and changes in Aβ aggregation with time. As seen in Figure 3. 1, the kinetics of Aβ fibril formation, as indicated by Congo red binding, follow a similar trend with and without mixing, however the time scales for fibril formation under the two conditions differ by a factor of two to four. In both cases, fibril formation follows a characteristic sigmoidal curve, with a lag phase at early incubation times, followed by a fibril growth phase, then a saturation phase. The phase lags are about 4 hours and 16 hours for mixing and non-mixing conditions, respectively.

Size Characterization of Aβ Species during Aggregation

I used SEC to characterize the size of Aβ species associated with fibril formation when Aβ was aggregated with and without mixing to try to determine if significant differences occurred during aggregation under the different conditions. When freshly prepared, Aβ species that eluted at volumes consistent with monomer and dimer species were observed with an approximate 1:2 ratio of absorbance of monomer to dimer. When

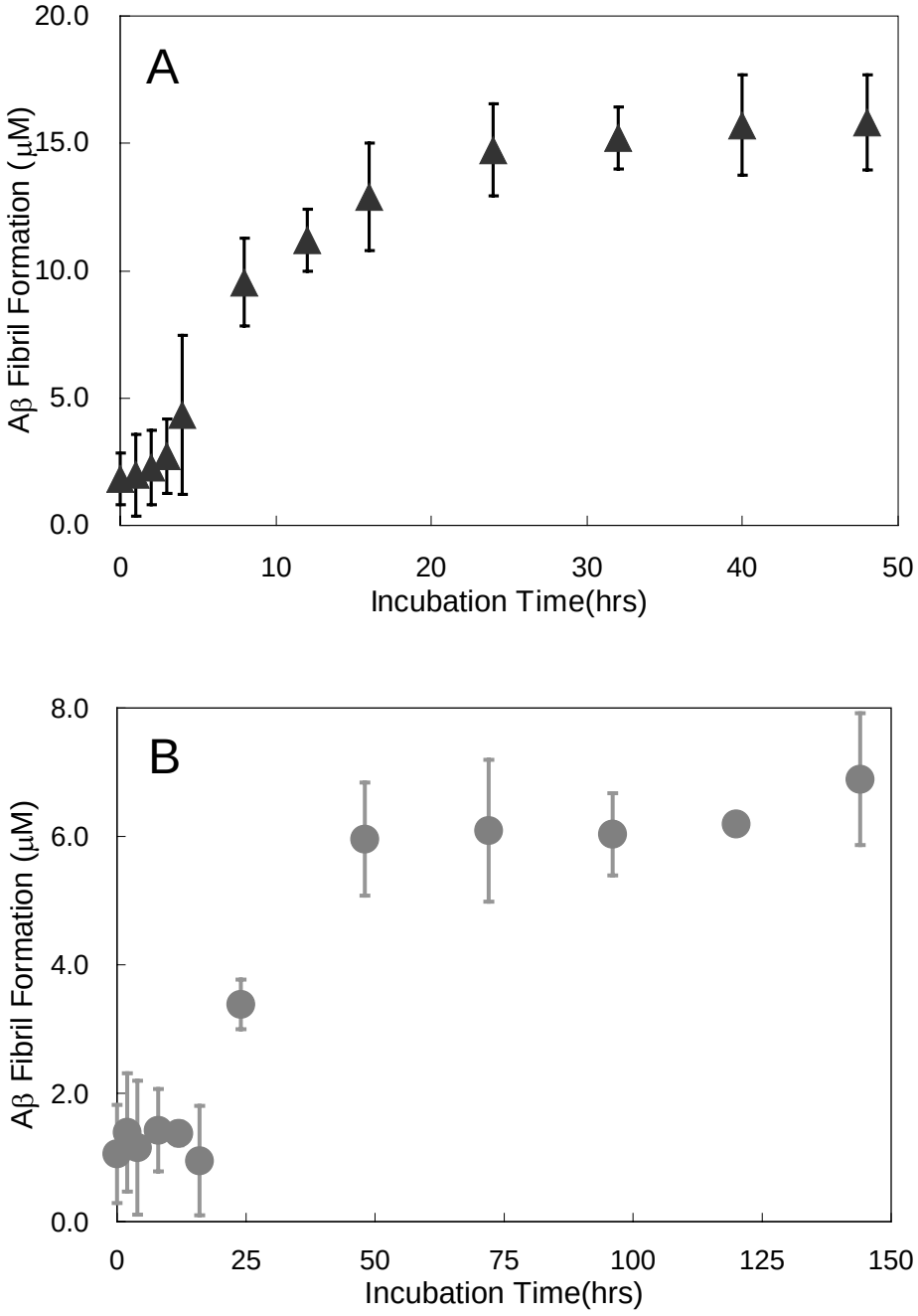

Figure 3. 1. Aβ aggregation scanning with time by using Congo red. 100μM Aβ was incubated at 37^{o}C in the (A) presence and (B) absence of mixing.

mixing was employed during aggregation, large Aβ species (>1,500kDa) appeared in chromatograms along with monomer and dimer as early as 2 hours after the beginning of aggregation (Figure 3. 2). These large species were also seen at 4 hours into aggregation, however, after 4 hours, only monomer and dimer appeared on chromatograms as sample pretreatment (centrifugation at 7000rpm for 3 minutes) removed the largest aggregates formed. At 8 hours and 24 hours, the only Aβ species recorded in SEC chromatograms were monomer and dimer, however, the total amount of monomer and dimer species decreased with time, indicating that more of the Aβ initially present was incorporated into large aggregated species that were removed via centrifugation prior to chromatography at later times during aggregation. Throughout aggregation, the relative ratio of monomer to dimer appeared constant, suggesting the two species were in equilibrium.

Analogous to that observed in chromatograms taken during aggregation with mixing, in chromatograms taken of samples when aggregation proceeded without mixing, species eluting at volumes consistent with monomer and dimer of Aβ were present at all times, in an approximate 1:2 absorbance ratio, with their relative amount decreasing with time during aggregation (Figure 3. 2). Unlike aggregation with mixing, when aggregation proceeded without mixing, a species that eluted with an approximate molecular weight of a dodecamer was observed at 4 and 8 hours after the beginning of aggregation. At later times this species was no longer present. The relative amounts of Aβ species observed during aggregation with and without mixing were calculated and are displayed in Table 3. 1.

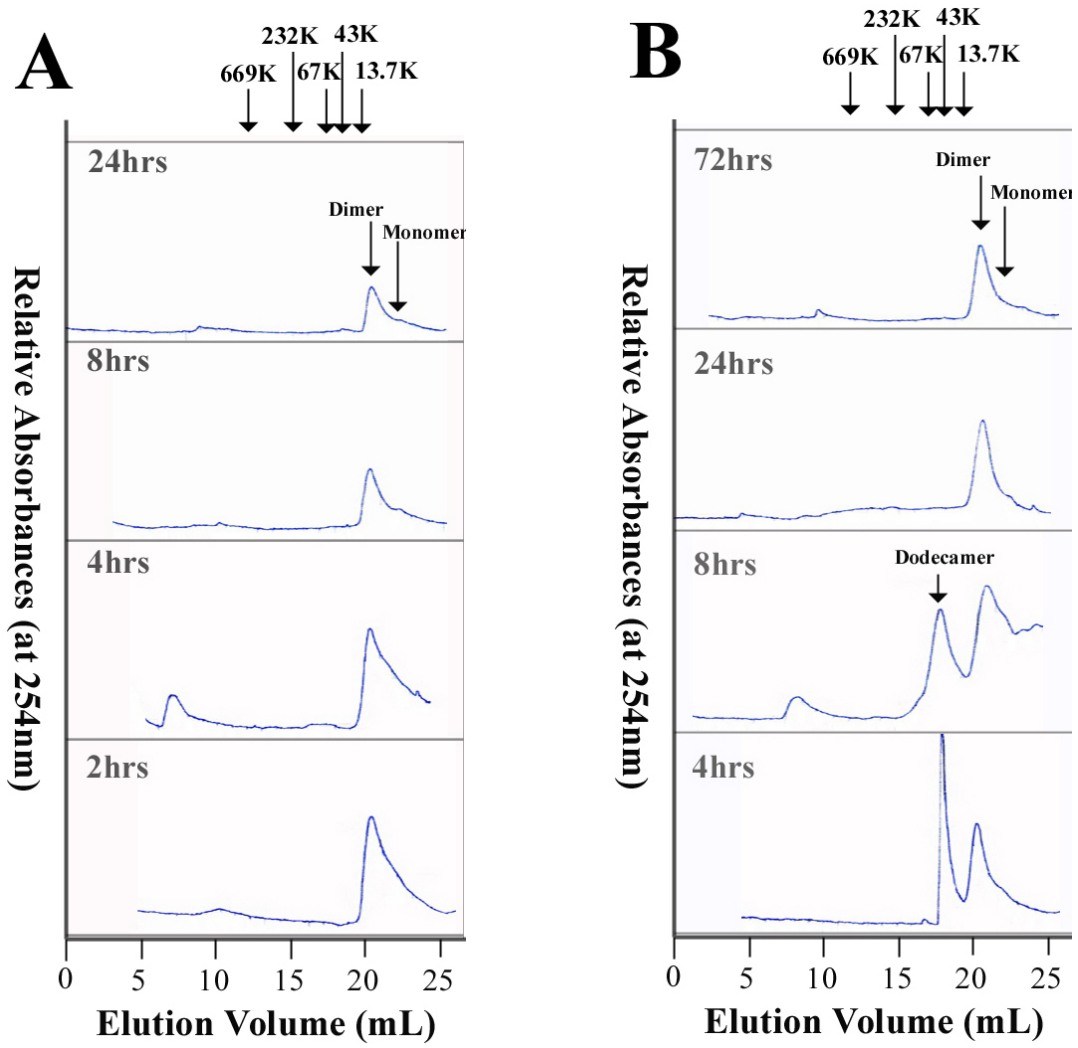

Figure 3. 2. Size characterization of Aβ species - representative SEC. 100μM Aβ samples were incubated at 37°C for (A) 2, 4, 8 and 24 hours in mixing condition and (B) 4, 8, 24, 72 hours in non-mixing condition.

Table 3. 1. Relative amount of Aβ species in percentage

	Mixing Condition				Non-Mixing Condition			
	Mono-mer	Di-mer	Dodeca-mer	Big species*	Mono-mer	Di-mer	Dodeca-mer	Big species*
2 hrs	21.3**	55.3**		2.0**				
4 hrs	14.7	38.7		15.3	18.0	40.7	41.3	
8 hrs	8.7	22.0			6.0	28.0	35.3	12.7
24 hrs	4.7	14.7			3.3	29.3		
72 hrs					2.0	26.7		

* Big species mean Aβ species that have the molecular masses of 1,500-2,000kDa.

** All values used in this table are percentage calculated by the equation of (Each species area/total 100μM Aβ area) x 100

Electron Micrographic Images of Aβ Species during Aggregation

Electron microscopy was used to visualize the images of Aβ species formed during aggregation with and without mixing. As seen in Figure 3. 3A, there were no distinct structures observed in micrographs of fresh Aβ. At times 2 hours after aggregation with mixing (Figure 3. 3B), small globular species with diameters under 5 nm could be observed.

At 4 and 8 hours after the initiation of aggregation with mixing, small globular species along with some fibril species could be seen in micrographs (data not shown). At 24 hours, dense mats of fibrils could be observed (Figure 3. 3C). When aggregation proceeded without mixing, at 8 hours after initiation of aggregation, uniform spherical species with diameters of 20~30nm were seen (Figure 3. 3D). Species with this size and structure were never seen when aggregation proceeded with mixing. At 72 hours, fibrils could be seen in micrographs that appeared more crystalline than fibrils observed under mixing conditions (Figure 3. 3E).

Changes in Aβ Secondary Structure during Aggregation

Circular dichroism (CD) was used to examine secondary structure changes of Aβ during aggregation. As seen in Figure 3. 4, the CD spectrum of fresh Aβ indicated that the fresh peptide contained a β-sheet rich structure with some α-helix and random coil contribution. When aggregation proceeded with mixing, while changes in the CD spectrum were observed, they did not indicate a change in the basic secondary structure elements of the aggregating peptide (Figure 3. 4A). However, when Aβ was aggregated

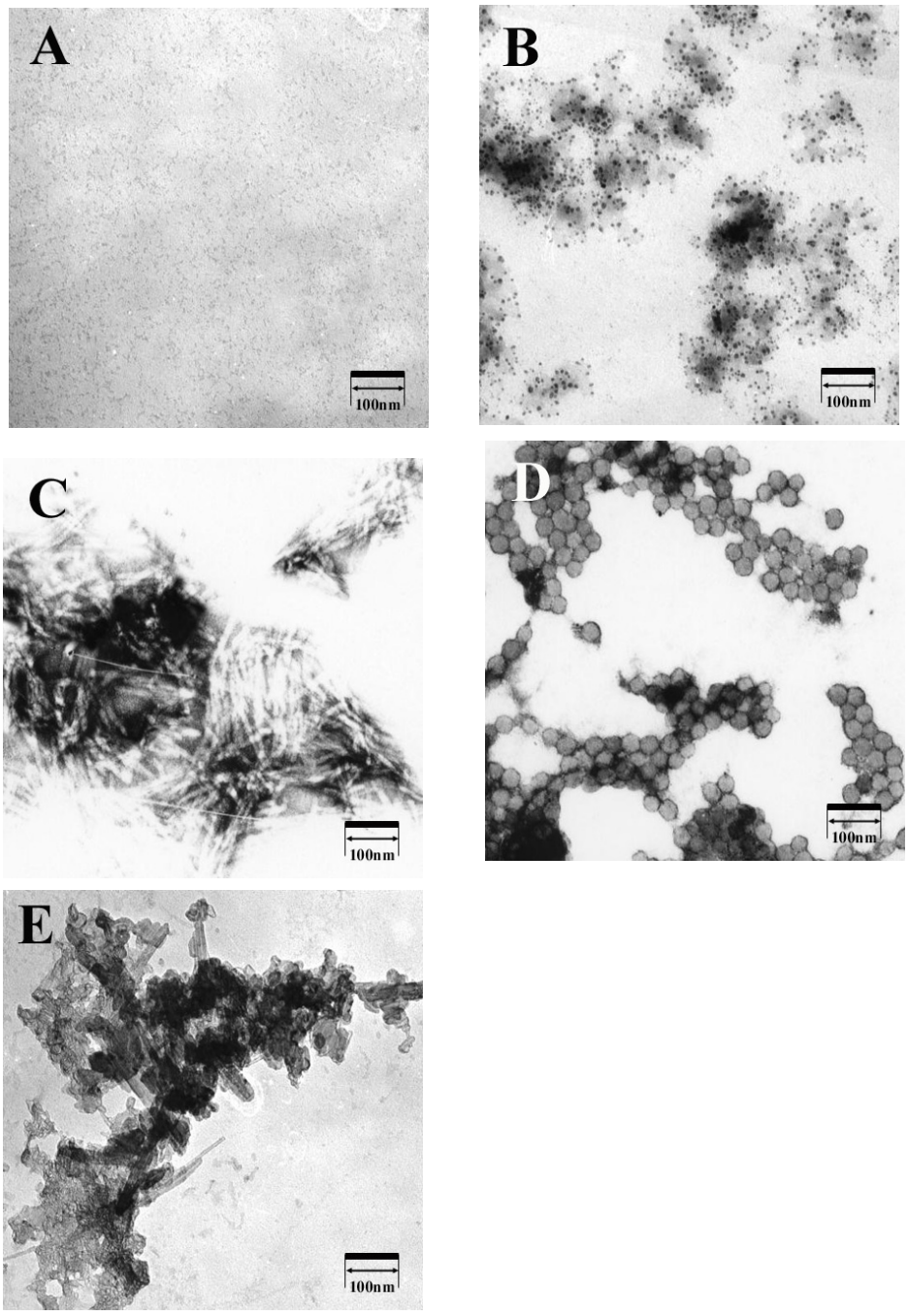

Figure 3. 3. Representative EM images of 100μM Aβ with time. (A) fresh Aβ, (B) 2 hours in mixing condition, (C) 24 hours in mixing condition, (D) 8 hours in non-mixing condition, and (E) 72 hours in non-mixing condition.

without mixing, a significant spectral shift in the CD spectrum was observed at times between 4 and 10 hours after initiation of aggregation, consistent with a decrease in β sheet and and increase in random coil structure (Figure 3. 4B). The appearance of the spectral shift in CD structure at intermediate times during aggregation without mixing coincides with the observation of the large (20 nm) globular species on electron micrographs and the peak that elutes at an approximate molecular weight of 53kDa on SEC chromatograms. At longer times after initiation of aggregation, the secondary structure of the aggregating Aβ took on more β-sheet content.

Stability of Aβ Species to Structure Change in Denaturant

In order to obtain a relative measure of stability of different Aβ species that were intermediates or end points during aggregation under different conditions, I examined structural changes of the Aβ species upon incubation with a denaturant, guanidine hydrochloride, somewhat analogous to typical protein unfolding experiments that would be used to examine stability of folded proteins. (Pace 1990) I made no attempt to quantify changes in energy associated with unfolding as it is not clear that equilibrium folding models apply to Aβ aggregation, however, in Figure 3. 5, I present the change in Aβ structure as measured by CD as a function of different concentrations of detergent. Fresh Aβ and Aβ fibrils formed without mixing require more denaturant before undergoing the maximum observed structural change, while Aβ fibrils formed with mixing and intermediate species formed during Aβ aggregation without mixing required the least amount of denaturant to undergo the maximum observed structural change.

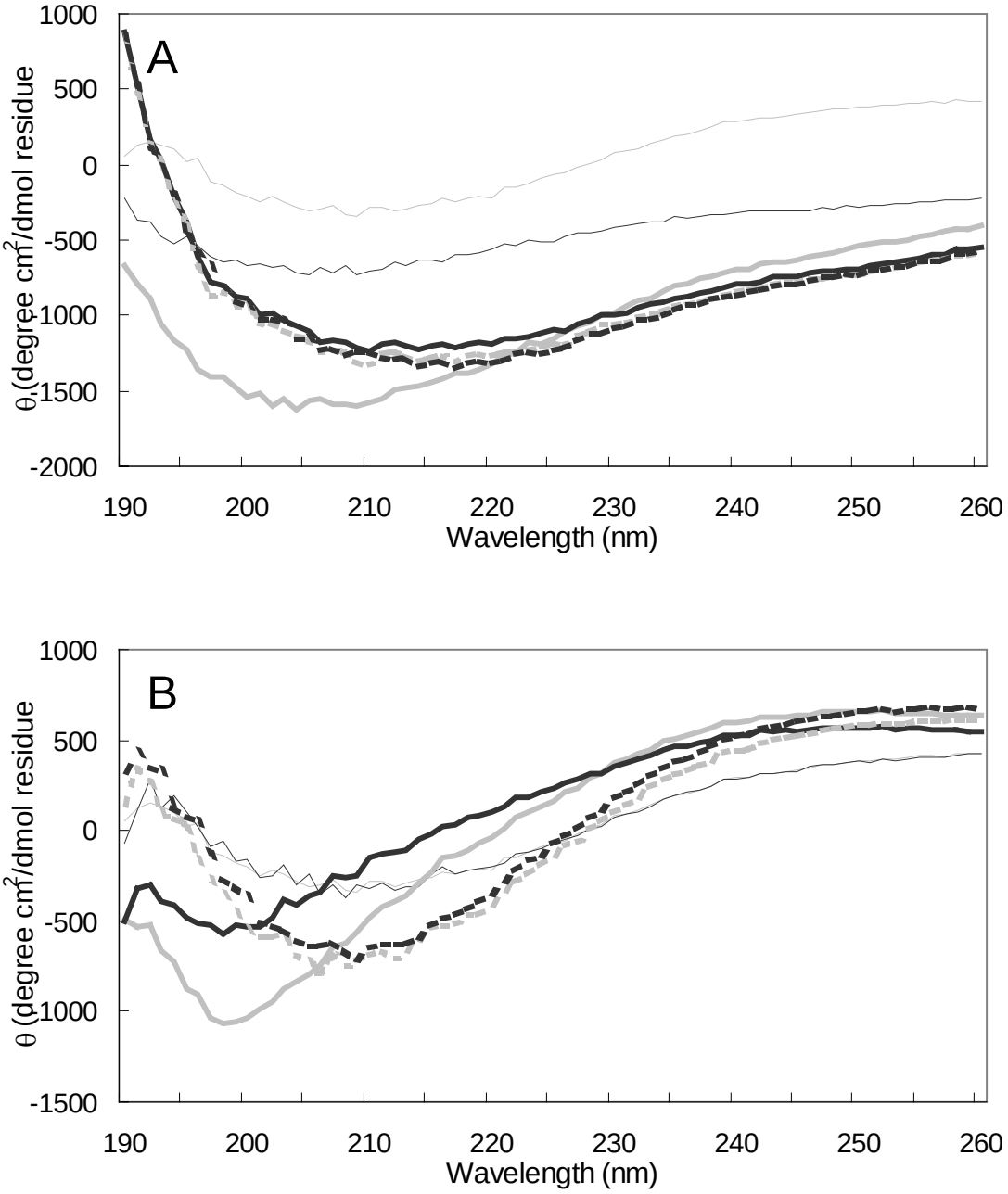

Figure 3. 4. Conformational changes in Aβ aggregation with time. 100μM Aβ at 37°C in the (A) presence, and (B) absence of mixing [light thin solid line- fresh Aβ; dark thin solid line- 2 hours; light thick solid line- 4 hours; dark thick solid line- 8 hours; light thick broken line- 10 hours; dark thick broken line- 12 hours]

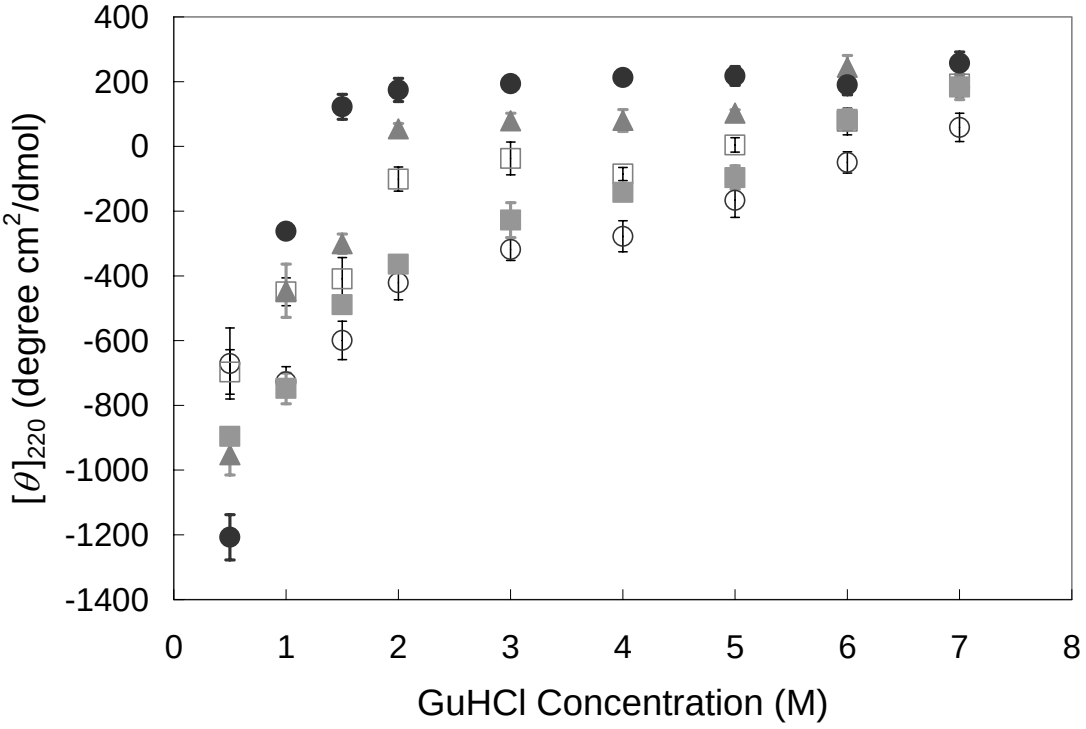

Figure 3. 5. Aβ stability with guanidine hydrochloride (GuHCl). Aβ samples were mixed with GuHCl to final concentration of 10μM Aβ and 0.5 - 7M GuHCl. Aβ samples in GuHCl were incubated for 2 hours at 37^{o}C until it reached equilibrium. CD intensities at 220nm were used for Aβ stability tests. [open circles - Fresh Aβ; open squares – mixed Aβ for 24 hours; closed triangles – non mixed Aβ for 4 hours; closed circles – non mixed Aβ for 8 hours; closed squares - non mixed Aβ for 72 hours]

Biological Activities of Aβ Species

Aβ is known to be toxic to neuron-like cells when aggregated, however it is not clear if fibrils or aggregation intermediates formed by different pathways have the same toxicity. I therefore examined viability of, differentiated SH-SY5Y cells were treated with Aβ samples prepared with or without mixing using a relatively fast viability assay (2 hour incubation with Aβ) in order to minimize structural and morphological changes of Aβ during incubation with cells.

Two markers were used for viability, annexin-V-PE which binds to phophatidyl serine on the surface of early apoptotic cells and 7-AAD which binds to membrane permeable (late apoptotic or nectrotic) cells. Viable cells were taken as those that were both annexin-PE and 7-AAD negative. A positive and negative controls were used to determine assay sensitivity over the short incubation time, with viable cells 23% ± 1% and 54% ± 3% of total cells in the positive and negative control samples, respectively. Relative cell viabilities were calculated by using the equation described in the methods. Relative cell viabilities of cells treated with Aβ samples aggregated under different conditions are shown in Figure 3. 6. Cells treated with fresh Aβ had almost the same cell viability (102% ± 9%) as negative control population ($p>0.05$). Aβ species prepared at different times of aggregation with mixing were significantly more toxic than controls ($p<0.05$), and toxicity increased with time of aggregation of the peptide. When Aβ was aggregated without mixing, a different pattern of toxicity with time of aggregation was observed. The toxicity of species formed within the first 8 hours of aggregation without mixing increased to a maximum observed toxicity at 8 hours. Species formed after 24 or

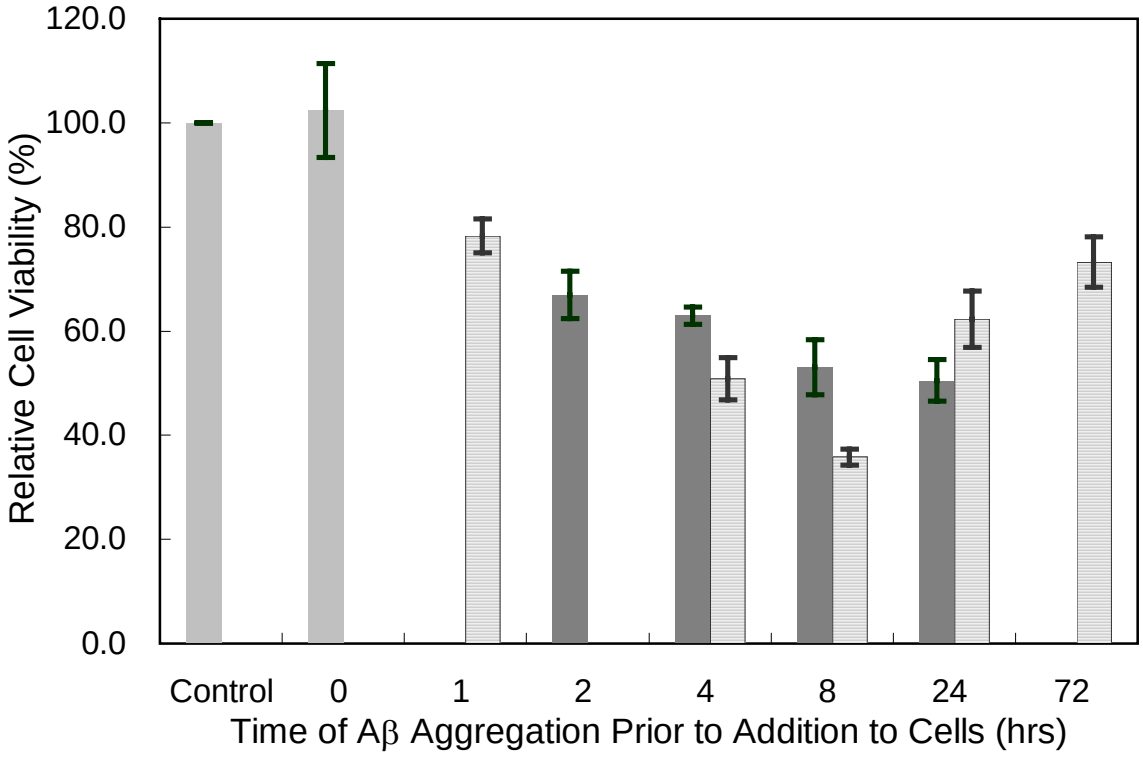

Figure 3. 6. Relative cell viability of differentiated SH-SY5Y cells. SH-SY5Y cells were treated with 100μM Aβ samples with time; [dark solid bar- mixing condition; stripe bar- non-mixing condition; light solid bar- negative control and fresh Aβ]

more hours of aggregation, however, had significantly less toxicity than those formed at earlier times. In addition, the toxicity of fibrils formed with mixing (24 hours) was significantly greater than fibrils formed without mixing (72 hours) ($p<0.05$).

DISCUSSION

In the effort to develop new methods of preventing toxicity associated with Aβ of Alzheimer's disease, many investigators have sought to elucidate both the mechanism of Aβ aggregation (Lomakin et al. 1997; Esler et al. 2000; Pallitto and Murphy 2001) and the relationship between Aβ structure and toxicity. (Lambert et al. 1998; Walsh et al. 1999; Ward et al. 2000; Klein et al. 2001; Walsh et al. 2002; Chromy et al. 2003; Hoshi et al. 2003) In this work, I show that when Aβ is aggregated under different conditions, different mechanisms of aggregation appear to occur, and structures formed during aggregation, that appear to have similar morphology, have different toxicities.

As seen in Figure 3. 1, kinetics of Aβ aggregation, regardless of the presence or absence of mixing, appears similar. The characteristic lag in development of extended β-sheet structure to which Congo red binds is typical of a nucleation mechanism of aggregation that a number of investigators propose for Aβ fibril formation. (Lomakin et al. 1997; Tseng et al. 1999; Esler et al. 2000; Serio et al. 2000; Pallitto and Murphy 2001) However, data obtained from size exclusion chromatography, CD spectroscopy and electron microscopy (Figures 3. 2 – 3. 4) suggests that there are significant differences in the mechanism of aggregation with and without mixing of Aβ.

SEC chromatograms indicate that throughout aggregation under conditions with or

without mixing, species that elute at volumes consistent with monomer and dimer species were in equilibrium as the ratio of peak areas for both species was constant in all chromatograms. Others have made similar observations of Aβ aggregation. (Pallitto and Murphy 2001) The relative amounts of monomer and dimer decreased with time, corresponding to increases in fibril formation as indicated by Congo red binding. (Table 3. 1) Different investigators have suggested that monomer or dimer are the building blocks for fibril nucleation or growth. (Garzon-Rodriguez et al. 1997; Roher et al. 2000; Hwang et al. 2004)

In the solvent used in our studies, Aβ was initially in a largely β-sheet conformation. CD data suggest that Aβ did not undergo significant structural rearrangements when aggregated with mixing, however, when aggregated without mixing, a dramatic shift in structure was observed at intermediate times (approximately 4-8 hours after aggregation is initiated), which corresponds to the presence of a intermediate sized species in chromatograms (approximate molecular weight as estimated from elution volume on SEC of 53kDa) and large globular species in electron micrographs. None of these intermediate species were observed when aggregation proceeded with mixing.

A number of investigators have observed Aβ aggregation intermediates, formed either at low temperature or via a particular preparation method, sometimes referred to as Aβ derived diffusible ligands (ADDLs) (Lambert et al. 1998; Klein et al. 2001) that have molecular weights within the range I observed via SEC. A number of reports indicate that these ADDLs are the (or one of the) toxic Aβ oligomers. (Lambert et al.

1998) Others have described spherical species of various sizes (Harper et al. 1999; Westlind-Danielsson and Arnerup 2001; Hoshi et al. 2003) that are Aβ aggregation intermediates with sizes ranging from 3 to 20 nm, and some up to 100 nm depending on starting peptide and preparation method. (Lambert et al. 1998; Harper et al. 1999; Klein et al. 2001; Westlind-Danielsson and Arnerup 2001; Hoshi et al. 2003) Toxicity of the spherical Aβ species has also been reported. (Hoshi et al. 2003) The approximate 53kDa species observed via SEC may be distinct from the spherical species observed via electron microscopy, however, it is not possible to tell from our data. Others have observed the formation of Aβ micelles (Soreghan et al. 1994; Lomakin et al. 1996; Yong et al. 2002; Kim and Lee 2004), which might appear as a large globular species via EM, but would certainly change apparent molecular size during chromatography. Alternately, it is probably that via SEC I would not be able to detect a globular protein aggregate of 20 nm diameter as it would be removed from our sample during our pretreatment, nor would I be able to detect 53kDa proteins via EM as they would be below the resolution of the microscope used.

That I observe dramatic structural rearrangements with aggregation when mixing was not used, but did not observe the same structural rearrangements when aggregation occurred with mixing is not surprising. If Aβ aggregation is nucleation dependent as others propose (Lomakin et al. 1997; Serio et al. 2000), then with mixing, one would expect more rapid collisions of molecules are faster nucleation. The faster rate of nucleation would mean that Aβ would have less time to undergo any intramolecular structural rearrangements that might be energetically favorable and increase stability of

the fibril formed. Without mixing, the rate of peptide collision with other peptides would be slower, allowing more time for intramolecular rearrangement of the peptide before combining with other peptides to form an aggregation intermediate. In short, mixing would favor intermolecular rearrangements to bury hydrophobic surfaces which would lead to aggregation, while static (or non-mixed) conditions would favor intramolecular rearrangements to bury hydrophobic surfaces. These intramolecular rearrangements could lead to formation of aggregation intermediates not seen when intermolecular interactions predominate.

Based on the results presented, I propose the mechanism for Aβ aggregation with and without mixing depicted in Figure 3. 7. Initially, a mixture of Aβ monomer and dimer are present, in predominantly β-sheet form. As demonstrated by others, the solvent used to initially dissolve Aβ would certainly affect this initial peptide conformation. (Barrow and Zagorski 1991; Barrow et al. 1992; Snyder et al. 1994; Shen and Murphy 1995; Fezoui and Teplow 2002; Kawooya et al. 2003; Stine et al. 2003) With mixing, either monomer or dimer combine, without structural rearrangement, to form nucleating species, from which fibrils grow. Under static conditions where no mixing is present, small Aβ species, possibly monomer as suggested by others (Pallitto and Murphy 2001), undergo a structural rearrangement, forming a larger oligomeric species or possibly micelles. It is from this larger oligomeric species or micelle that fibrils are initiated. There is some support for the role of Aβ micelles in fibril formation. (Soreghan et al. 1994; Lomakin et al. 1996; Yong et al. 2002; Kim and Lee 2004) Aβ critical micelle concentration is reported to be 100μM (Yong et al. 2002), the

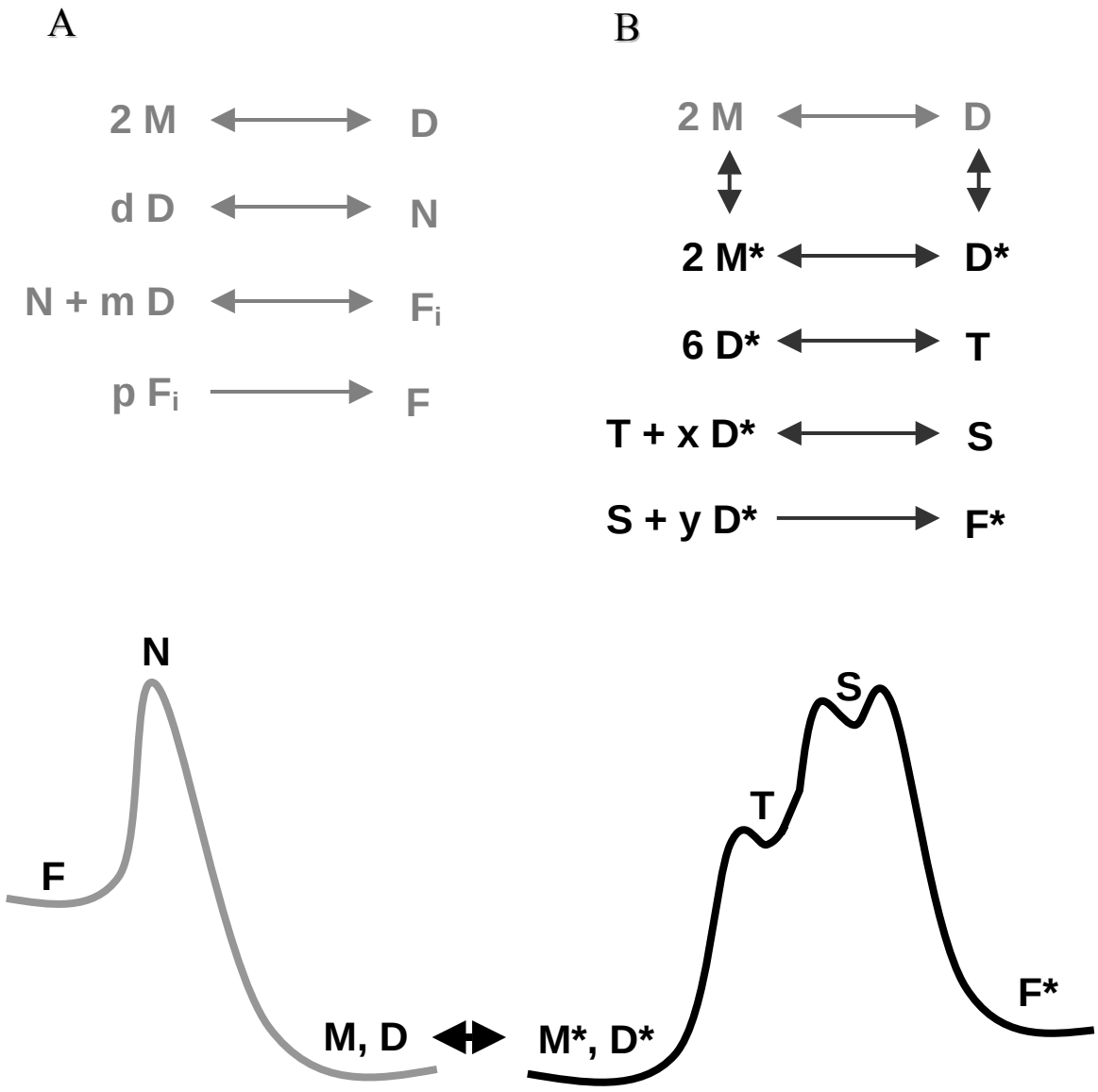

Figure 3. 7. Schematic mechanism and energy barrier of Aβ aggregation. (A) in mixing condition and (B) in non-mixing condition.

concentration used in studies reported here. When analogous experiments were performed of Aβ aggregation without mixing at lower concentrations of Aβ (20μM and 50μM), the same intermediate species were not observed via either SEC or EM. (data not shown)

The relative stability of species formed during aggregation in the presence and absence of mixing can be inferred from data collected on conformation change of Aβ in a denaturant (Figure 3. 5). When Aβ was aggregated with mixing, fibrils underwent conformation change in denaturant more readily than monomer, suggesting that a less stable or higher energy species was formed. When Aβ was aggregated without mixing, aggregation intermediates underwent conformation change more easily than either fresh or fibril Aβ suggesting the intermediate was least stable or had the highest energy. This interpretation is reflected in the mechanism of aggregation presented in Figure 3. 7. However, given that changes in free energy associated with unfolding (Pace 1990) or conformation change were not calculated given the difficulties in defining an equilibrium model for Aβ aggregation or unfolding, the interpretation of the stability data is only qualitative.

I examined biological activity or toxicity of fibrils and aggregation intermediates formed with mixing and without mixing (Figure 3. 6). Fibril toxicity was greater when formed with mixing, while toxicity of aggregation intermediates formed between 4 and 8 hours after initiation of aggregation without mixing were more toxic than other species formed. Fibrils formed with mixing and aggregation intermediates formed without mixing changed structure more readily in denaturant than other species examined

(Figure 3. 5). It is tempting to claim that the difference in stability in denaturants correlates with toxicity. A number of investigators have suggested that Aβ membrane interactions via Aβ conformational changes are important in the mechanism of Aβ toxicity. (McLaurin and Chakrabartty 1997; Terzi et al. 1997; Ege and Lee 2004) Behavior of Aβ in a membrane and in a denaturant might be analogous. Thus, one could speculate that toxicity of an Aβ species may be related to its ability to change structure within the cell membrane.

There are several alternative explanations of the data presented. Others have reported that Aβ oligomers with structures similar to those I describe forming during aggregation without mixing are more toxic than fibrils. (Hoshi et al. 2003) When comparing toxicity of fibrils formed via different methods, it has been very difficult to characterize concentration or number of fibrils in a solution. Others have shown that the average length of fibrils changes with aggregation condition (Walsh et al. 1999; Ward et al. 2000), so number of fibrils might also change. With mixing, one would expect larger numbers of smaller fibrils than would be formed without mixing. Thus differences in toxicity observed may simply be due to differences in oligomer or fibril concentrations in solution

In summary, I report structure and toxicity of Aβ species formed during aggregation via different methods. I show that fibrils formed via different methods, while structurally similar, do not have the same toxicity or the same apparent stability to denaturants. Aggregation intermediates which are similar to Aβ oligomer species reported by others such as ADDLs, were of comparable toxicity and stability to

denaturants as fibrils formed during mixing. This work contributes to the understanding of the relationship between Aβ structure, stability and toxicity.

CHAPTER IV

THE STABILITY OF Aβ SPECIES IN UREA AND CORRELATION WITH Aβ TOXICITY

OVERVIEW

β-Amyloid (Aβ) is a main protein component of senile plaques in Alzheimer's disease. Aβ aggregation is important in Aβ toxicity. Recently I found that Aβ aggregated via different pathways when incubated under different environmental conditions of mixing and non-mixing. Aggregation under the different environmental conditions resulted in different aggregation intermediates, and aggregates with different morphologies, and biological activity. In the current work, I use urea unfolding of the Aβ aggregation species to estimate the stability of different Aβ oligomers and the role of accessible hydrophobic surface in biological activity. I find a significant correlation between toxicity of the aggregated species and the change in Gibbs free energy of unfolding in water, and the parameter "m" which relates the free energy change upon unfolding with change in urea concentration and is taken as a measure of change in accessible hydrophobic surface when the protein goes from water to detergent. The Aβ sample that was most toxic had the greatest Gibbs free energy of unfolding and m values of all peptide samples tested, 3658.07 ± 228.48 cal/mol and 846.01 ± 55.17 cal/mol M, respectively. These results suggest that Aβ stability in detergent, or possibly membrane environments, may be key in determining Aβ biological activity. This work

contributes to our understanding of the relationship between Aβ structure and other biophysical properties and Aβ toxicity and may help guide our understanding of the mechanism of toxicity of Aβ.

INTRODUCTION

Proteins are susceptible to environmental changes such as temperature, pH, pressure, and denaturants. (Creighton 1993) Protein stability is very important for therapeutic proteins and industrial enzymes, as well as in other protein applications. (Fersht et al. 1992; Creighton 1993) Protein stability has also been linked to the ability of a number of disease associated proteins to form amyloid fibrils (Hammarstrom et al. 2001; Dahlgren et al. 2002; Foguel et al. 2003). Much research has been performed over the past two decades to develop a framework in which to study protein stability (Pace 1990).

The classic approach to examining protein stability is to assume that there are two equilibrium states for a protein, a native and an unfolded state, and by measuring what fraction of a protein population is in either state, the equilibrium constant and the change in Gibbs free energy for unfolding can be estimated. (Pace and Shaw 2000) ΔG_{H2O} and m in the free energy difference equation ($\Delta G = \Delta G_{H2O} - m\,[Urea]$) can be used to describe protein stability; ΔG_{H2O} is a measure of the conformational stability of the protein without denaturant and m denotes the difference in accessible hydrophobic surface area between native and unfolded states. (Tanford 1970; Myers et al. 1995; Spudich and Marqusee 2000)

Many diseases are related to protein unfolding and aggregation such as Huntington's disease which is associated with polyglutamine aggregation, and Parkinson's disease which is associated with α-synuclein aggregation. (Ross and Poirier 2004) One of the diseases in this category is Alzheimer's disease (AD), a neurodegenerative disease of central nervous system that is associated with the aggregation and accumulation of β-amyloid (Aβ). One of the hypotheses in AD pathology is that AD is caused by the toxicity of Aβ aggregates, especially Aβ soluble oligomeric species. Aβ is the main protein component of senile plaques in AD. Several studies show that Aβ forms fibrils via conformational transition from α-helix/random coil to β-sheet.(Walsh et al. 1997; Walsh et al. 1999) Aβ conformation depends on environmental factors such as solvents, pH, temperature, and ionic strength. (Stine et al. 2003). Recent research indicates that Aβ conformational change can be induced by membrane mimicking lipid vesicles. (McLaurin and Chakrabartty 1997; Terzi et al. 1997) Acidic phospholipids such as phosphatidylinositol induce an Aβ conformational change from random coil to β-sheet efficiently at low lipid to protein ratios. (Terzi et al. 1995; McLaurin and Chakrabartty 1997) At higher lipid to protein ratios, the Aβ conformational transition is observed from β-sheet to α-helix. (Terzi et al. 1997) These data suggest that Aβ conformational changes are strongly related to its interaction with lipid membranes. Other work suggests Aβ toxicity is also related to its interaction with lipid membranes. Cellular responses to Aβ that have been postulated to result in toxicity encompass destabilization of calcium homeostasis, membrane depolarization, increased vulnerability to excitotoxins, increased membrane permeability due to free radical

generation, blockage or functional loss of potassium channels, and direct disruption of membrane integrity (Busciglio et al., 1993, Koh et al., 1990, Arispe et al., 1993, Behl et al., 1994, Butterfield et al., 1994, Butterfield, 1997, Good et al., 1996, Hensley et al., 1994, Mattson et al., 1997, McLaurin et al., 1998, Pike et al., 1993, Simmons and Schneider, 1993). Changing membrane properties by altering the electrostatic potential of the membrane was shown to inhibit Aβ neurotoxicity. (Hertel et al. 1997).

In this research, Aβ conformational change and Aβ stability in urea was monitored by circular dichroism (CD) at 220nm. The free energy difference between native and unfolded states of Aβ was calculated by linear regression. In urea Aβ conformation changes from β-sheet to random coil.(Kawooya et al. 2003; Stine et al. 2003) These differences in structure were used to estimate equilibrium constants and free energies of unfolding or structure change as a function of urea concentration. Structures of Aβ that had the lowest free energy of structure change and smallest change in energy in detergent, fresh Aβ and Aβ fibrils formed without mixing, also had the lowest toxicity. Aβ species with the largest free energy of structure change and largest change in energy in detergent, aggregation intermediates formed without mixing at 4 and 8 hours after the beginning of aggregation, were the most toxic. These data suggest that Aβ structural change, or Aβ stability is very closely related to the biological activity of Aβ. Structural stability in detergent may be related to Aβ changes in structure in lipid environments. This work may provide insights into the mechanism of toxicity of Aβ.

MATERIALS AND METHODS

Materials

β-Amyloid (Aβ)–(1-40) was purchased from AnaSpec (San Jose, CA). Urea was purchased from Sigma-Aldrich Co.. (St. Louis, MO). All other chemicals, unless otherwise specified were obtained from Sigma-Aldrich Co..

Protein Sample Preparation

Aβ1-40 was dissolved in 0.1% (v/v) Trifluoroacetic acid (TFA) solvent at the concentration of 10mg/ml. This solution was incubated at room temperature for 20~30 minutes in order to dissolve Aβ into the solvent efficiently. Filtered phosphate-buffered saline (PBS, 4.3 mM Na_2HPO_4, 137 mM NaCl, 2.7 mM KCl and 1.4 mM KH_2PO_4, pH 7.4) was added to the Aβ solution to make final concentrations of 100μM. For aggregation with mixing, Aβ samples were mixed on the rotator at 18 rpm and 37^{o}C, and samples were taken out with time. For aggregation without mixing, Aβ samples were incubated without disturbance in a 37^{o}C incubator.

Aβ Stability with Urea

100μM Aβ samples were prepared as described in protein sample preparation. Aβ samples at 37^{o}C incubator were taken out in 0 (fresh Aβ), 2, 4, and 24 hours for mixed samples and 4, 8, and 72 hours for non-mixed samples. Urea was dissolved in PBS buffer and prepared in different concentrations. Aβ samples were mixed with urea solution at the ratio of 1:9 (v/v). The final Aβ concentration in each sample was 10μM.

The final urea concentrations varied from 0.5M to 10M with 0.5M intervals. Aβ samples in different urea concentrations were incubated at 37^{o}C for 2 hours such that the protein could come to equilibrium with the urea.

Circular Dichroism (CD)

Secondary structures for Aβ were measured using PiStar-180 Circular Dichroism Spectrometer (Applied Photophysics; Leatherhead, United Kingdom)**.** CD spectrum at 220nm for Aβ were obtained using a 1 cm quartz cell, at 37^{o}C, using a Xe lamp as a light source, a 1.0nm bandwidth, 1.0nm step interval. The spectrometer was purged with nitrogen gas during measurement. PBS buffer was used for the calibration.

Free Energy Differences with Equilibrium Constant or Urea Concentraion

The free energy for the Aβ stability in urea can be obtained by the assumption that Aβ is in equilibrium of two states, folded or native state (N) and completely unfolded state (U) with no partially unfolded intermediates.

$$N \leftrightarrow U \tag{4-1}$$

Based upon the equilibrium of two states, the fraction of unfolded state can be calculated by

$$f_U = \frac{y_N - y_{obs}}{y_N - y_U} \tag{4-2}$$

where f_U is the fraction of unfolded state, y_{obs} is the observed variable, and y_N, and y_U are linear characteristics of native and unfolded states. The equilibrium constant for two transition states can be expressed by the fraction of unfolded protein and the

characteristics of native and unfolded states

$$K = \frac{[U]}{[N]} = \frac{f_U}{1 - f_U} = \frac{y_N - y_{obs}}{y_{obs} - y_u} \quad (4\text{-}3)$$

where K is the equilibrium constant between N and U, [U] and [N] are the concentrations of unfolded and native states. The free energy difference, ΔG, between native and unfolded states can be obtained by thermodynamic relationship between Gibbs free energy and the equilibrium constant.

$$\Delta G = - R T \ln K = - R T \ln \frac{y_N - y_{obs}}{y_{obs} - y_u} \quad (4\text{-}4)$$

where ΔG is the free energy difference between unfolded and native states, R is the gas constant and T is the absolute temperature. The free energy difference can be determined experimentally as a function of denaturant concentration. The denaturant concentration is generally in linear relationship with the free energy difference.

$$\Delta G = \Delta G_{H2O} - m[\text{Urea}] \quad (4\text{-}5)$$

where [Urea] is the concentration of urea, m is the slope of this equation, and ΔG_{H2O} is the free energy difference in the environment without urea. (the symbol of slope m has been given by Greene and Pace. (Greene and Pace, 1974)

Linear Regression of Aβ Denaturation with Urea and Data Fitting for ΔG_{H2O} and m

Experimental data of CD intensities of Aβ with urea were used for data fitting of ΔG_{H20} and m in equation (4-5). Prior to this calculation, ΔG values were obtained from equation (4-4). y_N and y_U were calculated by linear regression of native and unfolding states respectively. Data of 0.5M-2.5M and 0.5M-2.0M urea concentration were taken as raw data for y_N linear regression for mixed Aβ, and non-mixed Aβ samples

respectively. Data of 6.5M - 10.0M urea were used for y_U linear regression. ΔG_{H20} and m in equation (4-5) were estimated from a linear regression of ΔG with urea concentration. ΔG_{H20} was obtained by extrapolation at zero denaturant concentration.

Statistical Analysis

For each experiment, at least 3 independent determinations were made. Significance of results was determined via the student t test with $p<0.05$ (95% confidence interval) unless otherwise indicated. Data are plotted as the mean plus or minus the standard error of the measurement.

RESULTS

Secondary Structures of Aβ in Buffer or in Urea Solution

Fresh Aβ in PBS buffer and 10M urea solution were incubated at 37^{o}C for 2 hours. The structure of Aβ samples was assessed by measuring CD in the range of 190nm and 260nm. In Fig. 4. 1, fresh Aβ in PBS buffer (solid line) had a minimum CD intensity around 210nm, corresponding to β-sheet structure in the peptide, along with a spectral features between 200 to 220nm, corresponding to α-helix structure in the peptide. The CD spectrum of Aβ in 10M urea had blue shift relative to the spectrum of Aβ sample in buffer, with a minimum intensity around 200nm. The CD spectrum suggests that the dominant structure of Aβ samples in 10 M urea is random coil. The large difference in spectral characteristics between native Aβ and Aβ treated with urea (unfolded Aβ) in the region of 220 nm was used to characterize stability of Aβ to unfolding in urea.

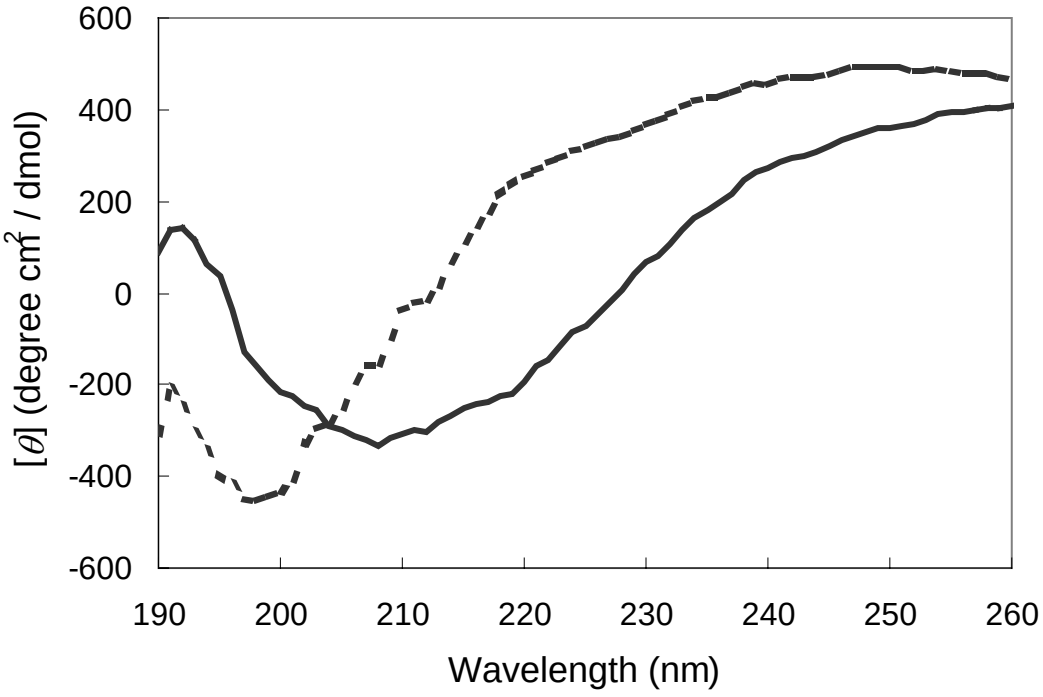

Figure 4. 1. Secondary structures of Aβ in buffer or urea solution. 100μM of fresh Aβ was mixed with buffer or urea solution to be final concentration of 10μM Aβ and 10M urea. Aβ samples were incubated at 37°C for 2 hours. Aβ samples in buffer (solid line) and in urea (broken line) were scanned by CD from 190nm to 260nm.

Aβ Stabilities with Urea in Different Incubation Conditions

Aβ aggregation depends on the environmental conditions such as temperature, pH, concentration, and ionic strength. Recently I found that different Aβ incubation condition affected the rate of fibril formation and intermediate Aβ species. Aβ formed fibrils in 24 hours when it was mixed. However fibrils formed more slowly, and unique aggregation intermediates were observed when Aβ was aggregated without mixing. Conformational stabilities of these Aβ species were estimated using urea unfolding.

MIXED Aβ STABILITIES WITH UREA

100μM Aβ was aggregataed as described in a previous chapter. The CD intensities at 220 nm of Aβ samples in urea were measured. As shown in Fig. 4. 2A, CD intensities decreased as urea concentration increased at low concentrations; from 0.5M to 2.5M urea. In 2.5M – 6M urea, CD intensities increased with urea concentration. All samples had a maximum CD intensity in around 6.5M urea. CD intensity reduced again with urea from 6.5M to 10M. The region from 0.5 M to 2.5 M urea was taken as the folded state of the peptide, while the region from 6.5M to 10 M urea was taken as the unfolded state. At concentrations of urea between 2.5 M and 6.5M, equilibrium constants and ΔG of unfolding were estimated. In this region, fresh Aβ structure changed at higher concentrations of urea than did any of the aggregated Aβ structures.

Linear regressions in the folded and unfolded regions were performed to estimate y_N and y_U. The regression results were displayed in Table 4. 1. At lower concentration between 0.5M and 2.5M, all mixed Aβ samples had similar slopes in y_N from –5.43 to –

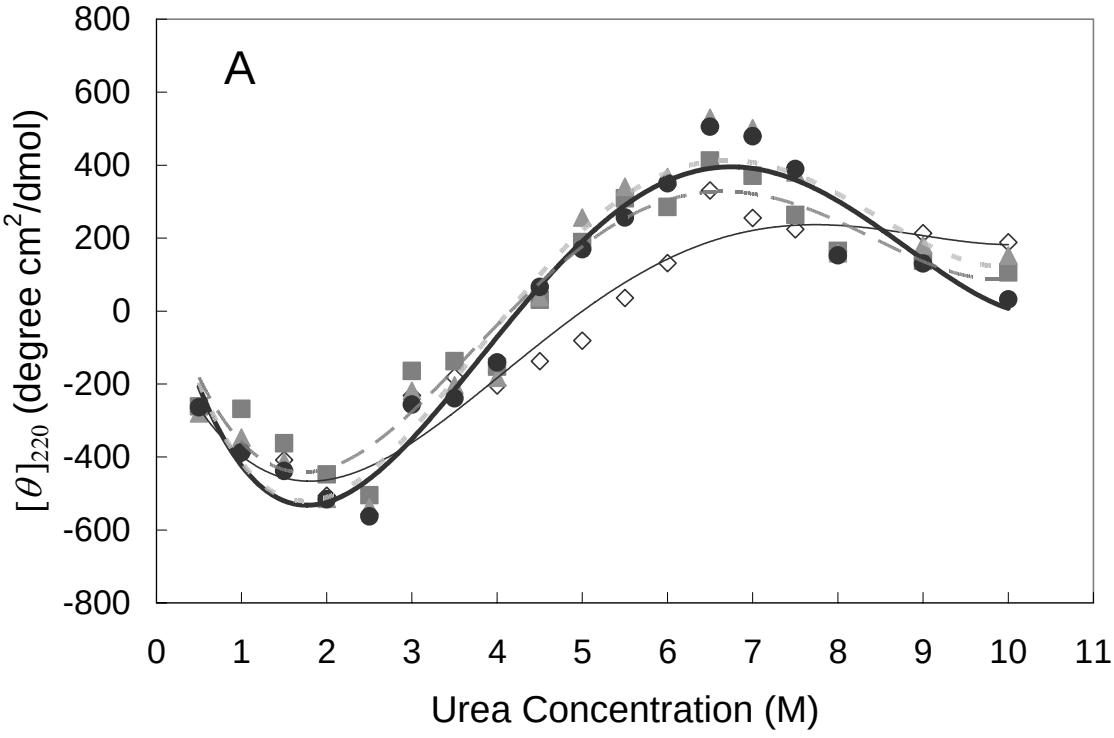

Figure 4. 2. Representative Aβ stabilities with urea concentrations. Aβ samples were mixed with urea to final concentration of 10μM Aβ and 0.5 - 10M urea with 0.5M intervals. Aβ samples in urea were incubated for 2 hours at 37^{o}C until it reached equilibrium. CD intensities at 220nm were used for Aβ stability tests. (A) Mixed Aβ stability with urea [open diamonds – fresh Aβ, closed squares – 2 hours, closed triangles – 4hours, closed circles – 24 hours; All lines are regressions for experimental data, thin solid line – fresh Aβ, dark large broken line – 2 hours, light small broken line – 4 hours, thick solid line – 24 hours]

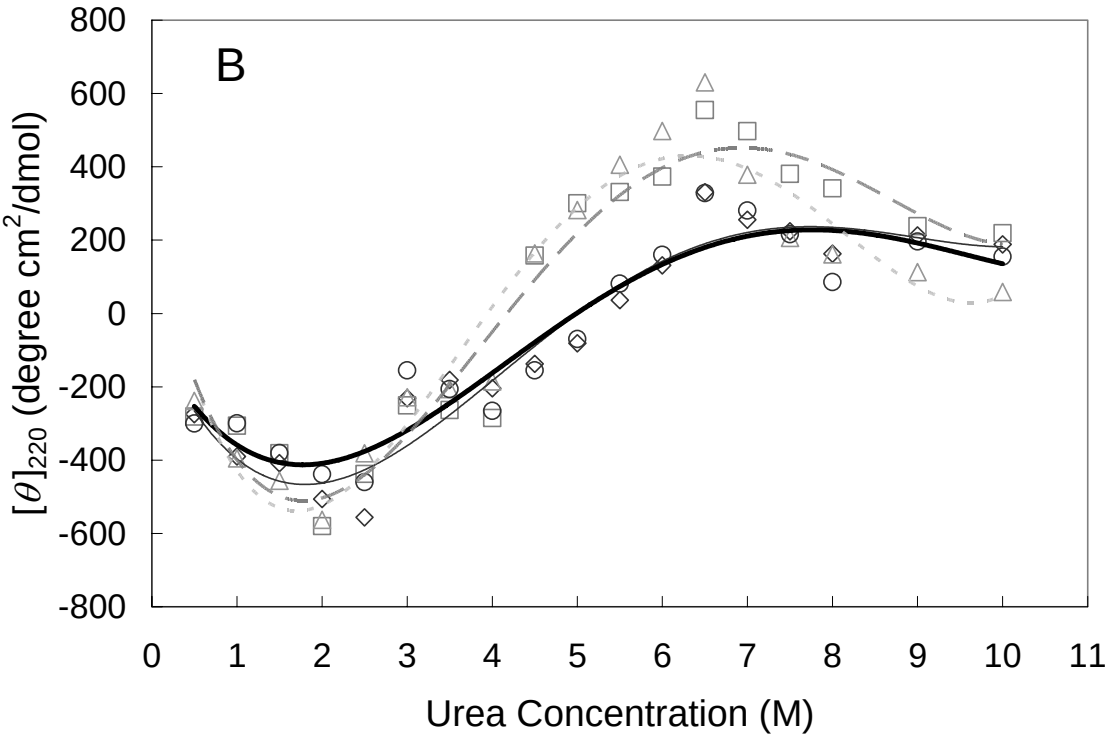

Figure 4. 2 Continued. (B) Non-mixed Aβ stability with urea [open diamonds – fresh Aβ, open squares – 4 hours, open triangles – 4hours, open circles – 24 hours; All lines are regressions for experimental data, thin solid line – fresh Aβ, dark large broken line – 4 hours, light small broken line – 8 hours, thick solid line – 72 hours]

5.81 and intercepts from –6.01 to –8.94. However the slopes and intercepts in y_U had more variation from –1.28 to –5.82 in slope and from 19.44 to 57.83. The 24-hour sample had the steepest y_U (y_U = -5.82 [urea] + 57.83) and fresh Aβ had the gentlest one (y_U = -1.28 [urea] + 19.44).

NON-MIXED Aβ STABILITIES WITH UREA

As seen in Fig. 4. 2B, Aβ samples prepared during aggregation without mixing displayed similar behavior in CD spectra exposed to urea as did Aβ samples prepared during aggregation with mixing. In the region associated with the change in structure from folded to unfolded state, both fresh and 72 hour aggregated fibril Aβ changed concentration at higher concentrations of urea than the aggregation intermediates formed without mixing. Given the variability of the CD measurements, it was not possible to discern if only two structure states were present in the Aβ samples in urea (native and unfolded) or if other folding intermediates were formed. Thus, the simplest two state model was used to estimate ΔG of unfolding in urea for the aggregated Aβ samples.

Free Energy Difference Calculation of Aβ Stabilities with Urea

Free energy differences were calculated by the assumption of two folding states - native and unfolded states were in equilibrium. Equilibrium was assumed because the analysis was performed several times, with different incubation times from 30 minutes to 2 hours allowed for unfolding in urea, all yielding similar unfolding curves. Equilibrium constants were estimated from concentration ratios of two folding states. The Free

Table 4. 1. Linear regression of native and unfolding Aβ with urea concentration

Mixed Aβ	y_N*	y_U**
0 hr –Fresh Aβ	y_N = -135.83 [Urea]** - 223.38	y_U = -32.115 [Urea] + 486.00
2hrs	y = -133.19 [Urea] - 169.25	y = -90.895 [Urea] + 969.65
4hrs	y = -136.49 [Urea] - 213.73	y = -117.75 [Urea] + 1259.3
24hrs	y = -145.37 [Urea] - 215.58	y = -145.55 [Urea] + 1445.8
Non-Mixed Aβ	y_N	y_U
4hrs	y = -194.4 [Urea] - 144.25	y = -99.306 [Urea] + 1166.4
8hrs	y = -206.95 [Urea] - 154.50	y = -140.94 [Urea] + 1385.6
72hrs	y = -99.35 [Urea] - 230.50	y = -44.206 [Urea] + 564.15

* y_N : Linear regression of native Aβ with urea. CD signals of Aβ in 0.5M-2.5M urea were taken for mixed Aβ and non-mixed 72-hour samples and those in 0.5M - 2.0M urea were taken for non-mixed 4- and 8-hour samples.

** y_U : Linear regression of unfolding Aβ with urea. CD signals of Aβ in 6.5M - 10.0M urea were used for this regression.

*** [Urea] : Urea concentrations in M

energy difference between two states was obtained from equation 4-4, and ΔG_{H2O} and m were calculated by linear regression of the data to equation 4-5.

FREE ENERGY DIFFERENCES OF MIXED Aβ

Free energy for unfolding was estimated as a function of urea concentration for aggregated Aβ samples prepared with mixing (Fig. 4. 3A). The slope of ΔG for unfolding of fresh Aβ as a function of urea was less than that for any of the aggregated Aβ samples. The slope m, and intercept ΔG_{H2O} of the equation, $\Delta G = \Delta G_{H2O} - m$ [Urea], are summarized in Table 4. 2. ΔG_{H2O} values were the intercept of free energy equation and obtained by extrapolation. A total of 3 experiments were performed independently for reproducibility and statistical analysis. Results are plotted in Fig. 4. 4. In Fig. 4. 4, slope m value of fresh Aβ was 470.19 ± 20.26 cal/mol M, whereas m values of other mixed samples were between 604.96 ± 26.94 cal/mol M (24-hour sample) and 642.26 ± 42.17 cal/mol M (4-hour sample). Two-tailed T-test showed that m value of fresh Aβ was statistically different from those of other samples. ($p = 0.0033$, 0.0032, and $0.0023 < 0.05$; with 2-, 4- and 24-hour samples respectively) m values between 2-, 4-, and 24-hour samples were not statistically different. ΔG_{H2O} values between the mixed samples were not statistically different.

FREE ENERGY DIFFERENCES OF MIXED Aβ

As shown in Fig. 4. 3B, slope m and intercept ΔG_{H2O} for the fresh Aβ and 72-hour sample were almost same, suggesting that the conformational stability of the two

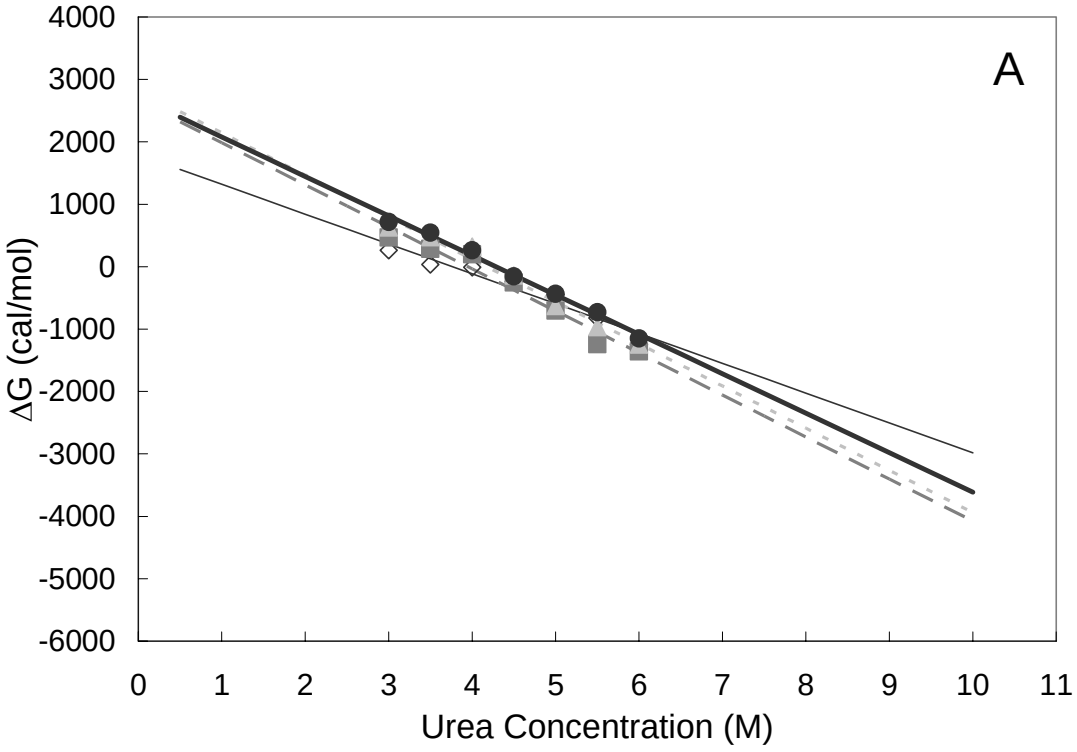

Figure 4. 3. Representative ΔG plot as a function of urea concentration. ΔG values were obtained by experimental data from Figure 4. 1 and linear regressions were done to predict the extrapolation. See the results in detail. (A) Mixed Aβ stability with urea [open diamonds – fresh Aβ, closed squares – 2 hours, closed triangles – 4hours, closed circles – 24 hours; All lines are regressions for experimental data, thin solid line – fresh Aβ, dark large broken line – 2 hours, light small broken line – 4 hours, thick solid line – 24 hours]

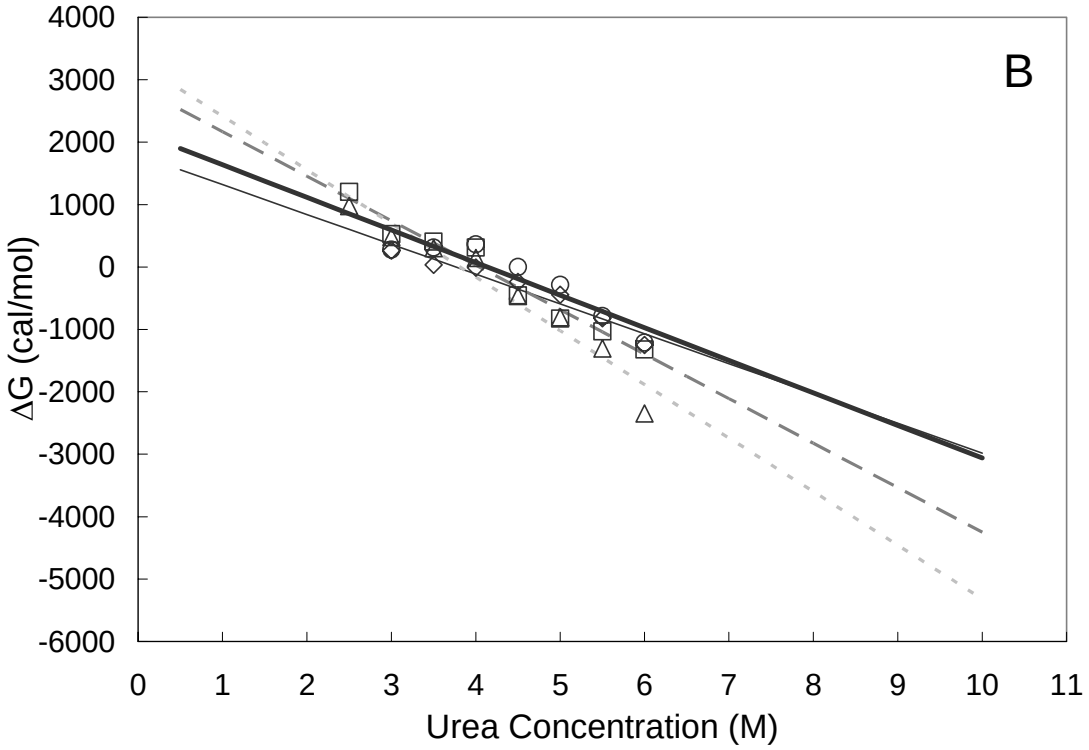

Figure 4. 3 Continued. (B) Non-mixed Aβ stability with urea [open diamonds – fresh Aβ, open squares – 4 hours, open triangles – 4hours, open circles – 24 hours; All lines are regressions for experimental data, thin solid line – fresh Aβ, dark large broken line – 4 hours, light small broken line – 8 hours, thick solid line – 72 hours]

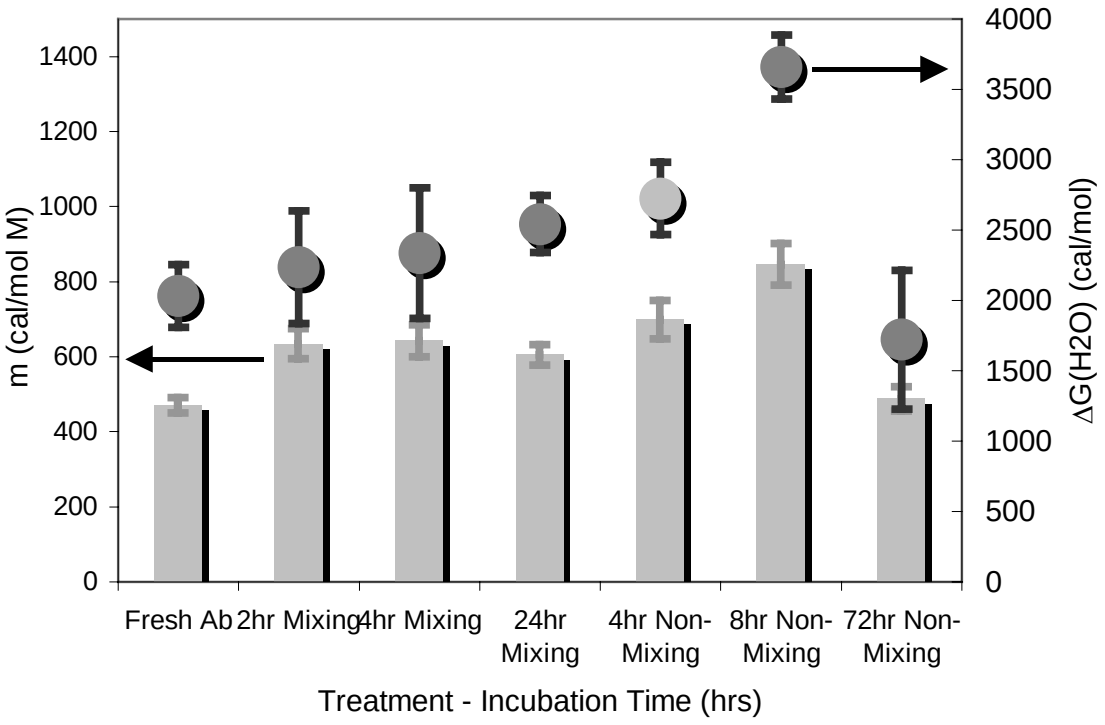

Figure 4. 4. Average and standard deviation plot for m and ΔG_{H2O}. Three independent experiments were done to get average and standard deviation of m (bar plot) and ΔG_{H2O} (scatter plot composed of circles).

Table 4. 2. Representative slope m, and intercept ΔG_{H2O} in the equation of $\Delta G = \Delta G_{H2O} - m$ [Urea]

Mixed Aβ	m (cal/mol M)	ΔG_{H2O} (cal/mol)
0 hr –Fresh Aβ	477.72	1796.3
2hrs	673.33	2656.9
4hrs	675.77	2818.3
24hrs	632.00	2708.5
Non-Mixed Aβ	m (cal/mol M)	ΔG_{H2O} (cal/mol)
4hrs	712.77	2880.0
8hrs	859.36	3725.0
72hrs	521.91	2158.6

This table was obtained by the linear regression of the data from Figure 4. 1.

samples in urea were similar. For aggregated Aβ samples prepared without mixing and collected 4 and 8 hours after the beginning of aggregation, the slope of the free energy curve with urea concentration was steepest. (Figure 4. 3B, Figure 4. 4) A two-tailed T-test showed that the m value of fresh Aβ (470.19 ± 20.26 cal/mol M) was not statistically different from that of the 72 hour-sample (487.35 ± 31.89 cal/mol M) ($p = 0.48 > 0.05$). The 8-hour sample was statistically different from that of 4-hour sample, and 4- and 8-hour samples were different from fresh and 72-hour samples in m and ΔG_{H2O} values.

In summary, ΔG_{H2O} and m values for the 8-hour non-mixed sample were statistically different from those of all other mixed samples. Mixed Aβ samples at 2, 4, and 24 hours were not different from each other. Fresh Aβ was not different from the 72-hour non-mixed sample, but was different from the other samples.

DISCUSSION

Proteins are very sensitive to their environmental conditions such as temperature, pH, pressure and denaturants. (Creighton 1993) They are in folded and native states when they are in optimum environments. However small environmental changes can cause structural change in proteins, which lead to protein unfolding or denaturation. Proteins in unfolded states lose their physiological activity. Protein aggregation can occur via transition from folded to unfolded or partially unfolded states. (Dobson 2003; Selkoe 2003)

While a number of other researchers in the past have studied unfolding and

stability of proteins associated with amyloid disease in order to understand factors associated with protein stability that lead to amyloidosis or protein aggregation (Hammarstrom et al. 2001; Foguel et al. 2003), in this work, I am interested in stability of Aβ after aggregation and the relationship between Aβ aggregate stability and its biological activity.

Depending on the aggregation state and how Aβ was aggregated, Aβ has different structures. Aβ is known to aggregate to form fibrils via conformational change to a β-sheet rich structure. (Walsh et al. 1997; Walsh et al. 1999) HoIver, other Aβ aggregation states that I have reported in earlier chapters have a mixture of secondary structures including random coil, especially for Aβ aggregation states produces without mixing at intermediate times (i.e. the large spherical species described previously). In urea, Aβ has a predominantly random coil structure. In this research, I use an analysis that typically is used to describe a transition form native to unfolded states. However, in this work, I are measuring a transition from aggregated species and unfolded.

AD is called a conformational disease since Aβ conformational changes are closely related to Aβ aggregation and toxicity. The mechanism by which Aβ aggregates cause toxicity and how Aβ conformational changes are related to cell toxicity is still unclear. Some investigators have suggested that lipid membrane induce Aβ conformational changes and Aβ aggregate - membrane interactions are important in the mechanism of Aβ toxicity. (McLaurin and Chakrabartty 1997; Terzi et al. 1997) Recently I examined the relationship between Aβ aggregation and toxicity using aggregation conditions analogous to those used in this work. Non-mixed Aβ samples formed large spherical

species during aggregation via a different mechanism of aggregation than that which mixed Aβ samples undergo upon aggregation. The biological activity of Aβ aggregated species were as follows: fresh Aβ samples and those aggregated for 72 hours without mixing were non toxic; mixed aggregated samples prepared between 4 and 24 hours after initiation of aggregation resulted in 30-50% cell toxicity; Aβ samples prepared without mixing at 8 hours after initiation of aggregation (large spherical species in electron micrographs) were the most toxic with 74% cell toxicity. In this work, I show that the toxicity of Aβ species is related to conformational change in denaturant and stability of Aβ. ΔG_{H2O} and m were estimated for the different Aβ aggregated species. ΔG_{H2O} represents the conformational stability of the protein without denaturant and m denotes the average change in accessibility of the protein groups upon denaturation. In Table 4. 2, fresh Aβ and 72-hour non-mixed samples have lower ΔG_{H2O} values (1780.4, and 2158.7 cal/mol), other samples have the values between 2656.9 and 2818.2 cal/mol, and 8-hour non-mixed sample has the highest value (3272.2 cal/mol). K_{H2O} which can be obtained by $K_{H2O} = \exp(-\Delta G_{H2O}/RT)$ makes ΔG_{H2O} meaning more clear. Fresh Aβ and 72-hour non-mixed samples have higher K_{H2O} values (0.056, and 0.030), other samples have the values between 0.009 and 0.013, and the 8-hour non-mixed sample has the lowest value (0.005). All of the samples tend to stay in the native or aggregated state in water relative to the unfolded state. Among Aβ samples used, the 8-hour non-mixed sample was most stable (had the greatest tendency to stay in the "native" state. The 8-hour sample also had the greatest m value (859.36 cal/mol M) and was different from other samples. Fresh Aβ and 72-hour non-mixed samples had lower m values (477.72,

and 521.91 cal/mol M), and other samples had m values between 632.00 and 712.77 cal/mol M. These results imply that there was the greatest change in accessible surface when the 8 hour Aβ sample was exposed to denaturant. Its structure was more readily disrupted in denaturant than the other samples.

The two-state transition model has some drawbacks to explain Aβ conformational change and stability. First of all, the data of CD intensities with urea (Fig. 4. 2) are scattered in the middle of the urea concentration range and do not have a single inflexion point. Another denaturant, Guanidine hydrochloride (GuHCl), shows this result more clearly; the data are less scattered therefore the lack of a single inflection point is easier to verify. The lack of a single inflection point in the data implies that there are more than two states (more than simply folded and unfolded states). The analysis is based on equilibrium calculations, however, it is not clear that aggregation states of Aβ, the initial states in these studies, can be in true equilibrium. Also, I start with aggregated species, not natively folded proteins, and it is likely that there is more than a single transition from aggregated to unfolded Aβ.

In order to avoid these dilemmas, a three-transition states model is proposed for analysis of Aβ stability.

$$N \leftrightarrow I \leftrightarrow U \qquad (4\text{-}6)$$

where N is the native state which has α-helix or random coil conformation. N is in equilibrium with I (intermediate state) which has a β-sheet structure. U is the unfolded state which has random coil structure upon exposure to the denaturant. Three-transition states will result in different estimates for m and ΔG_{H2O}, but the observed trends would

still be the same.

The results of this research suggest that the most toxic Aβ species, the 8-hour non-mixed sample, has the least stability and undergoes the most ready conformation change in denaturant, where as the other samples are more stable and less toxic. In addition, I examined stability of Aβ structures that morphologically appear similar in electron micrographs, and found that similar looking structures (mixed 24 hours and non-mixed 72 hours) had very different stabilities and toxicities. The protein stability of Aβ related to conformational change is strongly associated with biological activity.

This work may have other implications. Many speculate that Aβ biological activity or toxicity is associated with membrane interactions (Arispe et al., 1993, Butterfield et al., 1994, Butterfield, 1997, Good et al., 1996, Hensley et al., 1994, Mattson et al., 1997, McLaurin et al., 1998, Hertel et al., 1997). While I have measured stability in detergent, I postulate that change in conformation in detergent may correlate with protein changes in conformation in a phospholipid membrane. If this is true, then those Aβ aggregated species that most easily change structure in the cell membrane may cause the most damage to cells.

CHAPTER V

HSP20 PREVENTS Aβ FIBRIL FORMATION AND TOXICITY*

OVERVIEW

β-Amyloid (Aβ) is a major protein component of senile plaques in Alzheimer's disease, and is neurotoxic when aggregated. The size of aggregated Aβ responsible for the observed neurotoxicity and the mechanism of aggregation are still under investigation; however, prevention of Aβ aggregation still holds promise as a means to reduce Aβ neurotoxicity. In research presented here, I show that Hsp20, a novel α-crystallin isolated from the bovine erythrocyte parasite *Babesia bovis*, was able to prevent aggregation of denatured alcohol dehydrogenase when the two proteins are present at near equimolar levels. I then examined the ability of Hsp20 produced as two different fusion proteins to prevent Aβ amyloid formation as indicated by Congo red binding; I found that not only was Hsp20 able to dramatically reduce Congo red binding, but it was able to do so at molar ratios of Hsp20 to Aβ of 1 to 1000. Electron microscopy confirmed that Hsp20 does prevent Aβ fibril formation. Hsp20 was also able to significantly reduce Aβ toxicity to both SH-SY5Y and PC12 neuronal cells at similar molar ratios. At high concentrations of Hsp20, the protein no longer displays its

---

*Reprinted with permission from "Hsp20, a novel α-crystallin, prevents Aβ fibril formation and toxicity" by Sungmun Lee, Kenneth Carson, Allison Rice-Ficht, and Theresa Good, 2005. *Protein Science*, **14**, 593-601.

aggregation inhibition and toxicity attenuation properties. Size exclusion chromatography indicated that Hsp20 was active at low concentrations in which dimer was present. Loss of activity at high concentrations was associated with the presence of higher oligomers of Hsp20. This work could contribute to the development of a novel aggregation inhibitor for the treatment of Alzheimer's disease.

INTRODUCTION

Alzheimer's disease (AD), the leading cause of dementia in the aging population, is accompanied by the accumulation of β-amyloid peptide (Aβ) as amyloid fibrils in senile plaques in the cerebral cortex. It is hypothesized by many that Aβ contributes to the neurodegeneration associated with AD via the toxicity of the peptide in aggregated form.

Investigation of the relationship between aggregated Aβ peptide size, structure and toxicity is ongoing. In an aggregated state containing fibrils, protofibrils, and low molecular weight intermediates/oligomers, Aβ peptide has proven to be toxic to cultured neuronal cells (Koh et al. 1990; Pike et al. 1993; Lambert et al. 1998; Kayed et al. 2003). Aβ structures reported to be toxic include a non-fibrillar species of approximately 17 to 42 kDa (Lambert et al. 1998), protofibrils species with hydrodynamic radii on the order of 9 nm to 367 nm (Wang et al. 2002), and fibril species, with some investigators suggesting that the smaller oligomeric Aβ species are more toxic than fibril and protofibril forms (Dahlgren et al. 2002). Many believe that one strategy for preventing neurodegeneration associated with AD is the prevention of aggregation of Aβ into its

toxic oligomeric or fibril forms.

A number of investigators have developed inhibitors of Aβ aggregation with the aim of preventing Aβ toxicity (Ghanta et al. 1996; Lansbury 1997; Pallitto et al. 1999; Cairo et al. 2002). Some of these inhibitors have been small peptides with sequences that mimic the sequence of Aβ believed to be essential for aggregation and fibril formation (Pallitto et al. 1999). Peptide inhibitors of this class have been able to prevent Aβ toxicity by altering the aggregated structure when added at inhibitor to Aβ molar ratios of near 1:1 (Tjernberg et al. 1996; Pallitto et al. 1999). The use of molecular chaperones including α-crystallins and other small heat shock proteins has also been explored as a means of preventing Aβ aggregation and toxicity. Human sHsp27 inhibited Aβ1-42 fibril formation (Kudva et al. 1997). When αB-crystallin was examined, it was actually found to increase toxicity and β pleated sheet content of Aβ1-40 although it prevented fibril formation of Aβ *in vitro* at inhibitor to Aβ molar ratios of 1:1 or 1:5 (Stege et al. 1999).

In work described here, I use a novel small heat shock protein, Hsp20, isolated from the erythrocyte parasite *Babesia bovis* to prevent aggregation of Aβ and Aβ toxicity. Using two different Hsp20 constructs, a maltose binding protein fusion (Hsp20-MBP) and a polyhistidine fusion (his-Hsp20), I show that Hsp20 has α-crystallin-like properties, and that it can prevent aggregation of denatured alcohol dehydrogenase. Hsp20 is able to prevent amyloid formation of Aβ as indicated by Congo red binding at molar ratios of Hsp20 to Aβ of 1:1000. Hsp20 attenuates the toxicity of Aβ in SH-SY5Y and PC12 neuronal cells at analogous molar ratios. Hsp20 appears to be able to prevent

Aβ aggregation via a novel mechanism and at much lower concentrations than what has been necessary to prevent aggregation with other inhibitors. Hsp20 may be a useful molecular model for the design of the next generation of Aβ aggregation inhibitors to be used in the treatment of AD.

MATERIALS AND METHODS

Materials

Aβ(1-40) was purchased from Biosource International (Camarillo, CA). Cell culture reagents were purchased from GibcoBRL (Grand Island, NY). All other chemicals were obtained from Sigma (St. Louis, MO) unless otherwise stated.

Hsp20 Preparation

Hsp20 was produced in two forms, as an N-terminal fusion protein with maltose binding protein (Hsp20-MBP) and as an N-terminal polyhistidine fusion protein (his-Hsp20). Both proteins were produced in E. coli. The production of the maltose binding protein fusion has been previously described. (Brown et al. 2001) The N-terminal polyhistidine fusion protein was made with an intervening Tobacco Etch Virus (TEV) protease site (Carrington, et al., 1998) between Hsp20 and a polyhistidine tract. The construct was created through PCR of the Hsp20 coding sequence using a primer containing a 5' 21bp extension encoding the TEV protease site. The PCR product was introduced into the pTrcHis2 TOPO protein expression vector (Invitrogen) and transformed into chemically competent TOP10 cells (Invitrogen). His-Hsp20 was

prepared by growing cells to OD_{600} of 0.5 followed by induction with 1mM IPTG for 5 hours, and removal of media. The cells were then lysed in PBS using a French pressure cell and the insoluble his-Hsp20 pellet collected. The pellet containing his-Hsp20 was suspended in Denaturing Binding Buffer (Invitrogen) containing 8M urea and incubated with Probond resin for 1 hour to allow binding of his-Hsp20 to the nickel chromatography resin. The protein was eluted from the resin using 100 mM EDTA, dialyzed overnight into PBS pH 7.0, 20% glycerol and frozen at –80^{o}C. Protein purity and molecular weight were confirmed by SDS PAGE.

Aβ Peptide Preparation

Stock solutions of 10 mg/ml Aβ(1-40) peptides were dissolved in 0.1% (v/v) trifluoroacetic acid (TFA) in water. After incubation for 20~30 min. at 25°C, the peptide stock solutions were diluted to concentrations of 0.5 mg/ml by addition of sterile phosphate buffered saline (PBS; 0.01 M NaH_2PO_4, 0.15 M NaCl, pH 7.4). The peptides were diluted to final concentrations of 20 μM, 50 μM, and 100 μM by addition of PBS for Congo red and electron microscopy (EM) studies. Cell culture medium (below) replaced PBS in toxicity studies. These solutions were rotated at 60 revolutions per minute at 25°C for 24 hours to ensure aggregation**.**

Cell Culture

Human neuroblastoma SH-SY5Y cells (a gift of Dr. Evelyn Tiffany-Castiglioni, College of Veterinary Medicine, Texas A&M University, College Station, Texas) were

cultured in minimum essential medium (MEM) supplemented with 10% (v/v) fetal bovine serum (FBS), 3 mM L-glutamine, 100 U/ml penicillin, 100 μg/ml streptomycin, and 2.5 μg/ml amphotericin B (fungizone) in a humidified 5% (v/v) CO_2/air environment at 37°C. Rat pheochromocytoma PC12 cells (ATCC, Rockville, MD) were cultured in RPMI medium supplemented with 10% (v/v) horse serum, 5% (v/v) FBS, 3 mM L-glutamine, 100 U/ml penicillin, 100 μg/ml streptomycin, and 2.5 μg/ml fungizone in a humidified 5% (v/v) CO_2/air environment at 37°C. For the toxicity assays, cells were plated at a density of 1 x 10^5 cells/well in 96 well plates and aggregated peptide solutions were added to the cells 24 hours after plating.

Congo Red Binding

Congo red studies were performed to assess the presence of amyloid fibrils in Aβ solution. Congo red dye was dissolved in PBS to a final concentration of 120 μM. Congo red solution was added to the peptide solutions at the ratio of 1:9. The peptide solution and control solution were allowed to interact with Congo red for 30~40 minutes prior to absorbance measurement with a Model 420 UV-Vis spectrophotometer (Spectral Instruments, Tucson, AZ) at 25°C. The fibril formation of the samples was estimated from the absorbance using equation 5-1;

$$[A\beta_{Fib}] = \left({}^{541}A_t / 4780\right) - \left({}^{403}A_t / 6830\right) - \left({}^{403}A_{CR} / 8620\right) \qquad (5\text{-}1)$$

where $[A\beta_{Fib}]$ is the concentration of Aβ fibril, ${}^{541}A_t$, ${}^{403}A_t$ and ${}^{403}A_{CR}$ are the absorbances of the sample and Congo red at the wavelength of 541nm and 403nm, respectively (Klunk et al. 1999). From these data, relative fibril concentrations were

calculated as the ratio of sample fibril concentration to pure Aβ fibril concentration.

MTT Reduction Assay

Cell viability was measured 24 hours after peptide addition to cells using the 3, (4,5-dimethylthiazol-2-yl) 2,5-diphenyl-tetrazolium bromide (MTT) reduction assay. 10μl of 12mM MTT was added to 100μl of cells plus medium in a 96 well plate. The cells were incubated with MTT for 4 hours in a CO_2 incubator. Then, 100μl of a 5:2:3 N, N-dimethylforamide (DMF): sodium dodecyl sulfate (SDS): water solution (pH 4.7) was added to dissolve the formed formazan crystals. After 18 hours of incubation in a humidified CO_2 incubator, the results were recorded by using an Emax Microplate reader at 585 nm (Molecular Devices, Sunnyvale, CA). Percentage cell viability was calculated by comparison between the absorbance of the control cells and that of peptide or peptide: Hsp20 treated cells. Relative cell viability increase, was calculated from the ratio of the difference in cell viability of Hsp20: Aβ treated cells and cells treated with pure Aβ, divided by viability of cells treated with pure Aβ.

Electron Microscopy (EM)

200μl of Aβ peptide solution, prepared as described above, was mixed, placed on glow discharged grids, and then negatively stained with 1% aqueous ammonium molybdate (pH 7.0). Grids were examined in a Zeiss 10C transmission electron microscope at an accelerating voltage of 80 kV. Calibration of magnification was done with a 2,160 lines/mm crossed line grating replica (Electron Microscopy Sciences, Fort

Washington, PA).

ADH Turbidity Assay

Light Scattering of ADH and Hsp20 was performed as previously described (Horwitz 1992). Briefly, the aggregation of ADH and Hsp20 in solution was measured by the apparent absorption due to scattering at 360 nm in a Gilford Response II spectrophotometer at 58^{o}C. Solutions were mixed at room temperature in 50mM phosphate buffer, pH 7.0 and analyzed immediately. 1.625 μM ADH was used in all experiments. Hsp20 concentrations were varied to obtain different molar ratios of Hsp20 to ADH. Absorbance readings were taken at 1 minute intervals for one hour.

Size Exclusion Chromatography (SEC)

The size of his-Hsp20 oligomers as a function of concentration at room temperature was determined using size exclusion chromatography using a Pharmacia FPLC system. Protein samples at different concentrations were loaded on a Superose 6 HR 10/300 column (Pharmacia) and eluted using PBS. Eluted proteins were detected using UV absorbance at either 280 nm or 254 nm. Oligomer sizes were estimated based on the elution volumes of a set of calibration proteins run on the same column under similar conditions.

Statistical Analysis

For each experiment, at least three independent determinations were made.

Significance of results was determined via the student t test with $p<0.05$ unless otherwise indicated. Data are plotted as the mean plus or minus the standard error of the measurement.

RESULTS

Characterization of Hsp20

Hsp20 is a 177 amino acid, 20.1 kDa protein isolated from *Babesia bovis,* a protozoan bovine erythrocyte parasite. (Brown et al. 2001) Initial characterization by BLAST search of the NCBI database indicated significant sequence similarity with the α-crystallin family of small heat shock proteins. Hsp20 contains a region near its C-terminus that corresponds to the ~95 amino acid α-crystallin domain common to members of this protein family. These proteins are thought to be involved in the cellular response to stress. Previous work (Ficht, unpublished observation) has revealed that Hsp20 expression is up-regulated in times of thermal, nutritional and oxidative stress to the organism. Based on the apparent involvement of Hsp20 in the stress response coupled with its homology to the α-crystallins, α-crystallin activity assays were applied to Hsp20. A turbidity assay (Figure 5. 1) was used to quantitate the ability of Hsp20-MBP to solubilize target proteins at elevated temperatures. A solution of alcohol dehydrogenase when incubated at 58^{o}C for 60 minutes exhibited a dramatic increase in light scattering due to aggregation of the enzyme. When Hsp20-MBP was included in the solution at time zero in a molar ratio of 2:1 Hsp20:ADH, a 2.3 fold reduction in light scattering was observed at 60 minutes. To determine the most effective molar ratio for

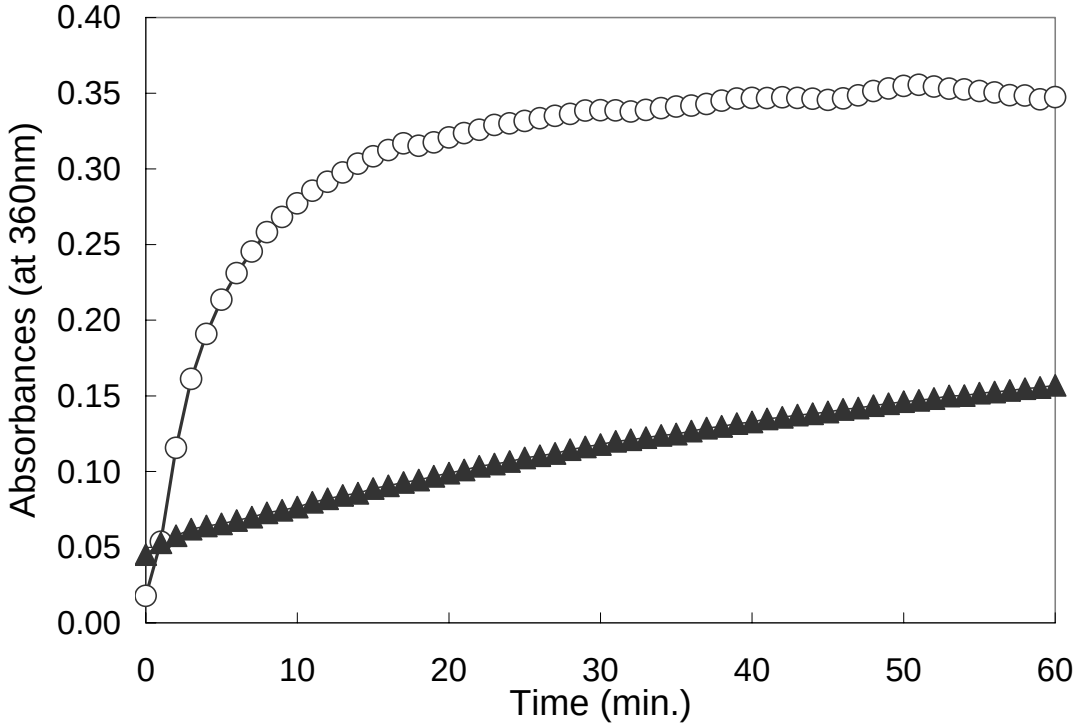

Figure 5. 1. Light scattering of ADH at elevated temperature. ADH was incubated in the presence and absence of Hsp20-MBP as determined by absorbance at 360 nm. ADH at a concentration of 1.625μM is incubated in phosphate buffer alone (open circles) and in the presence of 5.75μM Hsp20 (closed triangles) at 58°C for one hour. This data is obtained by Allison Rice-Ficht's group (Department of Medical Biochemistry and Genetics, Texas A&M University)

the reduction of light scattering, a series of experiments was conducted in which different mole ratios of Hsp20 was added the ADH (Figure 5. 2). At time infinity (determined by curve fitting software), the greatest reduction in light scattering was seen at a molar ratio of 2:1 (Hsp20 to ADH). Since Hsp20-MBP was prepared as a fusion protein with maltose binding protein, I examined the ability of maltose binding protein (MBP) alone to alter aggregation and turbidity of ADH in the same range of concentrations. MBP had no effect on ADH aggregation, suggesting the aggregation prevention activity was due to the presence of Hsp20. Having established the α-crystallin activity of Hsp20-MBP based standard assays, I then proceeded to test the ability of Hsp20-MBP to affect Aβ(1-40) fibril formation.

Effect of Hsp20-MBP on Aβ Fibril Formation Prevention

Given that Hsp20-MBP was able to prevent aggregation of denatured ADH, I then examined its ability to prevent aggregation and amyloid fibril formation of Aβ(1-40). I used Congo red binding as a simple indicator of amyloid formation. In these experiments, 20μM, 50μM, and 100μM concentrations of Aβ(1-40) were used to create fibrils. Hsp20-MBP at concentrations from 1 nM to 5 μM was added to Aβ(1–40) solutions prior to aggregation. This corresponds to molar ratios of Hsp20-MBP to Aβ of 1:20,000 to 1:20 or 0.00005 to 0.05. After 24 hours of incubation, sufficient time for typical fibril formation, Congo red was added to samples to assess fibril formation. Representative Congo red absorbance spectra are seen in Figure 5. 3. Hsp20-MBP alone did not alter Congo red absorbance. Pure Aβ(1–40) solutions caused a characteristic shift in

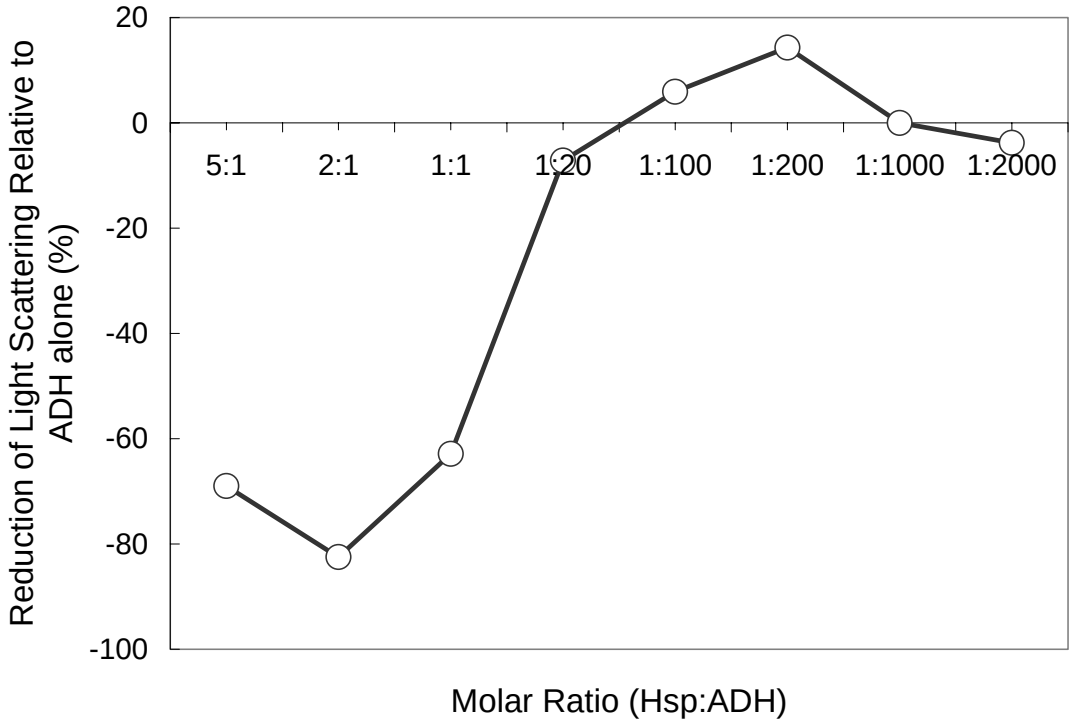

Figure 5. 2. Percent reduction of light scattering at time infinity of various solutions of ADH and Hsp20-MBP relative to ADH alone. Greatest reduction in light scattering is seen at 2:1 molar ratio (Hsp20:ADH). All experiments were performed at 58°C. ADH was included at 1.625μM in each experiment. Light scattering at time infinity was estimated from absorbance versus time curves for each mixture. This data is obtained by Allison Rice-Ficht's group (Department of Medical Biochemistry and Genetics, Texas A&M University)

absorbance to longer wavelengths and an increase in intensity. Hsp20-MBP, when added to Aβ prior to aggregation, attenuated the shift in absorption and increase in intensity associated with Aβ fibril formation. MBP alone, when added to Aβ at similar concentrations had no effect on fibril formation as assessed by Congo red binding.

I show in Figure 5. 4A the effect of Hsp20-MBP on reduction of Aβ fibril formation at different concentrations of Aβ and Hsp20-MBP. At Hsp20-MBP concentrations below 0.1μM, Aβ fibril formation decreased as a function of Hsp20-MBP concentration. However, Hsp20-MBP became less effective at preventing Aβ fibril formation in the higher concentration range. The concentration of Hsp20-MBP needed for optimal prevention of fibril formation appeared to be a function of Aβ concentration, with the lowest concentration of Aβ exhibiting the optimum in prevention of fibril formation at the lowest Hsp20-MBP concentration. In Figure 5. 4B, I replotted the fibril formation data as a function of molar ratio of Hsp20-MBP to Aβ at the three different Aβ concentrations. It appears from Figure 5. 4B that the three curves are now superimposed. The optimum in fibril formation for the three concentrations of Aβ tested occurred at or near the same molar ratio of Hsp20-MBP to Aβ, between 0.0005 and 0.001. The molar ratio of Hsp20-MBP to Aβ needed to optimally prevent fibril formation was several orders of magnitude lower than that needed to prevent aggregation of ADH. Electron micrographs of Aβ fibrils, Hsp20-MBP, and Aβ-Hsp20-MBP mixtures that correspond to conditions used in the Congo red binding studies are shown in Figure 5. 5. In the images, 100μM Aβ and 0.1μM Hsp20-MBP were used. As seen in Figure 5. 5A, Aβ formed long individual fibrils and groups of long fibrils under the aggregation conditions

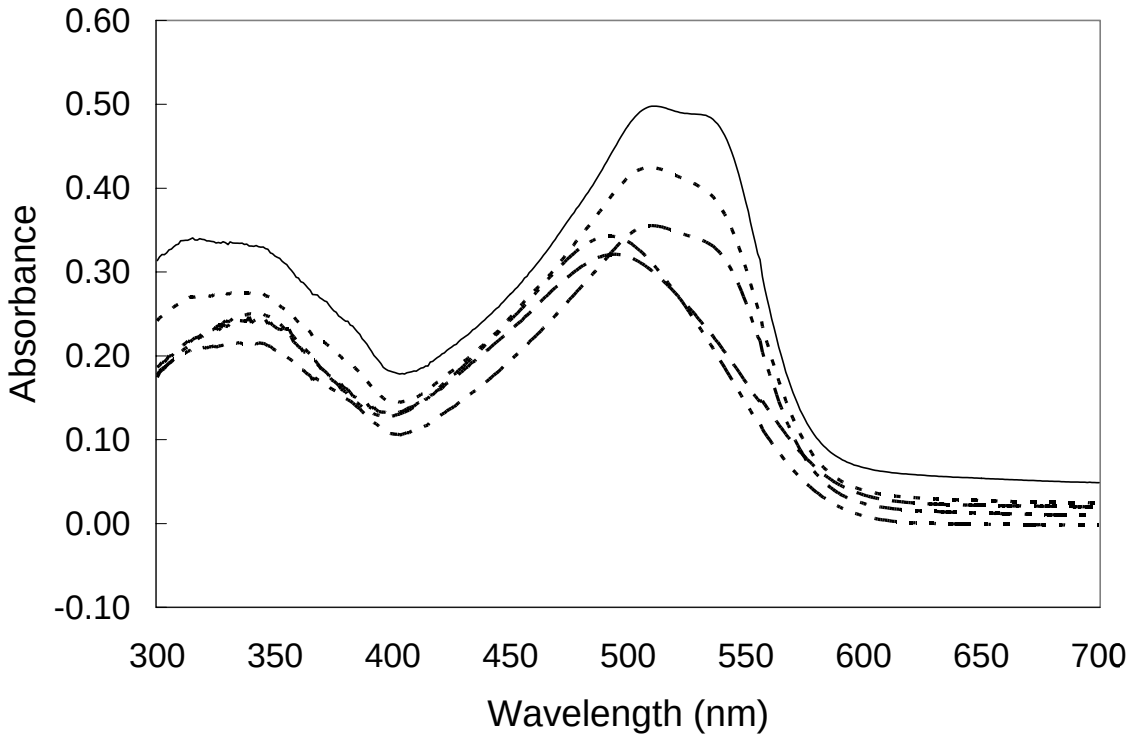

Figure 5. 3. Representative absorbance spectra of Congo red with Aβ and Aβ-Hsp20. 100μM Aβ(1-40) was used in all cases. Hsp20-MBP was added at the beginning of the 24 hour aggregation at room temperature with mixing. [bold line -Congo red alone; fine line- Aβ alone; light gray line - 1:100 Hsp20:Aβ; dark gray line - 1:1000 Hsp20:Aβ].

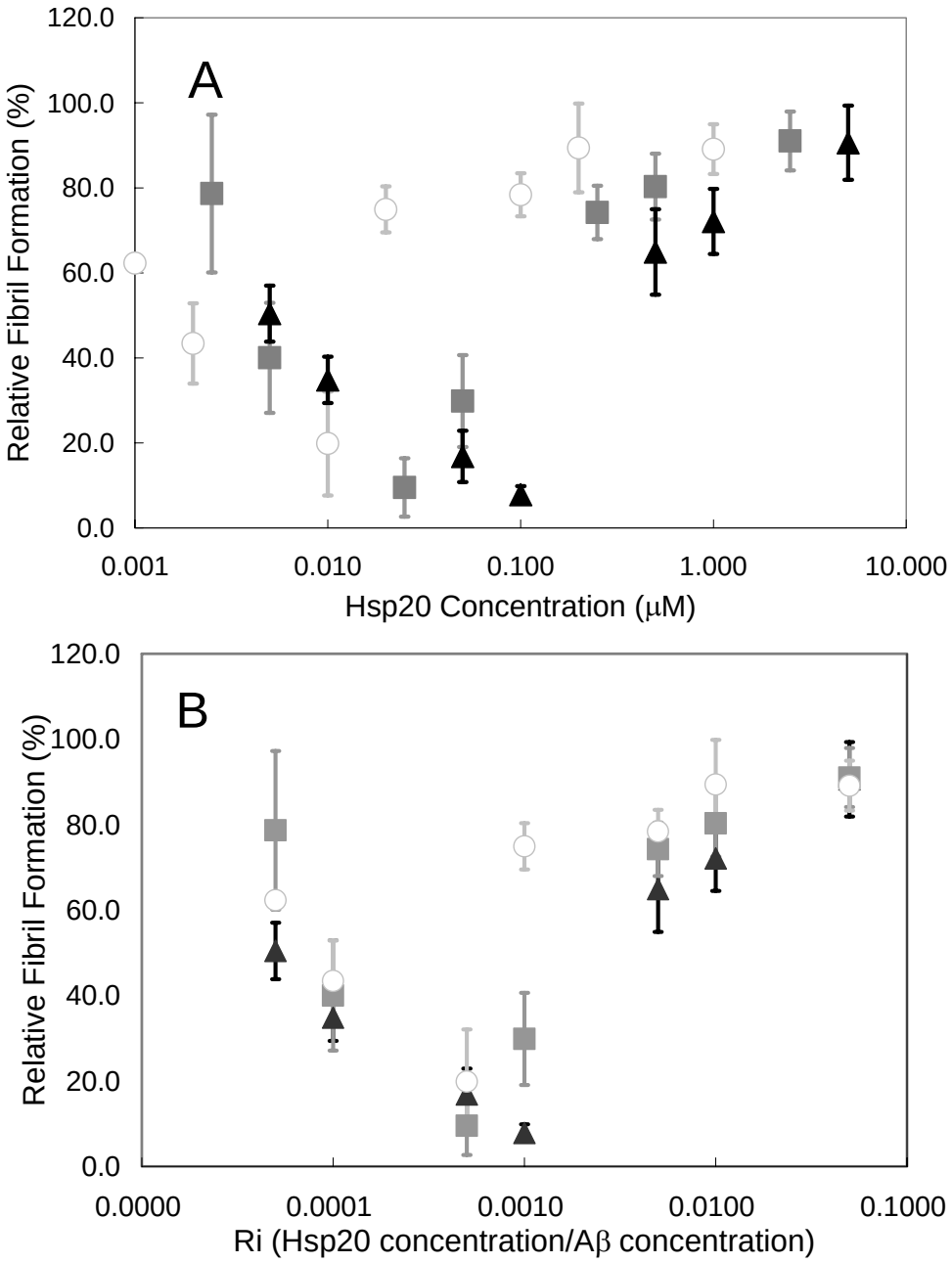

Figure 5. 4. Relative fibril formation as estimated from Congo red binding. Relative fibril formation. (a) as a function Hsp20-MBP concentration, and (b) as a function of the molar ratio of Hsp20-MBP to Aβ [open circles - 20μM Aβ; squares - 50μM Aβ; triangles - 100μM Aβ]

employed. Hsp20-MBP, at 0.1μM and room temperature, formed species of approximately 13.6 nm in diameter, composed of 2 subunits, 5.4 nm in width each, with a distance of 2.7 nm between subunits (Figure 5. 5B). In micrographs of the Aβ-Hsp20-MBP mixture (Figure 5. 5C), small globular species with a 16.3 nm diameter and variable length were observed. These species could be an Hsp20-Aβ complex, large Hsp20-MBP aggregates, and/or Aβ-protofibrils. Aβ fibrils were noticeably absent from micrographs of Aβ-Hsp20 mixtures.

Ability of Hsp20-MBP To Prevent Toxicity of Aβ

Aβ is typically toxic to neuron-like cells (SH-SY5Y cells, and PC12 cells etc.) when in aggregated form. In Figure 5. 6, I show the effect of Hsp20-MBP on Aβ toxicity as measured using the MTT assay for 100 μM Aβ added to SH-SY5Y cells and 2 μM Aβ added to PC12 cells. Hsp20-MBP by itself had no effect on SH-SY5Y or PC12 cell viability. However, Hsp20-MBP, when added to Aβ prior to aggregation, had a profound effect on Aβ toxicity observed in both cell types. MBP, when added to Aβ, did not attenuate Aβ toxicity. In Figure 5. 6, I plotted cell viability as a function of molar ratio of Hsp20-MBP to Aβ. As with fibril formation data presented in Figure 5. 4B, it appears that the two viability curves as a function of Hsp20 to Aβ molar ratio are superimposed. The molar ratio of Hsp20 to Aβ needed for optimal toxicity attenuation is approximately the same as the molar ratio needed for optimal fibril formation prevention.

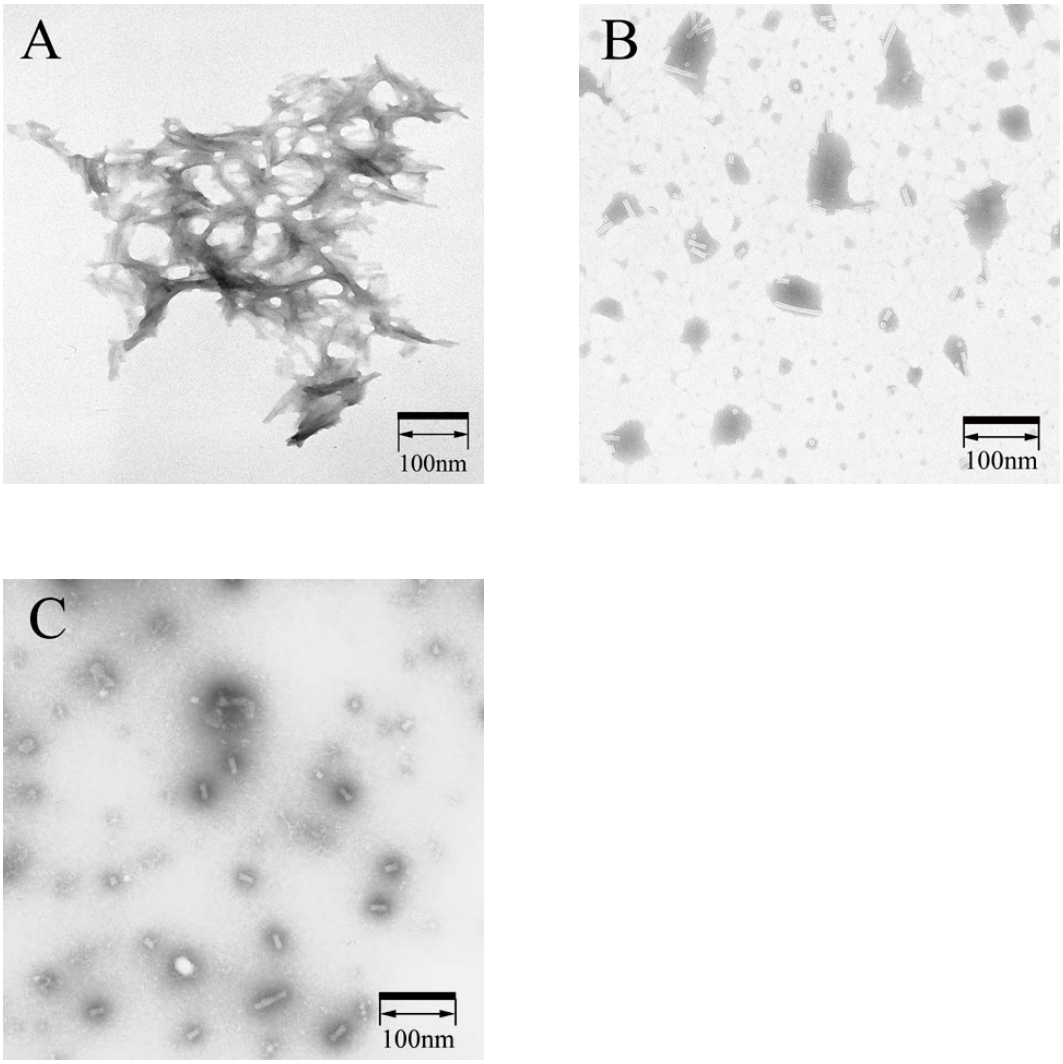

Figure 5. 5. Representative electron micrographs of Aβ and Hsp20-MBP. Samples were incubated for 24 hours of aggregation (a) 100μM Aβ, (b) 0.1μM Hsp20-MBP, and (c) 100μM Aβ + 0.1μM Hsp20-MBP.

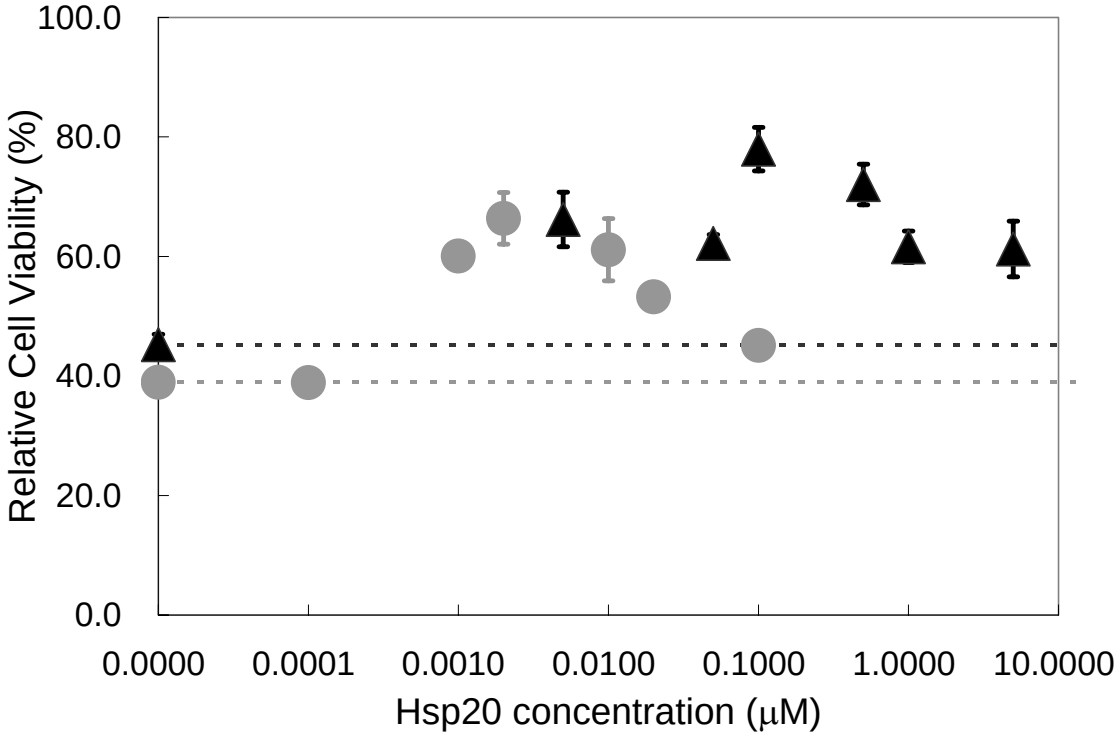

Figure 5. 6. Relative cell viability of SH-SY5Y cells (triangles) and PC12 cells (circles). Samples were treated with 100 μM (triangles) and 2 μM (circles) Aβ as a function of Hsp20-MBP concentration. Viability is measured via the MTT reduction assay. N is greater than or equal to 6. Aβ(1-40) was incubated for 24 hrs in the media prior to addition to the cells. Viability as a function of molar ratio of Hsp20-MBP to Aβ; viability is reported relative to control cells.

Ability of His-Hsp20 to Prevent Aβ Aggregation and Toxicity

While control experiments demonstrated that MBP alone had no effect on Aβ aggregation and toxicity, it was possible that the MBP fusion contributed to the function of Hsp20. To examine this possibility, I next generated a N-terminal polyhistadine-Hsp20 fusion protein. In experiments parallel to those described above, I examined if the polyhistadine-Hsp20 fusion protein could also prevent Aβ aggregation and toxicity as measured by Congo red binding and MTT reduction, respectively. As seen in Figure 5. 7, his-Hsp20 prevents Aβ aggregation and toxicity over a wider range of concentrations and at lower concentrations than the MBP fusion protein. Also, attenuation of toxicity approached 100% with the his-Hsp20 while the Hsp20-MBP attenuated Aβ toxicity to a lesser extent. However, as with the MBP fusion protein, there was a noticeable loss of his-Hsp20 activity at concentrations above 1 μM.

Size Exclusion Chromatography of His-Hsp20

To know the mechanism of loss of activity of His-Hsp20 at higher concentrations, I examined size of His-Hsp20 oligomers in solution as a function of concentration. Stock solutions of His-Hsp20 were diluted to 100 μM, 29 μM and 0.1 μM in PBS shortly before analysis. Chromatograms of His-Hsp20 at the different concentrations can be seen in Figure 5. 8. At the highest concentration (Figure 5. 8A), His-Hsp20 elutes as a mixture of a number of oligomers, ranging from an approximate 16-mer, 10-mer, 6-mer, tetramer, dimer and monomer, with dimer representing about 15% of total protein eluted the column. At intermediate concentrations, 0.1 μM (Figure 5. 8B), a concentration at

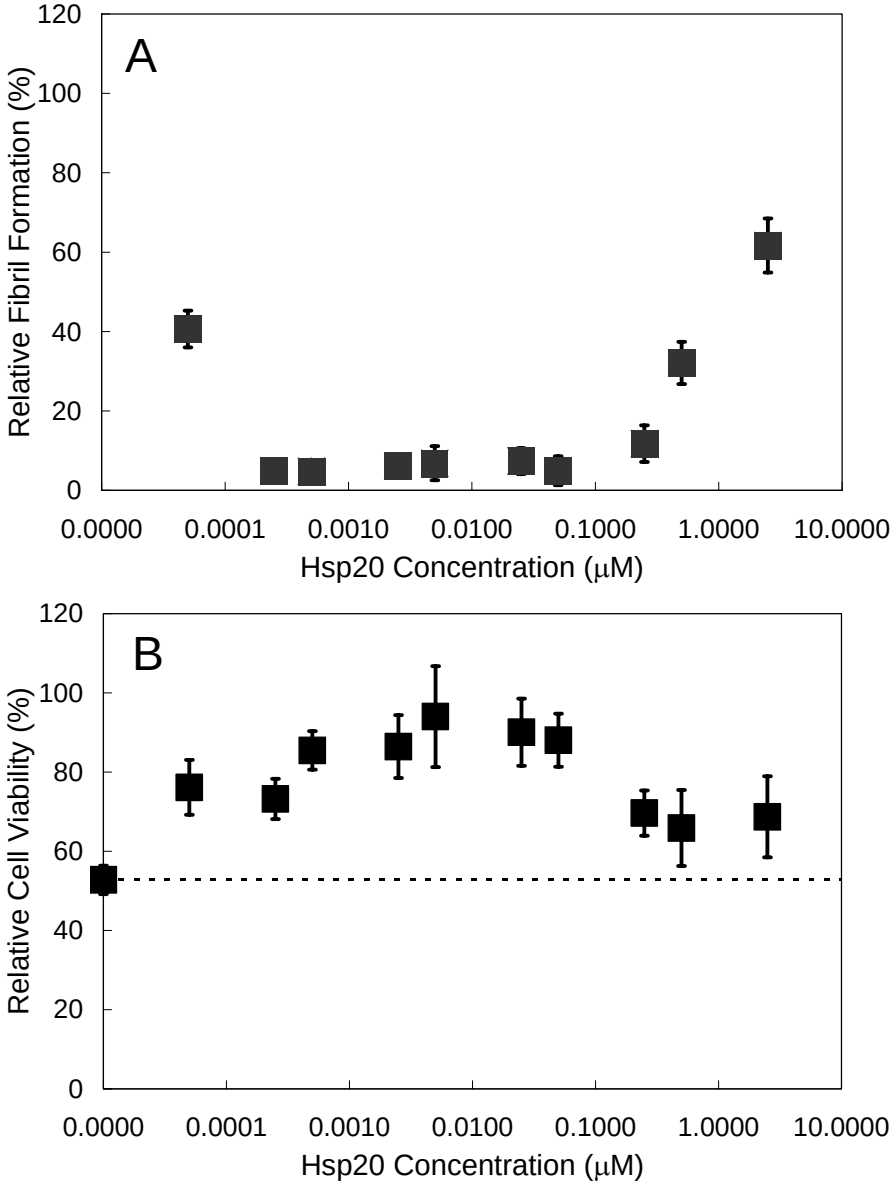

Figure 5. 7. Relative Aβ fibril formation and cell viability as a function of His-Hsp20 concentration. (A) Fibril formation using Congo red is reported relative to fibril formation in pure 50 μM Aβ solutions. (B) Cell viability was measured via MTT reduction and reported relative to cells untreated with Aβ or His-Hsp20. Aβ or His-Hsp20 mixtures were mixed, then aggregated with mixing at 37 C for 24 hours prior to treatment.

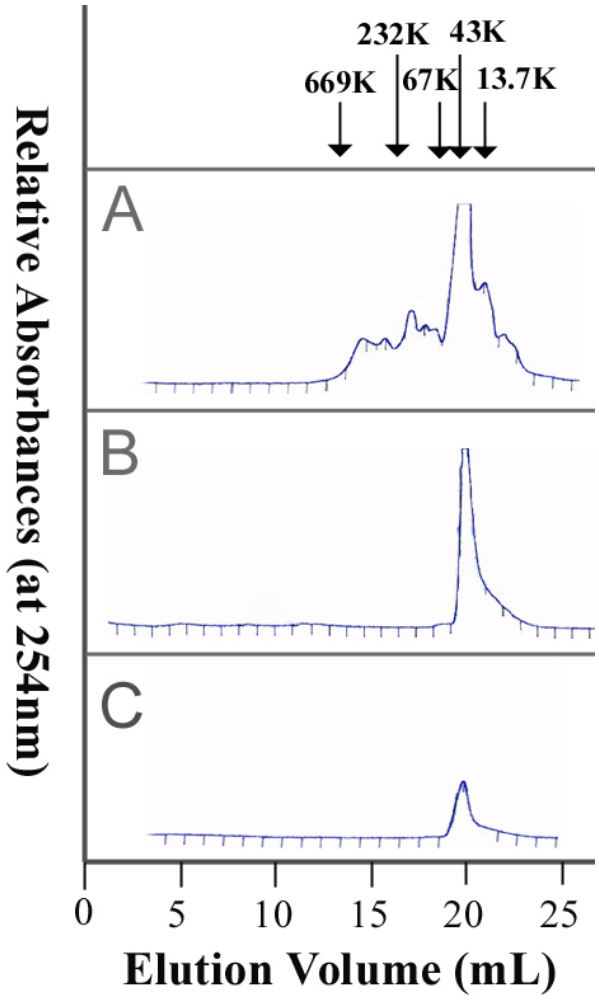

Figure 5. 8. Representative size exclusion chromatograms of His-Hsp20. (A) 1 μM His-Hsp20, (B) 0.1 μM His-Hsp20, and (C) 0.01 μM His-Hsp20. Separations were performed on a Pharmacia Superose 6 column at room temperature using phosphate buffered saline as an elution buffer.

which His-Hsp20 displays both high aggregation and toxicity prevention activities, only dimer was observed. At the lowest concentration (Figure 5. 8C), Hsp20 was mostly composed of dimers. Analytical ultracentrifugation was used to confirm the presence of high molecular weight oligomers of his-Hsp20 at high concentrations (data not shown).

Ability of Hsp20-MBP to Reverse Aβ Aggregation

I examined if, once Aβ was aggregated, addition of Hsp20-MBP could reverse fibril formation. I aggregated Aβ under conditions analogous to those described previously, and after 24 hours aggregation, I added Hsp20 at optimal concentrations for fibril formation prevention (100 nM), incubated for up to 2 days, and then assessed fibril content via Congo red binding. At all time points measured, fibril formation after addition of Hsp20 was equal to or greater than fibril formation of Aβ alone after 24 hours aggregation (data not shown). In all cases, viability of SH-SY5Y cells, as measured by the MTT assay, treated with solutions in which Hsp20 was added after 24 hour Aβ aggregation was not significantly greater than viability of cells treated with Aβ that had been allowed to aggregate for 24 hours (data not shown).

DISCUSSION

The superfamily of small heat shock proteins, sHSPs, are a diverse group of proteins involved in prevention of protein misfolding and the onset of programmed cell death (van den et al. 1999; Bruey et al. 2000). They typically exist as large multimeric complexes containing 4 to 40 subunits, with molecular masses of 40 kDa or less per

subunit. The sHSPs bind to their substrates with high affinity and prevent protein misfolding in an ATP independent reaction (Jakob et al. 1993).

Generally, the α-crystallins are considered to be sHSPs (Horwitz 1992; MacRae 2000). Circular Dichroism spectroscopy (CD) studies predict that β-pleated sheet dominates the secondary structure of the α-crystallins (Horwitz 2000; van Montfort et al. 2001). A conserved 90 amino acid sequence, located near the C-terminus, termed the α-crystallin domain, is the hallmark of all α-crystallins.

A protein, Hsp20, isolated by Rice-Ficht and coworkers from the bovine erythrocyte parasite *Babesia bovis* (Brown et al. 2001) has repeatedly demonstrated α-crystallin activity *in vitro*. The apparent light scattering of alcohol dehydrogenase in solution at 58°C was reduced when in the presence of equimolar concentrations of recombinant Hsp20 (Figure 5. 1). This indicates reduced aggregation of denatured ADH at the elevated temperature due to an interaction with Hsp20. The optimal Hsp20 to ADH binding ratio was 2:1 (Figure 5. 2), consistent with the stoichiometry of binding one Hsp20 dimer to one ADH molecule. This is consistent with the observations of van Montfort et al (van Montfort et al. 2001) that other alpha crystallins are active as dimers. In addition, Hsp20 is upregulated under heat shock conditions (42°C) and oxidative stress (molecular O_2 and H_2O_2); and, as other α-crystallins, it also forms higher order complexes as revealed through dynamic light scattering analysis (unpublished observation). Hsp20 has limited nucleotide and amino acid sequence homology to members of the α-crystallin family, with the majority of the identical/conserved amino acids occurring in the region corresponding to the α-crystallin domain. (Brown et al.

2001) The α-crystallin-like activity and ability to prevent protein aggregation of Hsp20 indicate that it may be potentially useful as an aggregation inhibitor (or a model for an aggregation inhibitor) for Aβ. In view of its divergent sequence, this α-crystallin may have entirely unique properties.

I show, in Figures 5. 3 – 5. 5 and Figure 5. 7, that Hsp20-MBP and his-Hsp20 prevent Aβ fibril formation as indicated by the absence of Congo red binding and of visible fibrils in electron micrographs, at molar ratios near 1:1000 Hsp20 to Aβ or lower. This is in sharp contrast to the near 1:1(2:1, or even 4:1 if ADH is considered a dimer) molar ratio needed to prevent ADH aggregation. A number of investigators have explored the ability of other small heat shock proteins, molecular chaperones, and α-crystallins to prevent fibril formation in several systems including Aβ (Kudva et al. 1997; Hughes et al. 1998; Stege et al. 1999; Hatters et al. 2001). Most have found that the chaperones or small heat shock proteins can inhibit Aβ aggregation at molar ratios of chaperone to Aβ of 1:10 to 1:100. The low concentrations of Hsp20 and other α-crystallins needed to prevent fibril formation, relative to that needed to prevent ADH aggregation, could be related to specificity of the α-crystallins for β-sheet or fibril forming proteins. Alternatively, the difference in molar ratios needed to prevent ADH aggregation relative to those needed to prevent Aβ fibril formation could be related to the temperature differences at which the experiments were carried out. The ADH aggregation experiments were carried out at elevated temperature, while the Aβ fibril formation experiments were carried out at room temperature. The quaternary structure of α-crystallins are generally temperature dependent; however, most often, more highly

active oligomers (dimers) are formed at higher temperatures (Abgar et al. 2001; van Montfort et al. 2001). Indeed, when I performed fibril formation and toxicity prevention experiments with Hsp20-MBP and Aβ at 37 C instead of room temperature, approximately 10 times less Hsp20-MBP was needed to prevent fibril formation (or 1:10,000 Hsp20 to Aβ mole ratio) relative to that needed to maximally prevent fibril formation at room temperature (data not shown).

Another plausible explanation for Hsp20 activity is that Hsp20 interacts with an oligomer of Aβ in a near 1 to 1 molar ratio; however, the Aβ oligomer may be very dilute in Aβ solutions. In models of Aβ aggregation, investigators postulate that Aβ forms micelles or multimeric nuclei from Aβ monomers or dimers via a high order process (Lomakin et al. 1997; Pallitto and Murphy 2001; Yong et al. 2002). It is from these micelles or nuclei that fibril growth is initiated. Micelles or nuclei would be far less abundant than monomeric Aβ. I propose that binding to or removal of these fibril initiating species from solution would be sufficient to prevent Aβ fibril formation.

The difference in fibril prevention activity of the two Hsp20 constructs tested, Hsp20-MBP and his-Hsp20 are clearly demonstrated in Figure 5. 7. I spectulate that the almost 100 fold increase in effectiveness of the his-Hsp20 compared to the Hsp20-MBP at preventing fibril formation is due to higher affinity of the his-Hsp20 for Aβ than Hsp20-MBP affinity for Aβ. Differences in Hsp20 structure or stability in the two different constructs may also affect fibril prevention activity of the protein.

As seen in Figures 5. 4 and 5. 7, there is an optimum concentration of Hsp20 for Aβ fibril formation prevention. I suggest several possible explanations for this

observation. Oligomerization dynamics of α-crystallins are concentration dependent (McHaourab et al. 2002). Hsp20 may aggregate to form a less active structure at higher concentrations. High molecular weight oligomers of heat shock proteins, which tend to form at high concentrations, are less active than the low molecular weight oligomers (Liang 2000). Additionally, equilibrium distribution of oligomeric Hsp20 species are likely dependent upon conformers or oligomers of substrate Aβ present in solution. Size exclusion chromatography (SEC) data presented in Figure 5. 8 supports the hypothesis that Hsp20 oligomerization is concentration dependent. At concentrations where his-Hsp20 has high Aβ fibril prevention activity, his-Hsp20 elutes as a dimer from the SEC column, suggesting that the active form of his-Hsp20 is a dimer. At concentrations of his-Hsp20 where the protein displays less fibril prevention activity or no activity, a complex mixtures of oligomers were detected via both SEC (Figure 5. 8) and analytical ultracentrifugation (data not shown). These data suggest that oligomers larger than the dimer are inactive. Hsp20-MBP becomes inactive in the fibril formation assay at lower concentrations than his-Hsp20, suggesting that the MBP construct contributes to the destabilization of the active dimer. Changes in oligmerization of Hsp20-MBP at low concentrations could not be confirmed because of limits of sensitivity of detection of the FPLC system in the range of concentrations where Hsp20-MBP was active.

Analogous to fibril formation prevention data, Hsp20 attenuates Aβ toxicity at similar molar ratios (Figures 5. 6 and 5. 7). These data suggest that the Aβ species which bind Congo red and have fibril appearance in electron micrographs are toxic, or, more probably, Aβ species which are associated with the formation of Congo red

binding or fibril species are toxic. While non-fibrillar ADDLs, low molecular weight oligomers, protofibrils, and fibrils have all been found to be toxic (Iversen et al. 1995; Lambert et al. 1998), recent evidence suggests that oligomeric Aβ are the toxic (or most toxic) species (Wang et al., 2002, Kayet et al., 2003, Dahlgren et al., 2002, for example).

A careful examination of electron micrographs of Aβ-Hsp20 mixtures under optimal fibril formation and toxicity prevention conditions (Figure 5. 5) reveals the presence of small globular species with a 16.3 nm diameter and variable length. The globular species are not yet well characterized, however, size analysis suggests that the species may be an Hsp20-Aβ complex rather than Aβ protofibrils since the width of these species (16.3nm) is atypical for Aβ micelles (5 ~11 nm), protofibrils (4~8nm), or fibrils (6~10nm) (Yong et al. 2002).

A number of different approaches have been explored for prevention of Aβ amyloid fibril formation and toxicity. Pentapeptides such as KLVFF (Pallitto et al. 1999), LPFFD (Soto et al. 1998), GVVIN, and RVVIA (Hetenyi et al. 2002) have been used to disrupt Aβ fibril formation and neurotoxicity. These pentapeptides have the same or similar residues as segments of Aβ essential for fibril formation, bind to Aβ, and alter the structure that Aβ adopts (Soto et al. 1998). Generally, 1 to 1 molar ratios of peptide inhibitors to Aβ are needed in order to effectively prevent fibril formation (Pallitto et al. 1999). Amphipathic molecules such as hexadecyl-*N*-methylpiperidinium (HMP) bromide or sulfonated molecules such as Congo red have also been used to prevent Aβ fibril formation and toxicity.

Other small heat shock proteins and α-crystallins have also been examined for

their ability to prevent Aβ and other amyloid fibril formation, with good success at relatively low molar ratios of α-crystallin to amyloid (Kudva et al. 1997; Hughes et al. 1998; Stege et al. 1999; Hatters et al. 2001). However, in none of these studies has toxicity inhibition been reported. Indeed, in work reported by Stege and coworkers (Stege et al. 1999), αB-crystallin prevented Aβ fibril formation but enhanced toxicity. Thus, I believe that I have found, with Hsp20, a novel protein, which both reduces Aβ fibril formation at very low molar ratios, and reduces Aβ toxicity at similar molar ratios. Upon further investigation of the mechanism of Hsp20 fibril formation and toxicity prevention, I hope to identify essential interactions between Aβ and Hsp20 essential for prevention of the formation of toxic Aβ species.

CHAPTER VI

THE EFFECT OF VARIOUS SMALL HEAT SHOCK PROTEINS ON PREVENTION OF Aβ AGGREGATION AND TOXICITY

OVERVIEW

β-amyloid (Aβ) is a main component of senile plaques in Alzheimer's disease (AD). Aβ readily forms fibrils via conformational changes. Aβ is toxic *in vitro* when it is aggregated. Many research groups have focused on prevention of Aβ aggregation and toxicity. Recently I found that Hsp20 from *B. Bovis* prevented Aβ aggregation and toxicity at very low mole ratios of small heat shock protein to Aβ. (Lee et al. 2005) In this work, I explore the mechanism of Hsp20 interaction with Aβ and compare its activity to several other small heat shock proteins. Our results suggest that Hsp20 interacts with Aβ via multivalent binding, which leads to productive aggregation prevention and toxicity prevention over a very limited range of protein concentrations. Other small heat shock proteins interact with Aβ via different mechanisms and while they are able to prevent Aβ aggregation, they can't prevent Aβ toxicity. These results highlight the unique properties of Hsp20 in Aβ aggregation and toxicity prevention. Understanding the mechanism of Hsp20-Aβ interaction may provide insights on how best to design the next generation of aggregation and toxicity inhibitors for AD.

INTRODUCTION

Alzheimer's Disease (AD) is the progressive disease that destroys a person's memory, judgment, and personal abilities gradually. Senile plaques and neurofibrillary tangles are two hallmarks of AD. β-amyloid peptide (Aβ) is the major component of senile plaques, which are clumps of proteins in fibril form that accumulate extracellularly in the brain. Aβ forms fibrils via a conformational change. Aβ toxicity is linked to its aggregation. (Iversen et al. 1995; Lambert et al. 1998) Recent studies show that soluble oligomeric forms of Aβ are more toxic than large fibrillar species. (Dahlgren et al. 2002; Chromy et al. 2003; Kayed et al. 2003) Aβ-derived diffusible ligands (ADDLs) composed of Aβ1-42 are toxic to neuron type of cells. (Lambert et al. 1998) Globular ADDLs have molecular weights between 17 to 42kDa with hydrodynamic radii between 3 to 8nm (Lambert et al. 1998; Klein et al. 2001; Chromy et al. 2003). Protofibrils of Aβ1-40 with hydrodynamic radii ranging from 9 nm to over 300 nm are toxic *in vitro*. (Walsh et al. 1999; Ward et al. 2000; Wang et al. 2002) Spherical aggregates with radii over 15 nm have also been reported to be toxic. (Hoshi et al. 2003)

Based on the Aβ aggregation hypothesis, many research groups have focused on finding the agents that prevent or reduce Aβ aggregation and toxicity. (Ghanta et al. 1996; Lansbury 1997; Pallitto et al. 1999; Cairo et al. 2002) Some chemicals such as polyphenol (Choi et al. 2001; Ono et al. 2004), apomorphine (Lashuel et al. 2002) and hexadecyl-*N*-methylpiperidinium (HMP) bromide (Wood et al. 1996) are reported to prevent Aβ aggregation and toxicity. Pentamer peptides, KLVFF (Tjernberg et al. 1996; Pallitto et al. 1999), LPFFD (Soto et al. 1998), GVVIN, and RVVIA (Hetenyi et al.

2002) have been used to prevent Aβ aggregation. Hydrophobic parts in the middle of Aβ including KLVFF are known to be very important in Aβ1-42 aggregation. (Tjernberg et al. 1999) Small heat shock proteins (sHsp) which had chaperone like activity have also been investigated to prevent Aβ aggregation or toxicity. Human sHsp27 inhibited Aβ1-42 fibril formation (Kudva et al. 1997). αB-crystallin, one of α–crystallin subunits prevented Aβ fibril formation *in vitro*, but increased the toxicity of Aβ1-40 (Stege et al. 1999).

Recently I found that novel heat shock protein, Hsp20 from *B. Bovis* can prevent Aβ aggregation and toxicity at very low concentrations of small heat shock protein relative to Aβ (1:1000). (Lee et al., 2005) The protein, however, lost activity at high concentrations of Hsp20. I originally postulated that the loss of activity was due to self assembly of the Hsp20 at high concentrations, and suggested that only dimer of Hsp20 was active, while higher order assembly was inactive.

In the work presented here, I describe a series of experiments in which I examine the mechanism of Hsp20 activity and compare it to activity of other small heat shock proteins. A novel Hsp20 construct was prepared that was missing 11 residues from the C-terminus which are partly responsible for Hsp20 assembly. This form of Hsp20 forms stable dimers under most conditions. I compare activity of the non-aggregating form of Hsp20 and the aggregating Hsp20, and find little difference in their aggregation prevention and toxicity behaviors. These results suggest that the binding ratio between Hsp20 and Aβ (stoichiometric binding) is more important in Aβ aggregation prevention than Hsp20 assembly. I examine aggregation and toxicity prevention properties of two

other small heat shock proteins, Hsp17.7 from carrot, and human recombinant Hsp27. Both sHsps inhibited Aβ1-40 aggregation but not toxicity. Electron microscope images of Hsp-Aβ complexes that formed under conditions and where both aggregation and toxicity prevention were observed were compared to Hsp-Aβ complexes that formed when only aggregation prevention was seen. In cases where both aggregation and toxicity prevention were seen, a large ring structure was observed repeatedly, which was absent when aggregation was prevented, but toxicity was not prevented. From these results, I postulated a mechanism for Hsp20-Aβ interaction that leads to both toxicity and aggregation prevention. Understanding how proteins prevent aggregation and toxicity of Aβ may provide insight in how best to design the next generation of Aβ aggregation inhibitors to be used in AD.

MATERIALS AND METHODS

Materials

β-Amyloid (Aβ)–(1-40) was purchased from AnaSpec (San Jose, CA). Recombinant human Hsp27 was purchased from MBL International Corporation (Woburn, MA). Human neuroblastoma SH-SY5Y cells (ATCC number: CRL-2266) were purchased from ATCC (Manassas, VA). Cell culture reagents were purchased from Invitrogen Life Technologies (Carlsbad, CA). Congo red was purchased from Fisher Chemicals. (Pittsburgh, PA). All other chemicals, unless otherwise specified Ire obtained from Sigma-Aldrich Co..

Heat Shock Protein 20 (Hsp20) Preparation

Hsp20 is isolated from *Babesia bovis,* (Brown et al. 2001) and Hsp20 was produced in two forms, as an N-terminal polyhistidine fusion protein (His-Hsp20) and as an N-terminal polyhistidine fusion protein (His-Hsp20) without 11 residues in C-terminus. Both proteins were produced in E. coli. The N-terminal polyhistidine fusion protein was made with an intervening Tobacco Etch Virus (TEV) protease site (Carrington et al. 1998) between Hsp20 and a polyhistidine tract. His-Hsp20 was prepared by growing cells to OD_{600} of 0.5 followed by induction with 1mM IPTG for 5 hours, and removal of media. The cells were then lysed in PBS using a French pressure cell and the insoluble His-Hsp20 pellet collected. The pellet containing his-Hsp20 was suspended in Denaturing Binding Buffer (Invitrogen) containing 8M urea and incubated with Probond resin for 1 hour to allow binding of his-Hsp20 to the nickel chromatography resin. The protein was eluted from the resin using 100 mM EDTA, dialyzed overnight into PBS pH 7.0, 20% glycerol and frozen at –80^{o}C. Protein purity and molecular weight were confirmed by SDS PAGE.

Heat Shock Protein 17.7 (Hsp17.7) Preparation

The gene, encoding Hsp17.7 from carrot, was cloned in *E.coli*. (Malik et al. 1999) *E.coli* was grown in the LB media (Trypton (10g/L), Yeast Extract (5g/L) and NaCl (10g/L)) with 50μg/ml kanamycin broth on the wheel for aeration overnight. The tubes of LB broth were inoculated at a 1:200 dilution and put on wheel at 37^{o}C. 100mM IPTG was added to cells in order to induce Hsp17.7 when *E.coli* reached an OD_{600} of 0.6.

E.coli was put back on the wheel and Hsp17.7 was expressed at 37^{o}C overnight. The cells were harvested by centrifugation at 6,000rpm for 10 minutes and frozen at -20^{o}C overnight. The cells were lysed with 20mM imidazole and 10min sonication. Hsp17.7 was purified by using a metal affinity column (POROS® MC) (Framingham, MA) with copper chromatography resin. (Self Pack™ POROS® 20MC Media) (Framingham, MA) The protein was eluted by pH gradient from pH 7.4 (Phosphate buffer, 50mM NaH_2PO_4, and 300mM NaCl) to pH 4.5 (Phosphate buffer). Protein purity and molecular weight were confirmed by size exclusion chromatography.

Protein Sample Preparation

Aβ1-40 was dissolved in 0.1% (v/v) Trifluoroacetic acid (TFA) solvent at the concentration of 10mg/ml. This solution was incubated at room temperature for 20~30 minutes in order to completely dissolve the Aβ. Filtered phosphate-buffered saline (PBS, 4.3 mM Na_2HPO_4, 137 mM NaCl, 2.7 mM KCl and 1.4 mM KH_2PO_4, pH 7.4) was added to the Aβ solution to make the final concentrations used in experiments. For cell viability assays, MEM medium was used instead of PBS buffer. For aggregation with mixing, Aβ samples were mixed on the rotator at 18 rpm and 37^{o}C, and samples were taken out as a function of time. For aggregation without mixing, Aβ samples were incubated without disturbance in a 37^{o}C incubator. sHsps were added to the Aβ samples before the samples were incubated (prior to aggregation).

Congo Red Binding

Congo red was dissolved in PBS at the concentration of 120μM and syringe filtered. The Congo red solution was mixed with protein samples at 1:9 (v/v) ratios to make the final concentration of Congo red 12μM. After a short vortex, the mixtures were incubated at room temperature for 30~40 minutes. Absorbance measurements from 400nm to 700nm were taken (UV-Vis spectrometer model UV2101, Shimadzu Corp.; Kyoto, Japan). Alternatively, Congo red absorbance was read at 405 nm and 540 nm using an Emax Microplate Reader (Molecular Devices, Sunnyvale, CA). In both cases, PBS buffer was used as a blank. The concentration of Aβ fibrils was estimated from Congo red binding via equation 6-1:

$$[A\beta_{FIB}] = ({}^{541}A_t/4780) - ({}^{403}A_t/6830) - ({}^{403}A_{CR}/8620) \qquad (6\text{-}1)$$

where ${}^{541}A_t$ and ${}^{403}A_t$ are the absorbances of the Congo red-Aβ mixtures at 541 nm and 403 nm, respectively, and ${}^{403}A_{CR}$ is the absorbance of Congo red alone in phosphate buffer.(Klunk et al. 1999) In Microplate reader, absorbances at 405nm and 540nm were assumed to be same as those at 403nm and 541nm.

Size Exclusion Chromatography (SEC)

A Superose6 HR 10/30 Column attached to FPLC (Fast Performance Liquid Chromatography) (Pharmacia; Piscataway, NJ) was used to separate Hsp20 and Aβ complex from small species such as monomer and dimer. PBS buffer was used as a mobile phase with flow rate of 0.5mL/min. A 100μL sample loop was used. Aβ and Hsp20 mixture was mixed for 4 hours. 100μL of the Aβ and Hsp20 mixture was

centrifuged at 7,000rpm for 3 minutes prior to SEC separation. Supernatants of centrifuged samples were loaded in the 100μL loop and injected into the column. Aβ species were detected by UV detector at 254nm.

Electron Micrograph (EM)

200μl of Aβ peptide solution, prepared as described above, was mixed, placed on glow discharged grids, and then negatively stained with 1% aqueous ammonium molybdate (pH 7.0). Grids were examined in a Zeiss 10C transmission electron microscope at an accelerating voltage of 80 kV. Calibration of magnification was done with a 2,160 lines/mm crossed line grating replica (Electron Microscopy Sciences, Fort Washington, PA).

Cell Culture

SH-SY5Y cells were grown in Minimum Essential Medium (MEM) supplemented with 10% (v/v) Fetal Bovine Serum (FBS), 25mM Sodium bicarbonate, 100 units/ml penicillin, and 100 mg/ml streptomycin. Cells were cultured in a 5% (v/v) CO_2 environment at 37^{o}C incubator. Low passage number cells were used (<p20) in all experiments to reduce instability of cell line.

Biological Activity Assay

For biological activity tests, SH-SY5Y cells at a density of 1x10^{5}cells/well were grown in 96 well plates. Cells were fully differentiated by addition of 20ng/mL NGF for

8 days. Aβ samples in MEM medium were added to the differentiated SH-SY5Y cells and the cells were incubated with Aβ samples at 37°C for 2 hours. Negative controls (cells in medium with no Aβ) and positive controls (cells treated with 800μM H_2O_2 in 50% (v/v) medium for 2 hours) were also prepared. At least 3 wells were prepared for each Aβ treatment, and each positive and negative control.

Cell viability was determined by using the fluorescent nucleic acid dye, propidium iodode (PI). PI is mostly used fluorescent dye for staining DNA in cells. PI can enter the dead cells and bind DNA in dead or late apoptotic cells. PI is a DNA specific dye and can not cross the membrane of viable cells. In order to stain the dead cells, Aβ treated cells were washed with PBS 1~2 times and 150μL of enzyme free dissociation buffer from Gibco (Carlsbad, CA) was added to the cells in order to detach SH-SY5Y cells from the surface. The cells were incubated at 37°C for approximately 5 minutes. 5μL of 33μM PI was added to the cells and cells were incubated for 15~20 minutes at room temperature in the dark.. Stained cells in 96 well plates were loaded in the FACS array (BD FACSArray, BD Bioscience; San Jose, CA) and fluorescence histograms for cells were obtained. To set up gates for the cell viability assays, 2 sets of staining controls were prepared, unstained cells, and cells stained with PI alone. Cells not stained with PI dye were taken as live cells, and the relative cell viabilities were calculated using equation 6-2.

$$\text{Relative Cell Viability}\,(\%) = \frac{(\text{L.C.}_{\cdot\text{sample}} - \text{L.C.}_{\cdot\text{H2O2}})}{(\text{L.C.}_{\cdot\text{NControl}} - \text{L.C.}_{\cdot\text{H2O2}})} \text{ x } 100 \qquad (6\text{-}2)$$

where $\text{L.C.}_{\cdot\text{sample}}$ is live cells (%) of Aβ treatment, $\text{L.C.}_{\cdot\text{Ncontrol}}$ is live cells (%) of negative control, and $\text{L.C.}_{\cdot\text{H2O2}}$ is live cells (%) of H_2O_2 treatment (positive control).

Statistical Analysis

For each experiment, at least 3 independent determinations were made. Significance of results was determined via the student t test with $p<0.05$ unless otherwise indicated. Data are plotted as the mean plus or minus the standard error of the measurement.

RESULTS

Effect of Hsp20 Assembly on Prevention of Aβ Aggregation

In previous work, I found that an optimum Hsp20 concentration existed for prevention of Aβ aggregation and toxicity. I had speculated that Hsp20 self assembled at higher concentrations and the assembled forms were not effective at preventing Aβ aggregation and toxicity. Size exclusion chromatography results indicated that at low concentrations, when Hsp20 was active and able to prevent both aggregation and toxicity, Hsp20 was predominantly in dimer form, however at concentrations higher than the optimum observed for activity, Hsp20 was predominantly in the form of large multimers with very little dimer present. (Lee et al., 2005) These results suggested that Hsp20 at low concentrations (in dimer form) had more activity than large assemblies of Hsp20. Recently Allison Rice-Ficht's lab (Department of Medical Biochemistry and Genetics, Texas A&M University) succeeded in cutting off 11 residues in the C-terminus of Hsp20, which was partly responsible for Hsp20 self assembly. Size exclusion chromatography (SEC) results showed that His-Hsp20 self assembly was drastically reduced when the 11 C terminal residues were removed. As shown in Fig. 6. 1, Hsp20 are mostly dimer with

small amount of small oligomeric species. Even at concentrations of 20 μM, more than 70% of the Hsp20 migrated as a dimer when the C terminal truncated protein was tested. (data not shown) If self assembly of Hsp20 resulted in loss of activity at high concentrations, then this C terminal truncated protein should have aggregation and toxicity prevention activity at concentrations well above that seen in the original untruncated protein.

In Fig. 6. 2, aggregation of 100μM Aβ when mixed for 24 hours with His-Hsp20 with or without 11 residues in C-terminus is shown. Extent of aggregation and fibril formation was measured with Congo red binding. Unlike our predictions of improved Hsp20 activity with the C terminal truncation, both the original Hsp20 and the C terminal truncated protein exhibited the same concentration dependence for aggregation prevention. About 80% of Aβ aggregation was prevented at concentration ranges of 1nM-1μM His-Hsp20. However, above 1 μM His-Hsp20, aggregation prevention activity decreased in both constructs. At 5μM of His-Hsp20 with and without the 11 C terminal residues, both proteins were able to decrease Aβ aggregation to 40% of that observed in Aβ samples not treated with Hsp20.

Based on these results, it was clear that mechanism of interaction of Aβ with Hsp20 was not as originally envisioned. Therefore, I carried out several experiments designed to help elucidate how Hsp20 interacted with Aβ.

Kinetics of Hsp20-Aβ Interaction

For Hsp20 to be a useful aggregation inhibitor (or model for an aggregation

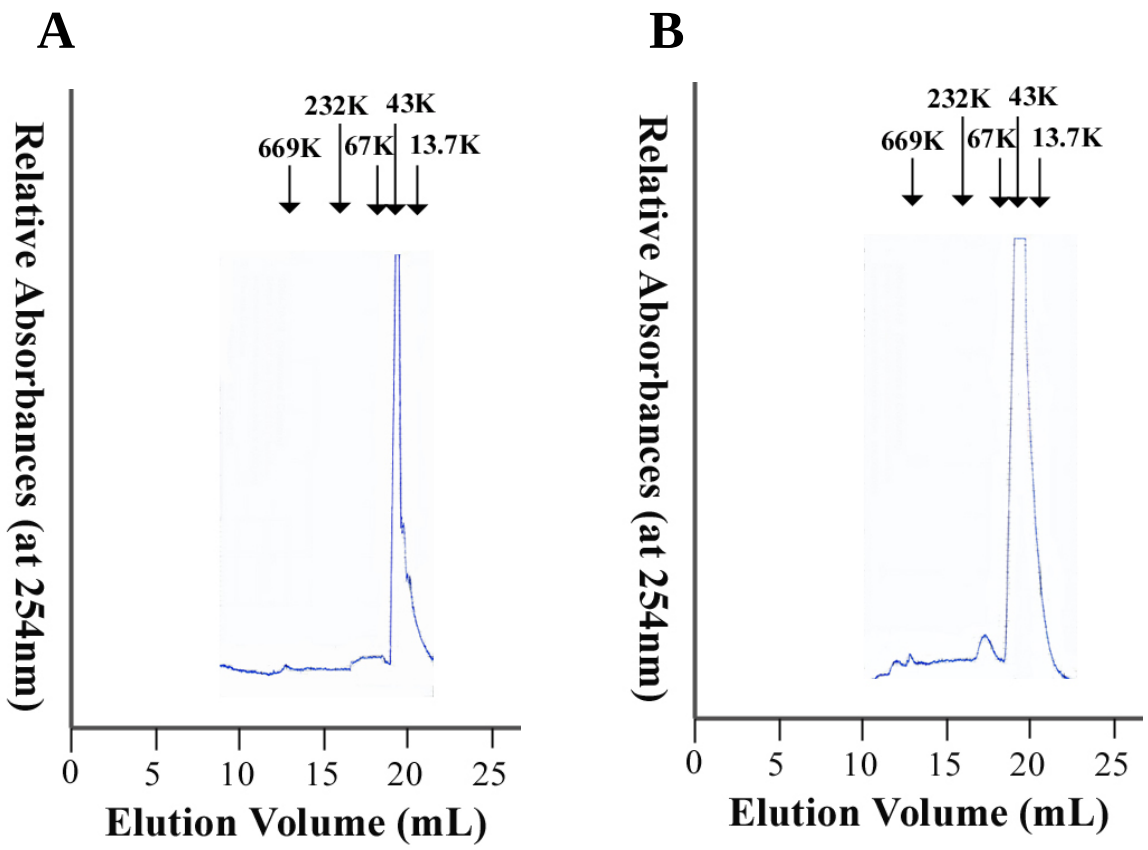

Figure 6. 1. SEC of His-Hsp20 without 11 residues in C-terminus. (A) 0.1μM of His-Hsp20 and (B) 5μM His-Hsp20

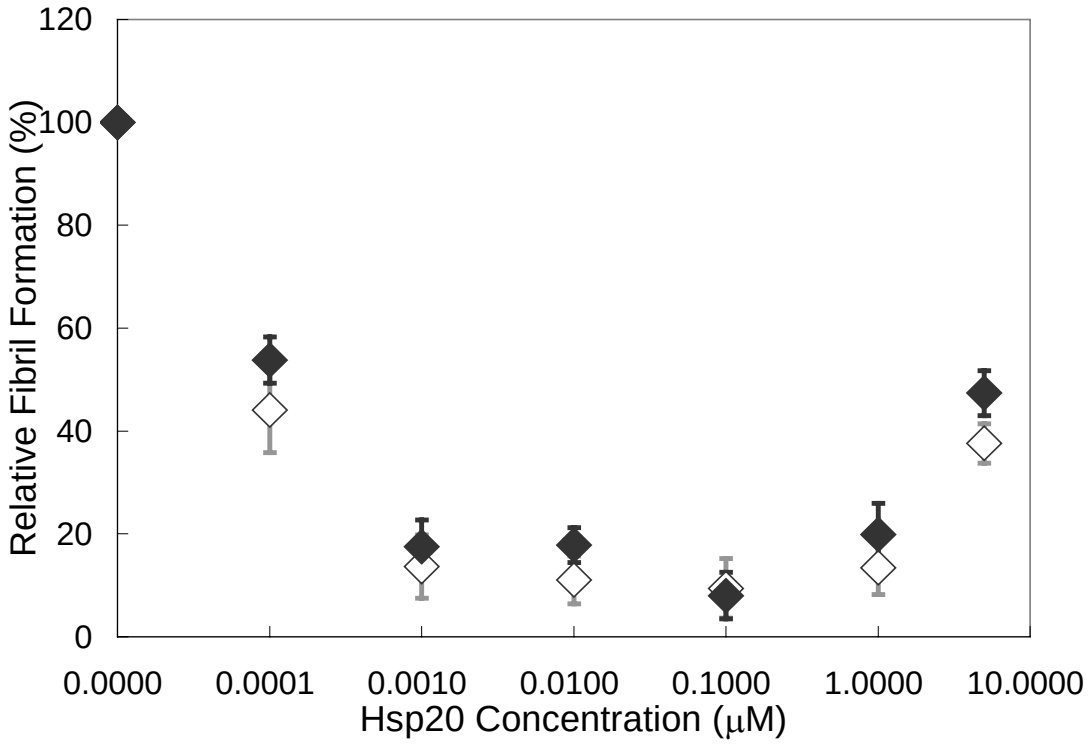

Figure 6. 2. Effect of His-Hsp20 with or without 11 residues on Aβ aggregation. Congo red was used as an indicator of Aβ aggregation. 100μM Aβ was mixed with His-Hsp20 at the beginning of Aβ incubation and the samples were mixed at 37^{o}C for 24 hours. [closed diamonds - His-Hsp20 with whole sequence, and open diamonds - His-Hsp20 without 11 residues in the C-terminus]

inhibitor) for Aβ, it was important to discern if Hsp20 simply slowed the rate of aggregation of Aβ, or actually altered the aggregation pathway of Aβ. To that end, I measured kinetics of Aβ aggregation as assessed via Congo red binding in the presence and absence of Hsp20. As seen in Fig. 6. 3, Aβ aggregation increases slowly at first, followed by a period of rapid increase in fibril content, which eventually saturates over time. When Hsp20 was added at the beginning of aggregation, fibril formation and Congo red binding followed a very different pattern. Initially, aggregation was accelerated, followed by a rapid loss in fibril content and ability to bind Congo red. These results suggest that Hsp20 does not simply slow the rate of Aβ aggregation, but actually changes the fibril formation pathway, possibly sequestering a fibril initiating species that forms early during aggregation and preventing further fibril growth.

In Fig. 6. 4, size exclusion chromatograms taken at different times during Aβ-Hsp20 incubation are shown. These chromatograms were collected in an attempt to isolated Aβ-Hsp20 intermediates to try to identify species formed in the mechanism of fibril formation prevention. Two peaks shown in Fig. 6. 4 corresponded to the molecular weights of around 87kDa, and 42kDa. The big peak of around 42kDa was the mixture of Aβ monomer and dimer and Hsp20 dimer. The small peak of around 87kDa was expected to be the complex of Aβ and Hsp20. I used mass spectrometry to try to confirm the presence of both Aβ and Hsp20 in complexes formed and to infer stoichiometry of binding, but with inconclusive results.

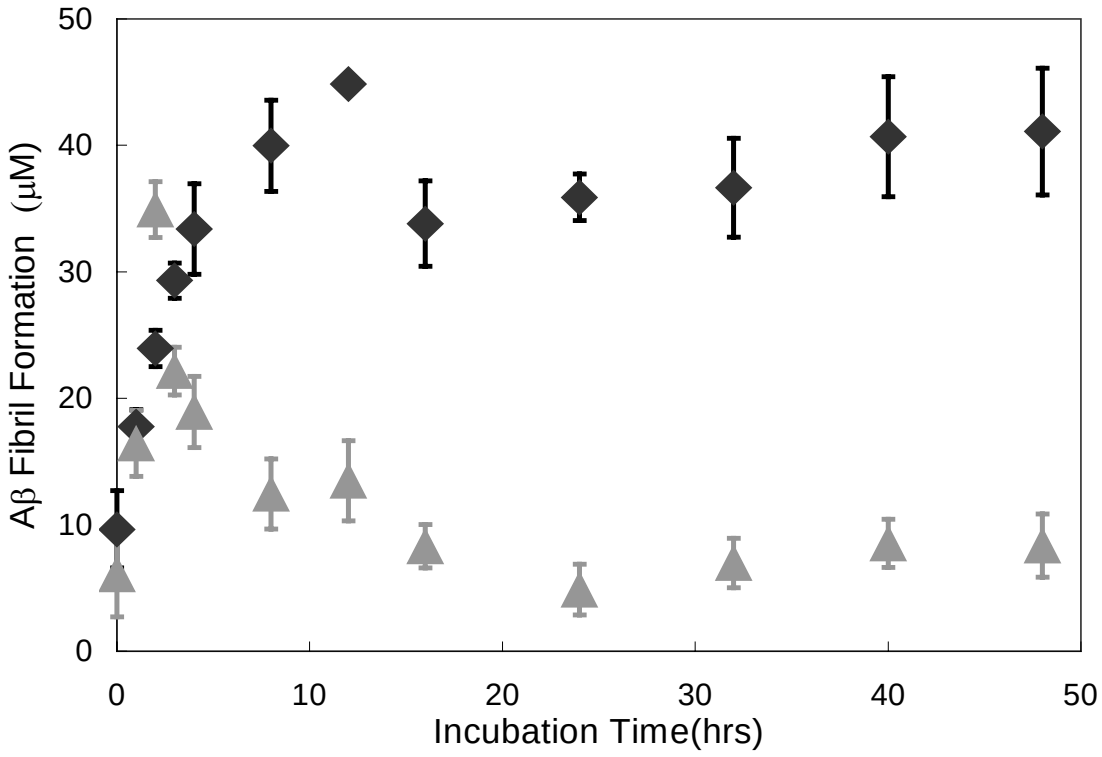

Figure 6. 3. Kinetics of Aβ aggregation using Congo red. [black diamonds – 100μM Aβ, gray triangles - 100μM Aβ and 0.1μM His-Hsp20]

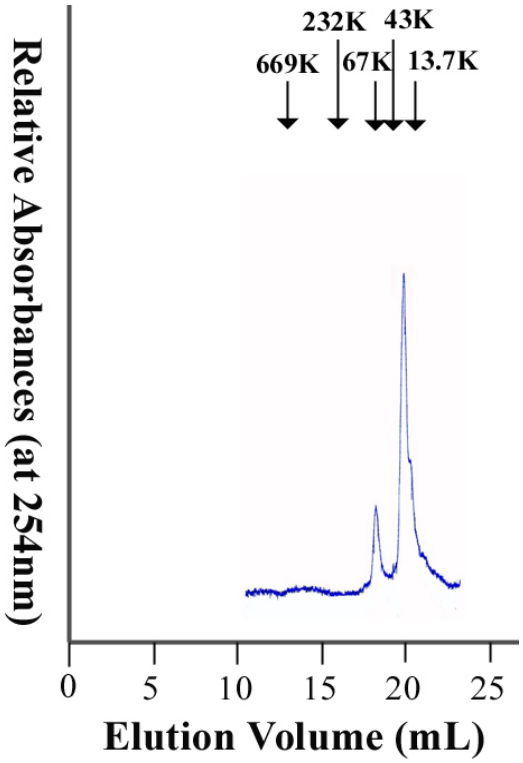

Figure 6. 4. Size Exclusion Chromatograms of the mixture of 100μM Aβ and 0.1μM His-Hsp20. Samples were mixed at the beginning of incubation, and incubated at 37^{o}C for 4 hours. After the incubation, samples are centrifuged at 7,000rpm for 3minutes and the supernatant is used for SEC.

Effect of His-Hsp20 on Non-Mixed Aβ Fibril Formation

I have shown in earlier work that Aβ aggregates via a different mechanism and forming different intermediates when aggregation is with mixing versus under static non-mixed conditions. If Hsp20 interacts with a fibril initiating species during aggregation that forms when Aβ is mixed, I wanted to assess if Hsp20 also interacted with Aβ when aggregation occurred without mixing. In Fig. 6. 5, I examined the effects of His-Hsp20 on the prevention of Aβ aggregation under static (non-mixing) conditions. A comparison of Fig. 6. 2 and Fig. 6.5 clearly indicate that while Hsp20 still reduces Aβ aggregation when aggregation occurs without mixing, Hsp20 is not nearly as effective at reducing aggregation as the maximum reduction in aggregation is 60 to 70% of the level of Aβ aggregation without Hsp20, while with mixing, between 90-100% of aggregation is prevented. In earlier work (Lee et al., 2005, Protein Science) I showed that the concentration of Hsp20 needed for optimal fibril prevention shifted to lower concentrations of Hsp20 when lower concentrations of Aβ were used. This appears to still be true when Aβ is aggregated without mixing. In Fig. 6. 5, 20μM, 50μM, and 100μM concentrations of Aβ1-40 were used for non-mixing aggregation experiments and 0.01nM to 5μM of Hsp20 was used for the prevention of Aβ aggregation. A broad range in optimal concentrations for fibril formation prevention was observed, with the lower end of the concentration ranges being near 1 nM, 2.5 nM, and 5 nM Hsp20 for Aβ concentrations of 20 μM, 50 μM, and 100 μM, respectively. At -Hsp20 concentration above 1 μM, His-Hsp20 was less effective at preventing fibril formation.

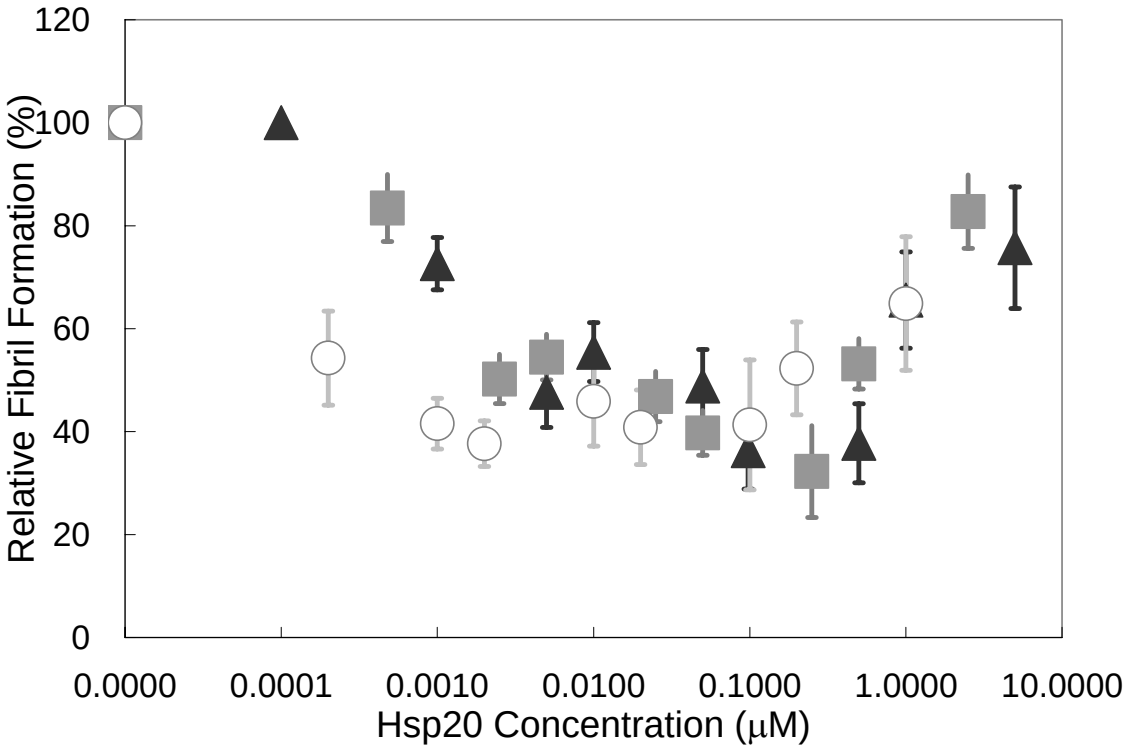

Figure 6. 5. Aβ aggregation with His-Hsp20 in non-mixing condition. 20, 50, 100μM Aβ was mixed with His-Hsp20 at the beginning of incubation, and those samples were incubated without mixing at 37^{o}C for 24 hours. After the incubation, Congo red binding experiment was done. [open circles – 20 μM Aβ, closed squares – 50 μM Aβ, and closed triangles – 100 μM Aβ]

Ability of His-Hsp20 To Prevent Toxicity of Aβ Under Mixing and Non-Mixing Condition.

Aβ is toxic to neuron-like cells when it is aggregated. The ultimate goal of Aβ aggregation prevention is to find agents which not only prevent aggregation, but also prevent Aβ toxicity. In order to assess the ability of His-Hsp20 to prevent Aβ toxicity, His-Hsp20 was added to mixed and non-mixed Aβ samples prior to Aβ aggregation, and toxicity of the Aβ-Hsp20 mixtures were tested as a function of time after incubation. As seen in Fig. 6. 6, His-Hsp20 was more at preventing the toxicity of mixed Aβ than non-mixed Aβ. This is consistent with data from Figures 6. 2 and 6. 5, where Hsp20 was more effective at preventing Aβ aggregation when mixed as compared to static non-mixed samples. Statistically, cell viabilities of mixed Aβ samples with His-Hsp20 at 2, 4, 8 hours were not different from negative control. ($p = 0.862$, 0.087, and 0.140 for 2, 4, and 8 hours respectively, p vales were obtained by two-tailed paired t test between samples and negative control, all p values were greater than 0.05) His-Hsp20 reduced the toxicity of non-mixed Aβ samples (viability was statistically different between Aβ sample and Aβ with His-Hsp20), but the non-mixed Aβ samples with His-Hsp20 still showed higher toxicities (about 30-40% toxicity) relative to negative controls.

Effect of His-Hsp17.7 on Aβ Aggregation and Toxicity

Results to date indicated that His-Hsp20 is very promising as an Aβ aggregation and toxicity inhibitor. However, while other research groups have investigated the use of other small heat shock proteins to prevent Aβ aggregation and toxicity, they have not

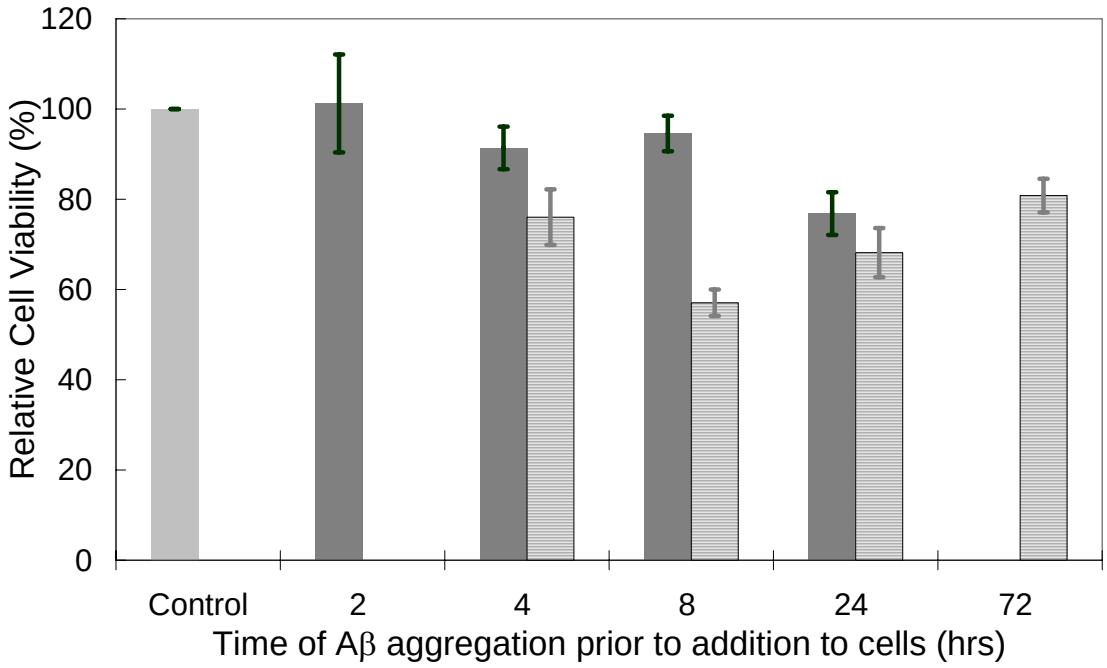

Figure 6. 6. Relative biological activities of Aβ species with His-Hsp20. 100 μM Aβ was mixed with 0.1 μM His-Hsp20 at the beginning of incubation. Some samples were mixed at 37^{o}C and taken out at 2, 4, 8, and 24 hours. The other samples were not mixed at 37^{o}C and taken out at 4, 8, 24, and 72 hours. These samples were added to SH-SY5Y cells, and incubated with the cells for 2 hours. [light solid bar - negative control (no Aβ treatment), dark solid bar – Aβ with His-Hsp20 in mixing condition, and stripe bar - Aβ with His-Hsp20 in non- mixing condition]

seen the same success. Thus, I set out to determine if other small heat shock proteins could prevent Aβ aggregation and toxicity in our hands, and if not, to elucidate differences between small heat shock protein activity in order to determine the mechanism of activity of Hsp20. I examined His-Hsp17.7, a small heat shock protein derived from carrot and cloned into *E.coli.,* for its ability to prevent Aβ aggregation and toxicity. Congo red was used as an indicator of Aβ aggregation. 20 μM of Aβ was used for aggregation and biological activity experiments. As seen in Fig. 6. 7A, His-Hsp17.7 prevented Aβ aggregation at all concentrations about 1 nM, without the apparent loss of activity seen Hsp17.7. Addition of Aβ to cells resulted in about 30% toxicity. Samples in which Aβ was treated with His-Hsp 17.7 had statistically the same toxicity as when Aβ alone was added to cells(all p values were greater than 0.05 between Aβ sample and other samples containing Hsp17.7). Thus, unlike Hsp20, Hsp17.7 prevented aggregation without preventing Aβ toxicity.

Effect of Hsp27 on Aβ Aggregation and Toxicity

Hsp27 is a human small heat shock protein and has been reported to be expressed in the brain of AD patients. (Renkawek et al. 1999) In experiments analogous to those used to examine the activity of Hsp20 and Hsp17.7, the aggregation and toxicity prevention activities of Hsp27 were examined. 100 μM of Aβ and 1nM-5 μM of Hsp27 were used for aggregation and biological activity experiments. As shown in Fig. 6. 8A, Hsp27 prevented Aβ aggregation at high concentrations as in the case of Hsp20. At higher concentration of 0.1μM up to 20μM, His-Hsp17.7 still exhibited the same or

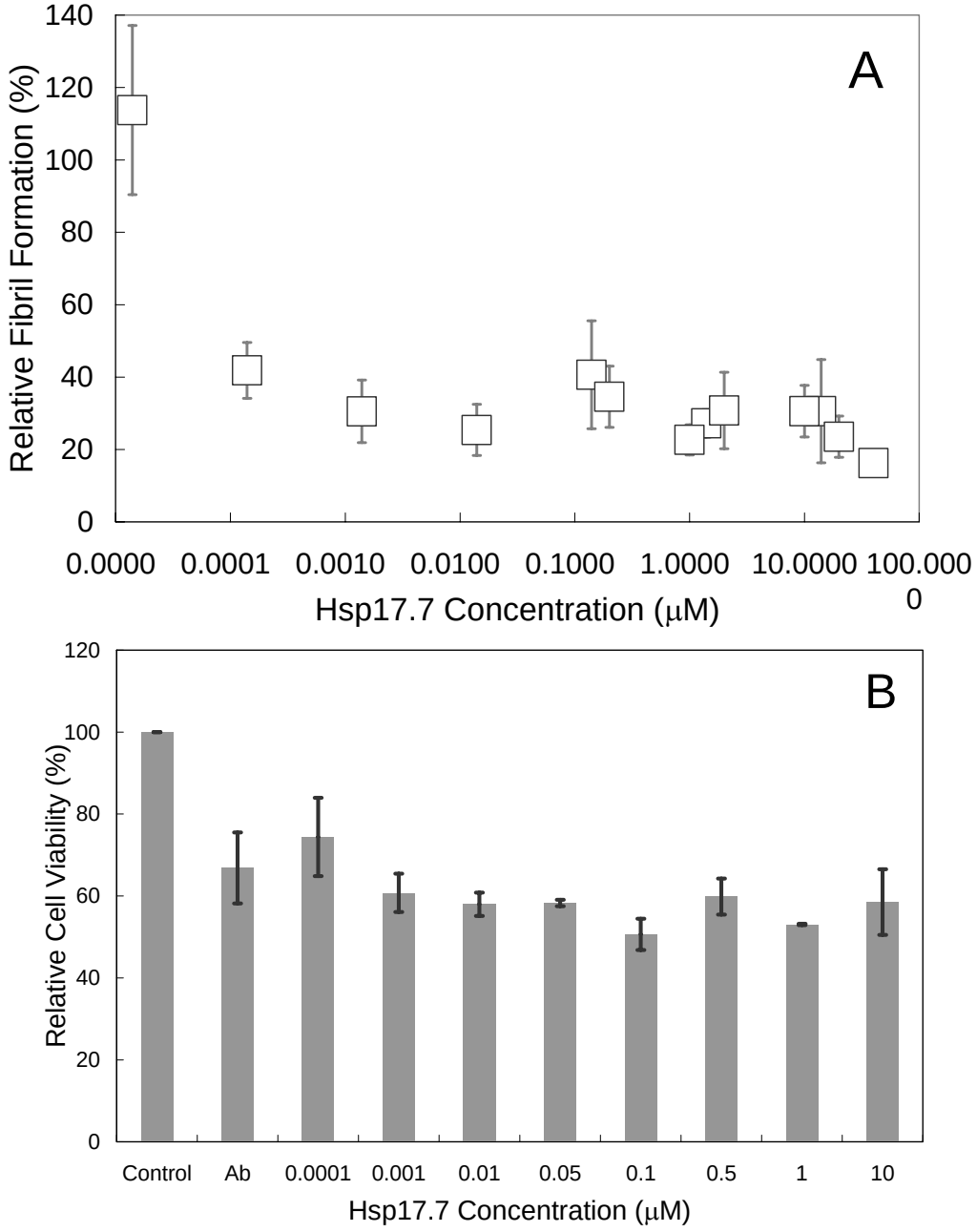

Figure 6. 7. Activities of His-Hsp17.7 to prevent Aβ aggregation and toxicity. All sample preparations were same as Aβ with His-Hsp20 in mixing condition. (A) Aβ aggregation with His-Hsp17.7 using Congo red (B) Biological activities of Aβ with Hsp 17.7 using two dyes in FACS array.

better activity at Aβ aggregation prevention. Fig. 6. 7B shows the biological activity of Aβ when incubated with His- with near the same effectiveness and at similar concentration ranges as Hsp17.7. Unlike Hsp20, Hsp27 did not loose its ability to prevent Aβ aggregation at high concentrations (5μM of Hsp27). In the toxicity experiments shown in Fig. 6. 8B, the samples containing Hsp27 incubated with Aβ had the same or more toxicity than the toxicity of Aβ alone. Statistically, cell viabilities of 100 μM Aβ with 5nM – 1 μM Hsp27 were not different from that of 100 μM Aβ. (all p values are greater than 0.05) 1nM and 5 μM Hsp27 increased the toxicity of 100 μM Aβ. In other words, Hsp27 did not protect the cells from the toxicity of 100 μM Aβ.

Electron Micrograph (EM) Images of Aβ with Small Heat Shock Proteins

I have data from 3 small heat shock proteins, each which prevent Aβ aggregation as measured by Congo red binding, however only one prevents Aβ toxicity. It is clear from these results that preventing extended β-sheet structure formation, the property which Congo red assesses, is necessary but not sufficient to prevent Aβ toxicity. To further exam the relationship between Aβ structure, sHsp-Aβ interactions, and aggregation and toxicity prevention activities, I used electron microscopy to examine structures formed by Aβ in the presence of the small heat shock proteins.

In one stet of experiments, I examined structures formed by 100 μM Aβ and 0.1 μM His-Hsp20 as a function of time during incubation with mixing, analogous to the kinetic data shown in Figure 6. 3. As seen in Fig. 6. 9, as early as 1-hour after incubation, Aβ and Hsp20 began to complex ring-like structures. At two hours, a more

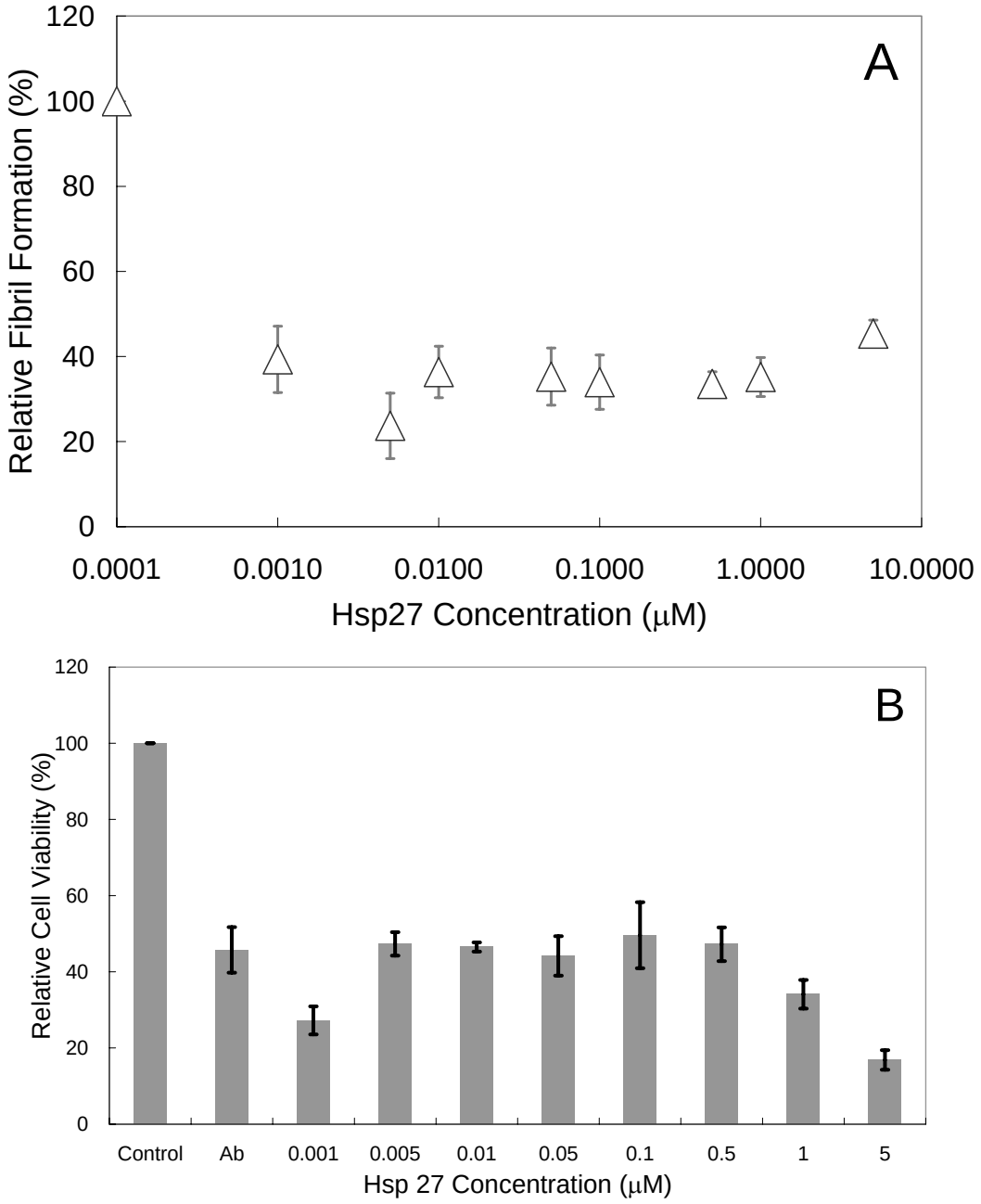

Figure 6. 8. Activities of recombinant Hsp27 to prevent Aβ aggregation and toxicity. All sample preparations were same as Aβ with His-Hsp20 in mixing condition. (A) Aβ aggregation with Hsp27 using Congo red (B) Biological activities of Aβ with Hsp27 using two dyes in FACS array.

well defined multi-ring structure was observed. The appearance of this large multi-ring structure corresponds to the maximum in Congo red binding seen in Aβ-Hsp20 mixtures seen in Figure 6. 3. At later times, the ring structures seem to fall apart, with few rings observed in micrographs at 24 hours after incubation. The large multi-ring structure was only seen in micrographs of Aβ and Hsp20 when 100 mM Aβ and 0.1 mM Hsp20 were used. When the same concentration of Aβ, but higher and lower concentrations of Hsp20 were used (1nM, 0.01 μM, 1 μM, and 5 μM Hsp20), the complex ring structure was not observed (data not shown). Thus, the formation of the large multi-ring complex observed in Figure 6. 9 appears to be dependent upon the stochiometery of the Aβ-Hsp20 interaction.

As seen in Figure 6. 10, similar electron microscopy studies were performed with Aβ and Hsp20 in non-mixing condition or Hsp17.7. At no time during incubation of Aβ and Hsp17.7 were the large multi-ring complexes observed in micrographs. I also examined structures formed 24 hours after incubation of Aβ and Hsp20 in non-mixing condition or Hsp17.7, as these structures would represent the complexes added to cells in culture for toxicity assays. Differences in these structures might point to clues as to the differences in structures formed and their relationship to cell toxicity.

DISCUSSION

Small heat shock proteins (sHsps) are expressed in almost all organisms when cells become stressed during exposure to unfavorable environments. Small heat shock proteins exist as large oligomeric complexes of 300-800kDa with monomeric molecular

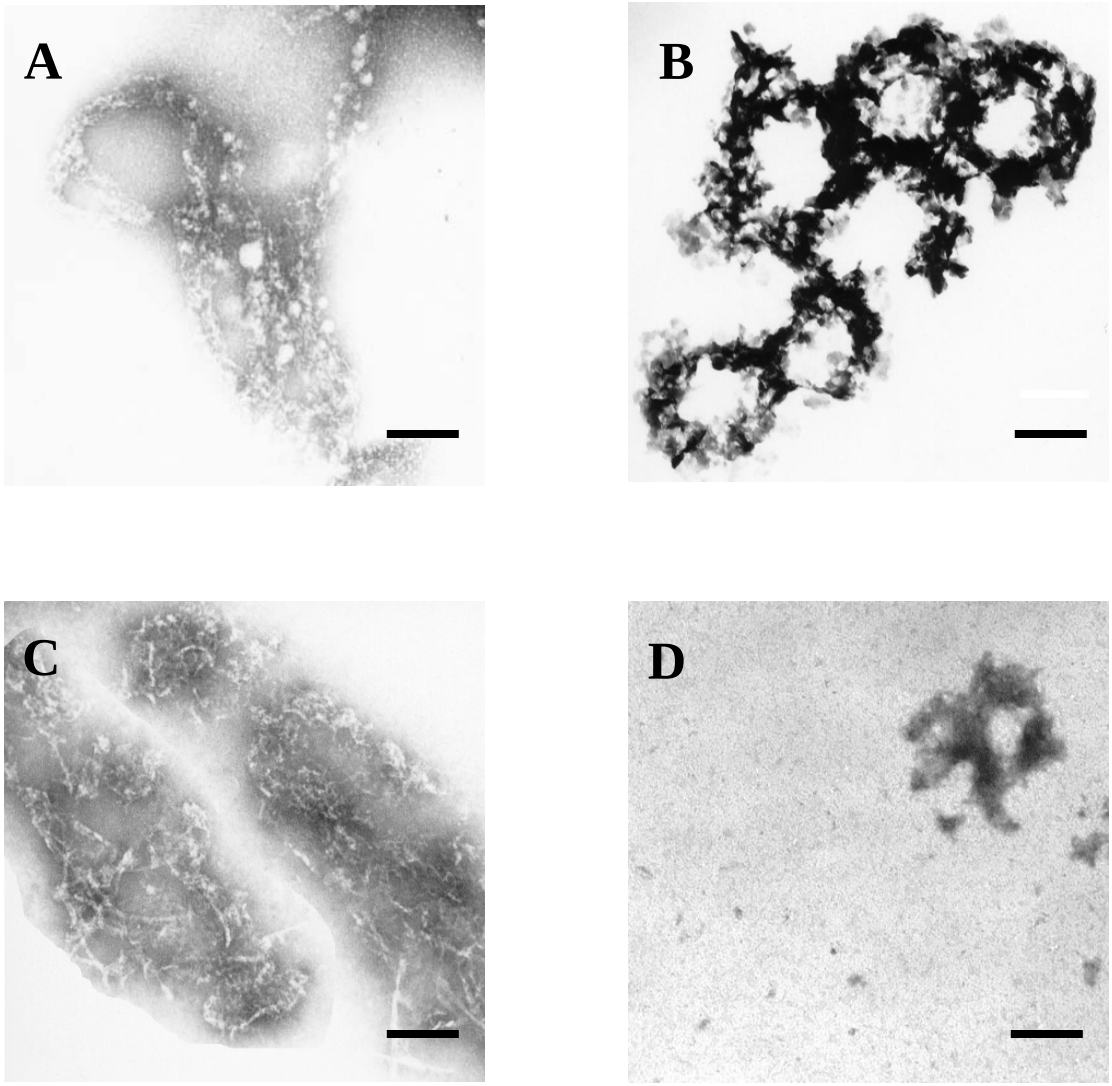

Figure 6. 9. Electron micrograph images of Aβ with His-Hsp20 in mixing condition. 100 μM Aβ with 0.1 μM His-Hsp20 in (A) 1 hour, (B) 2 hour, (C) 4hour, and (D) 24 hour incubation respectively. The length of scale bar is 100nm.

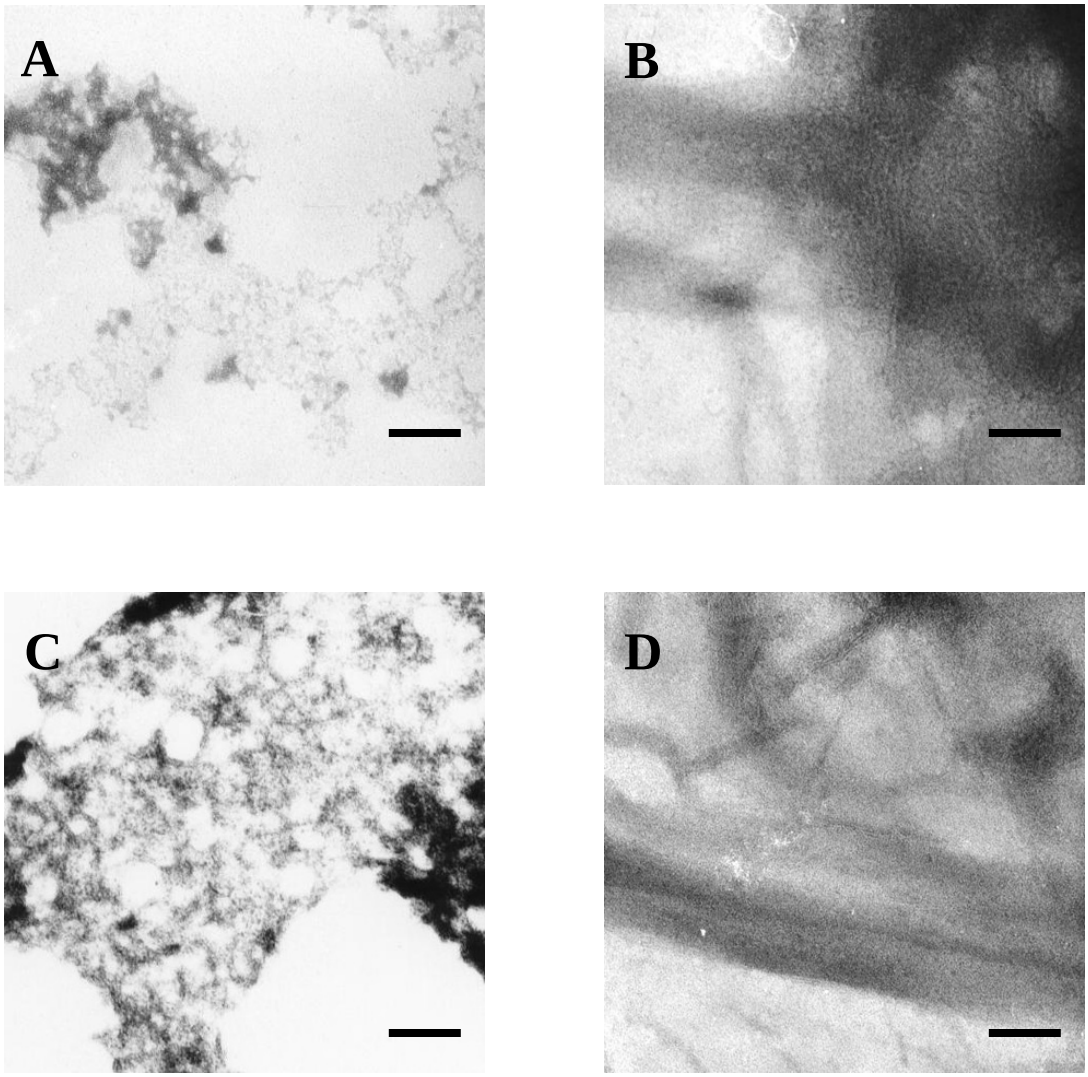

Figure 6. 10. Electron micrograph images of Aβ with His-Hsp17.7 and His-Hsp20. 100 μM Aβ with 2μM His-Hsp17.7 in mixing condition (A) 2 hour, (B) 24 hours, and 100 μM Aβ with 0.1 μM His-Hsp20 in mixing condition. (C) 8hours, (D) 72 hours incubation respectively. The length of scale bar is 100nm.

mass of 15-43kDa. (van den et al. 1999; Clark and Muchowski 2000; MacRae 2000) The primary roles of sHsps are to stabilize other proteins under stress conditions and protect them from aggregation. (van den et al. 1999; Bruey et al. 2000) sHsps are composed of three parts in the primary sequence, the N-terminal domain, the α-crystallin domain, and the C-termial extension. The α-crystallin domains, highly conserved 80-100 amino acid sequences located in the C-terminal regions, are very important for substrate binding. (de Jong et al. 1993) The N-terminal domain is responsible for sHsp assembly, which results in polydisperse sHsp. Some sHsps are active when they are assembled in large multimeric complexes, whereas some other sHsps are active when they are dissociated. In a previous chapter, I showed, using SEC that the dominant species of Hsp20 at concentrations below 0.1μM are dimers which are the active form to prevent Aβ aggregation. In the first Hsp20 constructs prepared, Hsp20 self assembles into large heterogeneous complexes at concentrations higher than 0.1μM. In this range, Hsp20 was less effective at preventing Aβ aggregation. (Lee et al., 2005) I suggested that the loss of Hsp20 activity at high concentrations was a result of its assembly into inactive multimers. In this work, I used a new Hsp20 construct, which is predominantly dimer at high concentrations, however, as seen in Figure 6. 2, its activity is indistinguishable from that of an Hsp20 construct which aggregates at high concentrations. These results suggest that the loss of activity at high concentrations of Hsp20 is not due to aggregation, but to some other phenomena. There are several possible explanations for the loss of Hsp20 activity at high concentrations, or the presence of an optimal activity at intermediate concentrations. Hsp20 could form micelles at high concentrations, thus

effectively reducing the concentration of Hsp20 available for binding to Aβ. Micelles of Hsp20 would fall apart under SEC conditions and thus not be detected. However, if micelles were formed, one would expect a critical micelle concentration at which Hsp20 looses activity regardless of the concentration of Aβ added. This is not the behavior I have seen, either in earlier work (Lee et al., 2005) or in this work (Figure 6. 5). Instead, I see that the range of activity of Hsp20 and the concentration at which Hsp20 begins to loose activity is always proportional to the concentration of Aβ used in the experiment.

Another possible hypothesis to explain the optimum Hsp20 activity at intermediate concentrations is that Hsp20 binds Aβ stoichiometrically. I still postulate that the Hsp20 dimer is the active form in Aβ aggregation prevention, but I postulate that there is multivalent binding between an Aβ species and the Hsp20 dimer, and at specific ratios of concentrations of active species, large complexes of the active species can form, much like an agglutination reaction with antibody and polyvalent antigen. Such an explanation would explain the formation of large multi-ring complexes of Aβ and Hsp20 (Figure 6. 9), much larger than what one would expect of dimer or Aβ species alone, that only form at specific concentration ratios.

Although the mechanisms of action and structures associated with the interaction between sHsps and their substrates are still under investigation, two possible mechanisms have been suggested. One mechanism is that partially unfolded proteins are refolding in the sHsp cavity which is formed by assembly of sHsp subunits. The other mechanism is that partially unfolded proteins interact with multiple α-crystallin domain of sHsp in the cleft of sHsp subunits. (Ganea 2001) It is not clear that Hsp20 can form a

large assembly with a cavity by itself. In electron microscope images, Hsp20 forms relatively disordered assemblies composed of subunits (dimers) at higher concentrations (data not shown), however, no cavity was observed in these assemblies. Based on two observations (Hsp20 dimer is the active form, and no cavity is observed in Hsp20 assemblies), I postulate that Hsp20 could prevent Aβ aggregation via the interaction of multiple α-crysatllin domains in Hsp20 with Aβ. In the stoichiometric binding hypothesis, at low concentrations of Hsp20, there is not sufficient Hsp20 to completely prevent Aβ aggregation. However, at higher concentrations of Hsp20, Hsp20 interferes with the interaction between Hsp20 and Aβ. According to Congo red results from 20μM, 50 μM, and 100 μM Aβ, those data are well overlapped when they are plotted as a function of mole concentration ratio (Hsp20/Aβ) rather than mole concentration of Hsp20. EM and MALDI-MS results show that the large ring structures are formed only at the optimum ratio between Aβ and Hsp20. Figures 6. 3 and 6. 9 indicate that Hsp20-Aβ complexes form a large species at 2 hours incubation. When an optimum ratio mixture of Hsp20 and Aβ (0.1 μM His-Hsp20 and 100 μM Aβ) were incubated for 2 hours, centrifuged (12,000 rpm for 3 minutes), then subjected to MALDI-MS, approximately 90% of both proteins were found in the centrifuged pellet, suggesting both proteins participated in forming a the large complex seen in EM. At concentrations other than the optimum ratio, only 50% of Aβ and Hsp20 were in the pellet. Congo red, EM, and MALDI-MS results suggest that Aβ binds to Hsp20 stoichiometrically to form the large multi-ring structure at only an optimum concentration ratio.

Fig. 6. 5 indicates that when Hsp20 with Aβ and incubated without mixing, that

Hsp20 is not as effective at preventing Aβ aggregation as occurs when mixing is used. One of the possible explanations for this result is the kinetics problem related to diffusion. In mixing conditions, Hsp20 can collide with Aβ before Aβ forms fibrils, whereas Aβ forms fibrils before Hsp20 can bind to Aβ in non-mixed condition (with mixing, the rate of Hsp20-Aβ collision and reaction is faster than fibril growth, where as without mixing, fibril growth is faster). Based on data comparing the rate of fibril growth with mixing and without mixing, I suggest that the rate of fibril nucleation or initiation is the slowest step in both cases, and that mixing greatly increases the rate of fibril nucleation. When Hsp20 is present, I postulate that Hsp20 binds to a fibril nucleating species or rare intermediate that forms prior to fibril nucleation. This species would be more abundant during mixing than during static conditions, making it far more probable that Hsp20 would collide with this nuclei or intermediate when mixing was used.

Another possibility is that Hsp20 can't bind multivalently to Aβ (as per the stochiometric binding hypothesis) in the non-mixing condition because the conformation of Aβ intermediates during aggregation are different when aggregation occurs with mixing versus under static conditions. I have shown in an earlier chapter that under static conditions, Aβ appears to undergo an intramolecular rearrangement prior to fibril growth that does not occur when Aβ aggregates with mixing. This would suggest that the fibril nucleating species have different structures and exposed hydrophobic surfaces when prepared with mixing or without mixing. The α-crystallin domain is known to play an important role in the interaction with the hydrophobic region of a partially unfolded

protein, (Stevens and Augusteyn 1997; Sharma et al. 1998) and results in protein folding of the substrate protein. Mutation studies in α-crystallin domain suggest that the substrate binds to the α-crystallin domain by multiple contacts. (Derham et al. 2001) The α-crystallin domain of Hsp20 would favor binding to the β-sheet structure of Aβ aggregation intermediate that is observed prior to fibril growth in mixing condition rather than random coil structure of the Aβ intermediate observed in non-mixing condition.

In Alzheimer's disease (AD) and in dementia associated with Parkinson's disease, an increased expression of Hsp27 and of αB-crystallin was found (Iwaki et al. 1989; Renkawek et al. 1999). These results suggest that chaperone activity of heat shock proteins may contribute to the pathogenesis associated with protein aggregation in Alzheimer's disease (Kudva et al. 1997). Other research groups showed that αB-crystallin prevented Aβ fibril formation *in vitro*, but not the toxicity. (Stege et al. 1999) Human Hsp27 inhibited fibril formation of Aβ1-42 *in vitro*, but it was less effective on the pre-formed amyloid. (Kudva et al. 1997) Fig. 6. 7 and 6. 8 show that both Hsp17.7 and Hsp27 prevent Aβ aggregation but not toxicity. Conclusively, Hsp17.7 and Hsp27 can prevent only Aβ1-40 aggregation, but Hsp20 prevents Aβ1-40 aggregation and toxicity. The α-crystallin domains of these sHsps could be the crucial parts of the proteins in preventing Aβ aggregation because the α-crystallin domains are well-conserved regions and are found in Hsp20, Hsp17.7, and Hsp27. The results of sequence homologies using the software CLUSTALW (EMBL-European Bioinfomatics Institude) show that sequences between sHsps are not homologous. (32% - αB-crystallin and

Hsp27, 15% - αB-crystallin and Hsp17.7, 8% - αB-crystallin and Hsp20, 17% - Hsp20 and Hsp17.7, 7% - Hsp20 and Hsp27, and 7% - Hsp17.7 and Hsp27) The sHsps lack sequence homology in both the N-terminus, and C-terminal extension. These differences could result in different binding affinity between sHsp and Aβ or in different mechanisms by which when they prevent Aβ aggregation. Only Hsp20 forms a large multi-ring structure with Aβ (at 2 hours in mixing condition), whereas the other sHsps were not observed to form ring structures. These data suggest that Hsp20 may have a unique mechanism of interaction with Aβ that results in different activity in Aβ toxicity prevention relative to other sHsps.

CHAPTER VII

FUTURE DIRECTIONS

The research presented in this dissertation indicates that different Aβ incubation conditions *in vitro* can affect the rate of Aβ fibril formation, the morphology, the toxicity and the conformation of intermediates in the aggregation pathway. And a series of experiments also show that small heat shock proteins (Hsp20, Hsp17.7 and Hsp27) can prevent Aβ aggregation. However only Hsp20 prevents Aβ toxicity *in vitro*, whereas Hsp17.7 and Hsp27 do not. Future work described in this chapter will focus on understanding the kinetics of Aβ aggregation. These studies will be helpful in understanding features of Aβ aggregation that lead to the formation of toxic oligomers. In other future work, studies to examine the mechanism of sHsps interaction with Aβ to prevent aggregation and toxicity will be discussed.

THE KINETICS OF Aβ AGGREGATION

Based on Congo red binding results, Aβ fibril formation follows a characteristic sigmoidal curve, with a lag phase at early incubation times, followed by a fibril growth phase, then a saturation phase. The characteristic lag phase implies that there is a classic nucleation dependent mechanism of aggregation. In this research, the kinetic mechanism of Aβ aggregation in with mixing will be based on the assumption that a nuclei initiates fibril formation. A proposed mechanism is shown:

$$2\,M \xleftrightarrow{k_1} D \qquad (7\text{-}1)$$

$$M \xleftrightarrow{k_2} U \tag{7-2}$$

$$n\,U \xleftrightarrow{k_3} N \tag{7-3}$$

$$N + j\,U \xleftrightarrow{k_4} f_j \tag{7-4}$$

$$m\,f_j \xrightarrow{k_5} F_j \tag{7-5}$$

where M, and D are monomer and dimer with α-helix/random coil structure, U is unfolded monomer with a β-sheet rich structure, N is a nuclei, f_j is a filament composed of nuclei and j unfolded monomer, F_j is fibril made from lateral aggregation of m filaments,. k_1, k_2, k_3, k_4, and k_5 are the forward rate constants in each steps. K_1, K_2, K_3, and K_4 are equilibrium constants corresponding to reactions 1 thru 4. n, j, and m are constants. The rate equation for fibril production based on this mechanism is

$$\frac{dF_j}{dt} = k_5\ f_j^{\,m} \tag{7-6}$$

Integration of equation (7-6) based on mass balance and equilibrium relationships gives

$$\sum_{i=1}^{2} A_i\,(M^{i-m(n+j)} - M_o^{\,i-m(n+j)}) + C\,(M^{n-m(n+j)} - M_o^{\,n-m(n+j)}) + D\,(M^{n-m(n+j)} - M_o^{\,n-m(n+j)}) = t$$

where M is the Aβ monomer concentration with time, M_o is initial Aβ monomer concentration, t is incubation time, A_1, A_2, C, and D are constants composed of equilibrium constants, rate constant, m, n, and j.

$$A_1 = \frac{K_2^{\,-m(n+j)}\,(1+K_2)}{m(n+j)\,k_5\,(K_3\,K_4)^m\,[1-m(n+j)]}$$

$$A_2 = \frac{4\,K_1\,K_2^{\,-m(n+j)}}{m(n+j)\,k_5\,(K_3\,K_4)^m\,[2-m(n+j)]}$$

$$C = \frac{n^2 K_3 K_2^{\,n-m(n+j)}}{m(n+j)\,k_5 (K_3 K_4)^m [\,n - m(n+j)\,]}$$

$$D = \frac{(n+j)^2\ K_3 K_4 K_2^{\,(1-m)(n+j)}}{m(n+j)\,k_5 (K_3 K_4)^m [\,n+j-m(n+j)\,]}$$

Equilibrium constants, rate constants, and stochiometric constants m, n, and j can be determined from experimental data.

Figure 7. 1 shows a preliminary result of a study of the kinetics of Aβ aggregation from SEC and turbidity data. Open diamonds are fibril amounts obtained by turbidity at 405nm. Closed triangles and circles are Aβ dimer and monomer respectively from SEC data. From these data, equilibrium constants, rate constants, m, n, and j can be estimated by nonlinear regression.

This type of analysis will enable us to examine the relative rate of different steps in Aβ aggregation, and how manipulation of individual rates (i.e. of nucleation or fibril growth) will affect the final morphology and toxicity of the Aβ aggregation species formed.

THE MECHANISMS OF HSP20 TO PREVENT Aβ AGGREGATION AND TOXICITY

All types of Hsp20 (Hsp20-MBP (maltose binding protein fusion), His-Hsp20 (polyhistidine fusion) and His-Hsp20 without 11 residues in C-terminus) are able to prevent Aβ1-40 aggregation and toxicity. However, Hsp17.7 and Hsp27 can inhibit Aβ1-40 aggregation but not its toxicity. For future drug development, it will be very

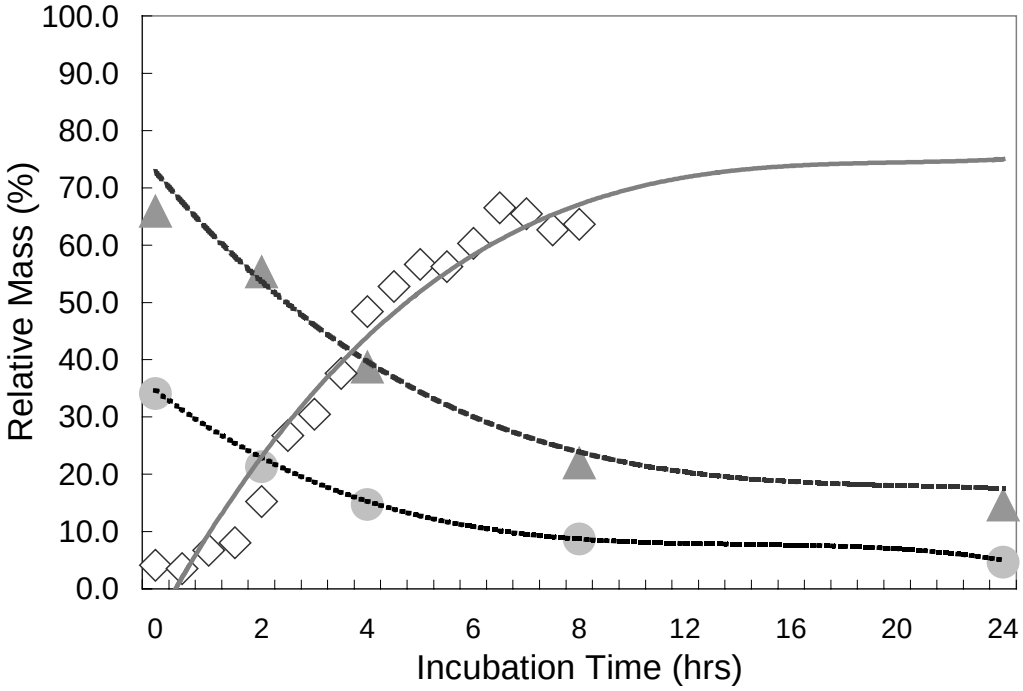

Figure 7. 1. Concentration change of Aβ species with time. Concentrations of monoer (closed circles) and dimer (closed triangles) were detected by SEC and fibrils (open diamonds) were detected by turbidity assay at 405nm.

important to understand the differences between Hsp20 and Hsp17.7/Hsp27.

One of the plausible hypotheses to explain the difference between Hsp20 and Hsp17.7/Hsp27 is that all sHsps prevent Aβ aggregation by a hydrophobic interaction of Aβ with the α-crystallin domains of the sHsps, but only Hsp20 inhibits Aβ toxicity by an electrostatic interaction with Aβ. In fibril formation, hydrophobic forces in the middle of Aβ sequences and at the end of C-terminus are very important. (Tjernberg et al. 1999) Electrostatic interactions in Aβ are associated with Aβ binding to membrane mimicking lipids. (Ege and Lee 2004) These data suggest that hydrophobic forces and electrostatic forces could be the dominant driving forces in Aβ aggregation and toxicity, respectively. Partially unfolded proteins interact with multiple α-crystallin domains of sHsp in the cleft of sHsp subunits. (Ganea 2001) The α-crystallin domain is known to play an important role in interaction with hydrophobic regions of partially unfolded protein, (Stevens and Augusteyn 1997; Sharma et al. 1998) and results in the correct folding of substrate protein. sHsps could prevent Aβ aggregation via the interaction of multiple α-crysatllin domains composed of hydrophobic β-sheet structures. According to a Kite and Doolittle (hydrophobicity) analysis, Hsp20 has less hydrophobic character (or more hydrophilic character) at the end of N-terminal domain and/or the beginning of α-crystallin domain, whereas other sHsps have less hydrophilic character (or more hydrophobic character in those regions.) The y axis of Kite and Doolittle plot is the hydrophobicity (positive values indicate hydrophobic character and negative values indicate hydrophilic character) and the x axis is the protein residues. In preliminary results of a Kite and Doolittle analysis, αB-crystallin (light line) and Hsp20 (dark line)

are shown in A, αB-crystallin (light line) and Hsp17.7 (dark line) in B, αB-crystallin (light line) and Hsp27 (dark line) in C.

In the result shown in Figure 7. 2A, both αB-crystallin and Hsp20 have hydrophobic character in the α-crystallin domain. Hsp20 has more hydrophilic residues at around 70-90, whereas αB-crystallin is hydrophobic at the corresponding residues. In the results shown in Figure 7. 2B and C, Hsp17.7 and Hsp27 have hydrophobic residues at α-crystallin domains like αB-crystallin and Hsp20. However, Hsp17.7 and Hsp27 have more hydrophobic residues like αB-crystallin where Hsp20 has more hydrophilic residues.

In order to determine if electrostatic binding between Aβ and sHsp plays a role in aggregation or toxicity prevention, a method of examining protein-protein interaction could be helpful. One of the programs used for predicting protein-protein interactions is Hex. First of all, Hex calculates all possible positions between ligand protein and receptor protein based on 3D parametric function by surface shape, electrostatic charges, and potential distributions. From these results, orthogonality properties (translational or rotational properties) can be calculated. After this step, steric hindrances and residue refinements are calculated. From a series of calculations, this program seeks protein-ligand positions which minimize the interaction energy. With the Hex program, better predictions are possible with smaller rigid proteins than larger molecules, and 3D structure information is necessary. Unfortunately, 3D structures of Hsp20, Hsp17.7, Hsp27, and αB-crystallin have not been characterized. Among sHsps, 3D structure information is only available for Hsp16.9 and Hsp16.5. The good news is that Hsp16.5

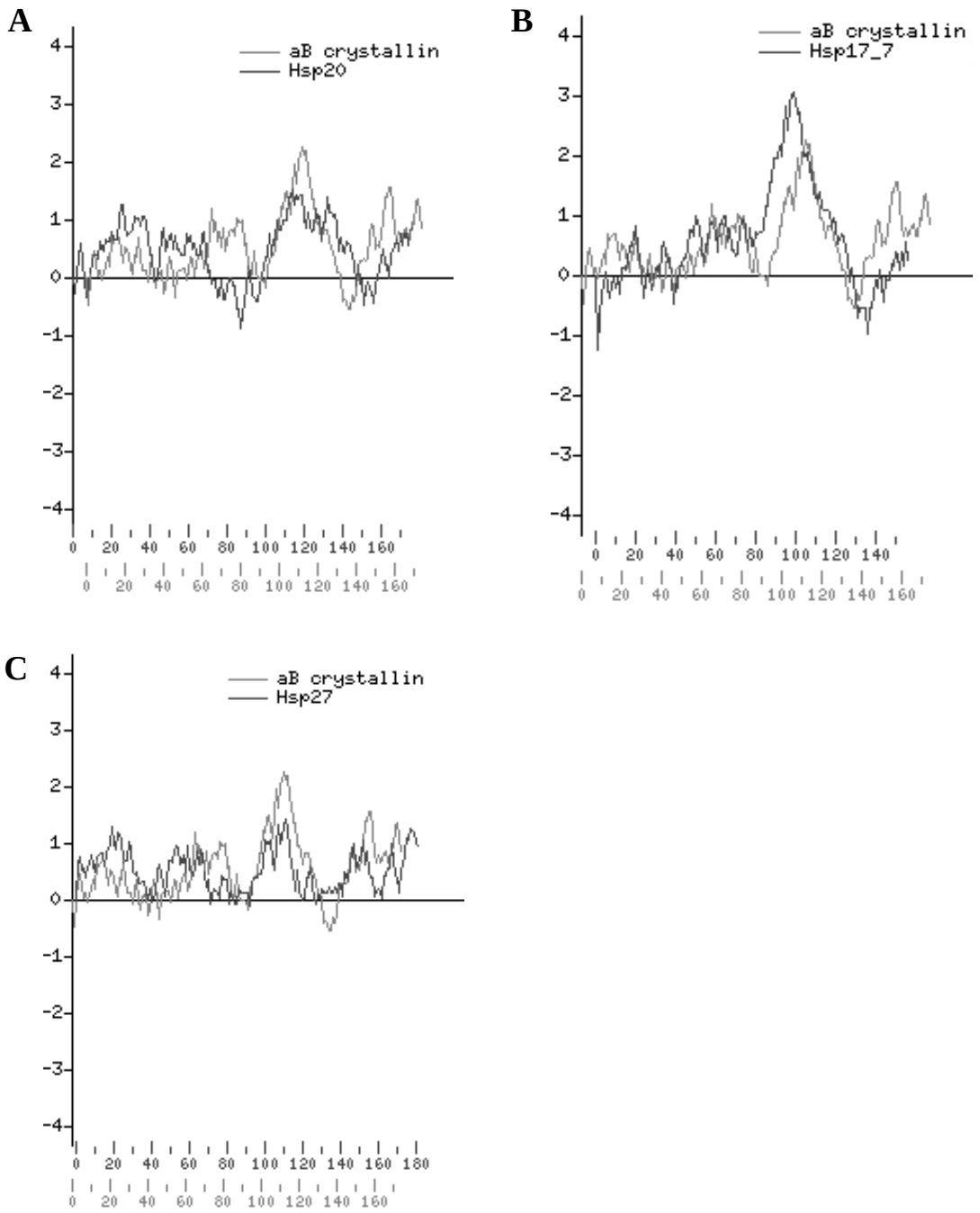

Figure 7. 2. Hydrophobicities of small heat shock proteins by using Kite and Doolittle. Light color lines – αB-crystallin and dark color lines - (A) Hsp20, (B) Hsp17.7, and (C) Hsp27

has a similar hydrophobic profile to Hsp20, and Hsp16.9 has a profile similar to αB-crystallin, Hsp17.7 and Hsp27. (Kite and Doolittle data are not shown). In order to examine the effect of electrostatic interactions, Aβ1-16 was used instead of whole peptides.

Figures 7. 3A and B are the result of the prediction of the interaction between Aβ1-16 and Hsp16.5 (A), and Hsp16.9 (B). Total energies of interaction between Aβ and the sHsp in A and B are –63.71, and –0.43, respectively. These results imply that Aβ1-16 is interacts more strongly with Hsp16.5 than with Hsp16.9, and that the electrostatic interactions between Aβ and Hsp16.5 (and by analogy Hsp20) are greater than those between Aβ and Hsp16.9 (and by analogy Hsp17.7, 27, and αB-crystallin).

The preliminary results of Hex protein-protein interaction predictions, and Kite and Doolittle analysis suggest that Hsp20 can bind to Aβ1-40 by hydrophobic forces as well as electrostatic forces. However, more evidence will be needed to confirm these results because I used models of all proteins Hsp16.5 and Hsp16.9 as model small heat shock proteins and Aβ1-16 instead of the full length Aβ sequence) in Hex program. I can try other computational approaches to predict protein-protein interaction, or I could block electrostatic forces experimentally (e.g. by changing pH or ionic strength).

Short term goals for future work include research into the factors that affect kinetic of Aβ aggregation and the mechanisms of Hsp20-Aβ interactions. Long term goals include the design of peptides (proteins) or chemicals to prevent Aβ aggregation, and toxicity. The drugs designed in the future research will be useful in treatment of AD or could be helpful in the treatment of some of the 20 other diseases related to amyloidoses.

A

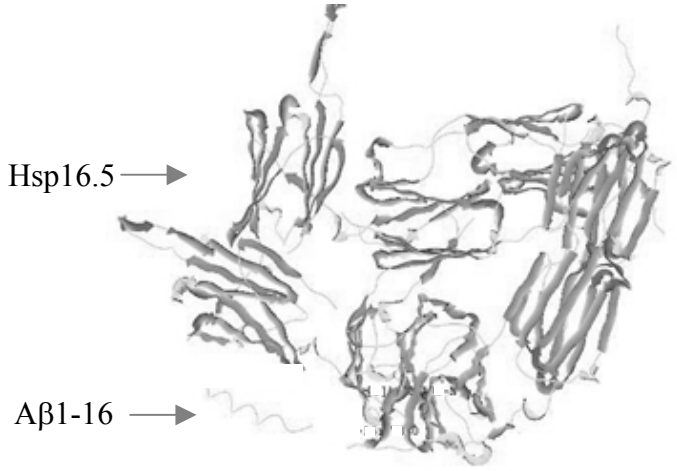

B

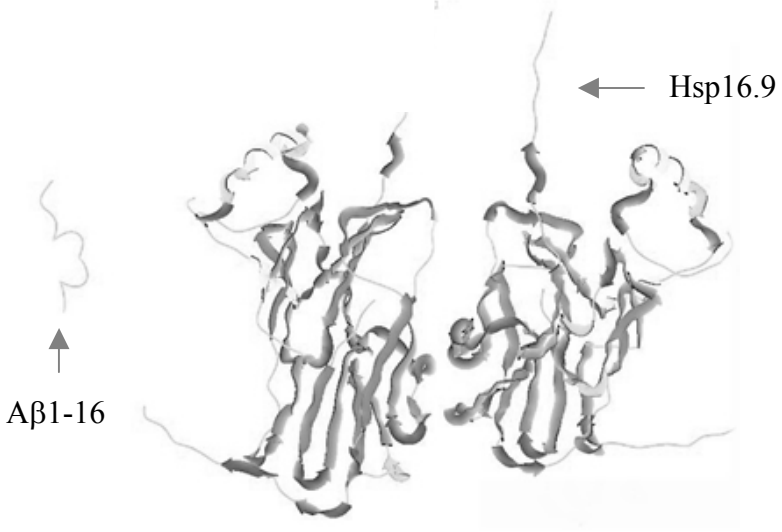

Figure 7. 3. Protein-protein interaction between Aβ1-16 and Hsps by using Hex. (A) Hsp16.5, substitution of Hsp20, (B) Hsp16.9, substitution of other Hsps.

CHAPTER VIII

SUMMARY AND CONCLUSIONS

The objectives of this research are to understand the characteristics of Aβ aggregation under different incubation conditions, and the role of small heat shock proteins in prevention of Aβ aggregation and toxicity. β-amyloid peptide (Aβ) is the main protein components of senile plaques that are one of the histopathological hallmarks in Alzheimer's disease (AD). Aβ readily forms fibrils via conformational changes to high β-sheet content, (Walsh et al. 1997; Walsh et al. 1999) and this fibril structure is associated with senile plaques in AD. Numerous environmental factors such as solvents, pH, temperature, and ionic strength that are associated with how investigators aggregate Aβ *in vitro* may affect Aβ structure. (Barrow and Zagorski 1991; Barrow et al. 1992; Snyder et al. 1994; Shen and Murphy 1995; Fezoui and Teplow 2002; Kawooya et al. 2003; Stine et al. 2003)

In work presented here, I determined that different Aβ incubation conditions (mixing and non-mixing condition) *in vitro* can affect the rate of Aβ fibril formation, the morphology, the toxicity and the conformational stability of intermediates in the aggregation pathway. According to Congo red binding results, the kinetics of Aβ aggregation appears similar regardless of the presence or absence of mixing. In both cases, fibril formation follows a characteristic sigmoidal curve, with a lag phase at early incubation times, followed by a fibril growth phase, then a saturation phase. The characteristic lag is typical of a nucleation dependent mechanism of aggregation that a

number of investigators propose for Aβ fibril formation. (Lomakin et al. 1997; Tseng et al. 1999; Esler et al. 2000; Serio et al. 2000; Pallitto and Murphy 2001) CD data suggest that Aβ does not undergo significant structural rearrangements when aggregated with mixing, however, when aggregated without mixing, a dramatic shift in structure is observed at intermediate times (approximately 4-8 hours after aggregation is initiated), which corresponds to the presence of an intermediate sized species in chromatograms (approximate molecular weight as estimated from elution volume on SEC of 53kDa) and a large globular species in electron micrographs. When Aβ is aggregated with mixing, fibrils undergo conformation change in denaturant more readily than monomer, suggesting that a less stable or higher energy species is formed during aggregation with mixing. When Aβ is aggregated without mixing, aggregation intermediates undergo conformation change more easily than either fresh or fibril Aβ suggesting that the intermediate is least stable or has the highest energy. Aggregation intermediates formed without mixing change structure more readily in guanidine hydrochloride than other species examined. The same trends are observed in Aβ stability using urea as a denaturant. Toxicity of fibrils is greater when formed with mixing, while toxicity of aggregation intermediates formed between 4 and 8 hours after initiation of aggregation without mixing are more toxic than other species formed. The difference in stability in denaturants could correlate with toxicity. A number of investigators have suggested that Aβ membrane interactions via Aβ conformational changes are important in the mechanism of Aβ toxicity. (McLaurin and Chakrabartty 1997; Terzi et al. 1997; Ege and Lee 2004) Behavior of Aβ in a membrane and in a denaturant might be analogous.

Small heat shock proteins (sHsps) are expressed in almost all organisms when cells become stressed in unfavorable environments. sHsps exist as large oligomeric complexes of 300-800kDa with monomeric molecular mass of 15-43kDa. (van den et al. 1999; Clark and Muchowski 2000; MacRae 2000) Important roles of sHsps are to stabilize other proteins under stress conditions and protect them from aggregation. (van den et al. 1999; Bruey et al. 2000)

In this research, several small heat shock proteins (sHsps) are tested to prevent Aβ aggregation and toxicity as drug candidates. sHsps used in this research are Hsp17.7 from carrot, human recombinant Hsp27, and Hsp20 from *B. Bovis* in different constructs, Hsp20-MBP (maltose binding protein fusion), His-Hsp20 (polyhistidine fusion) and His-Hsp20 without 11 residues in C-terminus. Cutting off the 11 residues from the C-terminus in Hsp20 improves the assembly properties of Hsp20. All types of Hsp20 are able to prevent Aβ1-40 aggregation at much lower concentrations than what has been necessary to prevent aggregation with other inhibitors. Hsp20 is able to optimally prevent amyloid formation of Aβ at molar ratios of Hsp20 to Aβ of approximately 1:1000 as indicated by Congo red binding. Hsp20 attenuates the toxicity of Aβ in SH-SY5Y and PC12 neuronal cells at analogous molar ratios. A careful examination of electron micrographs (EM) of Aβ-Hsp20-MBP mixtures under optimal fibril formation and toxicity prevention conditions reveals the presence of small globular species with a 16.3 nm diameter and variable length. The globular species are not yet well characterized, however, size analysis suggests that the species may be an Hsp20-Aβ complex rather than Aβ protofibrils since the width of these species (16.3nm) is atypical

for Aβ micelles (5 ~11 nm), protofibrils (4~8nm), or fibrils (6~10nm) (Yong et al. 2002). EM studies of Aβ-His-Hsp20 at the optimum ratio used to prevent aggregation taken at different times during aggregation show that Aβ-His-Hsp20 forms a huge ring structure complex at 2 hours. After 2 hours, the complex rings seem to break down and dissipate into the environment. In prevention of Aβ aggregation and toxicity, His-Hsp20 is more active than Hsp20-MBP, but His-Hsp20s show almost same activities regardless of the existence of the 11 residues in the C-terminus. Hsp17.7 from carrot and human recombinant Hsp27 can prevent Aβ1-40 aggregation, but not toxicity. Kudva et al., reported that Hsp27 inhibited fibril formation of Aβ1-42 *in vitro*.(Kudva et al. 1997) These sHsps do not appear to form the large ring structures when incubated with Aβ that are formed with Hsp20, suggesting that the formation of the large ring structure may be important in the mechanism of toxicity prevention.

Conclusively, I report structure and toxicity of Aβ species formed during aggregation via different methods. I show that fibrils formed via different methods, while structurally similar, do not have the same toxicity or the same apparent stability to denaturants. Aggregation intermediates that are similar to Aβ oligomer species reported by others such as ADDLs, are of comparable toxicity and stability in denaturants as fibrils formed during mixing. This work contributes to the understanding of the relationship between Aβ structure, stability and toxicity. All sHsps used in this research prevent Aβ1-40 aggregation, but only Hsp20 can inhibit Aβ1-40 toxicity. In drug development for AD, it will be very useful to understand the mechanism of Hsp20 in prevention of Aβ toxicity.

REFERENCES

Abgar, S., Vanhoudt, J., Aerts, T., and Clauwaert, J. 2001. Study of the chaperoning mechanism of bovine lens alpha-crystallin, a member of the alpha-small heat shock superfamily. *Biophys J* **80:** 1986-1995.

Aisen, P.S. 1996. Inflammation and Alzheimer disease. *Mol Chem Neuropathol* **28:** 83-88.

Aksenov, M.Y., Aksenova, M.V., Butterfield, D.A., Geddes, J.W., and Markesbery, W.R. 2001. Protein oxidation in the brain in Alzheimer's disease. *Neuroscience* **103:** 373-383.

Aleshkov, S., Abraham, C.R., and Zannis, V.I. 1997. Interaction of nascent ApoE2, ApoE3, and ApoE4 isoforms expressed in mammalian cells with amyloid peptide beta (1-40). Relevance to Alzheimer's disease. *Biochemistry* **36:** 10571-10580.

Allinson, T.M., Parkin, E.T., Condon, T.P., Schwager, S.L., Sturrock, E.D., Turner, A.J., and Hooper, N.M. 2004. The role of ADAM10 and ADAM17 in the ectodomain shedding of angiotensin converting enzyme and the amyloid precursor protein. *Eur J Biochem* **271:** 2539-2547.

Allinson, T.M., Parkin, E.T., Turner, A.J., and Hooper, N.M. 2003. ADAMs family members as amyloid precursor protein alpha-secretases. *J Neurosci Res* **74:** 342-352.

Alvarez, A., Toro, R., Caceres, A., and Maccioni, R.B. 1999. Inhibition of tau phosphorylating protein kinase cdk5 prevents beta-amyloid-induced neuronal death. *FEBS Lett* **459:** 421-426.

American Health Assistance Foundation, http://www.ahaf.org/alzdis/about/Amyloid Plaques .htm, Accessed on March 30, 2005

Barger, S.W. 2004. An unconventional hypothesis of oxidation in Alzheimer's disease:

intersections with excitotoxicity. *Front Biosci* **9:** 3286-3295.

Barinaga, M. 1995. New Alzheimer's gene found. *Science* **268:** 1845-1846.

Barrow, C.J., Yasuda, A., Kenny, P.T., and Zagorski, M.G. 1992. Solution conformations and aggregational properties of synthetic amyloid beta-peptides of Alzheimer's disease. Analysis of circular dichroism spectra. *J Mol Biol* **225:** 1075-1093.

Barrow, C.J., and Zagorski, M.G. 1991. Solution structures of beta peptide and its constituent fragments: relation to amyloid deposition. *Science* **253:** 179-182.

Basun, H., Forssell, L.G., Wetterberg, L., and Winblad, B. 1991. Metals and trace elements in plasma and cerebrospinal fluid in normal aging and Alzheimer's disease. *J Neural Transm Park Dis Dement Sect* **3:** 231-258.

Bayer, T.A., Wirths, O., Majtenyi, K., Hartmann, T., Multhaup, G., Beyreuther, K., and Czech, C. 2001. Key factors in Alzheimer's disease: beta-amyloid precursor protein processing, metabolism and intraneuronal transport. *Brain Pathol* **11:** 1-11.

Becaria, A., Campbell, A., and Bondy, S.C. 2002. Aluminum as a toxicant. *Toxicol Ind Health* **18:** 309-320.

Birks, J.S., and Harvey, R. 2003. Donepezil for dementia due to Alzheimer's disease. *Cochrane Database Syst Rev***:** CD001190.

Birks, J.S., Melzer, D., and Beppu, H. 2000. Donepezil for mild and moderate Alzheimer's disease. *Cochrane Database Syst Rev***:** CD001190.

Borchelt, D.R., Thinakaran, G., Eckman, C.B., Lee, M.K., Davenport, F., Ratovitsky, T., Prada, C.M., Kim, G., Seekins, S., Yager, D., et al. 1996. Familial Alzheimer's disease-linked presenilin 1 variants elevate Abeta1-42/1-40 ratio *in vitro* and *in vivo*. *Neuron* **17:** 1005-1013.

Brookmeyer, R., Gray, S., and Kawas, C. 1998. Projections of Alzheimer's disease in the United States and the public health impact of delaying disease onset. *Am J Public Health* **88:** 1337-1342.

Brown, W.C., Ruef, B.J., Norimine, J., Kegerreis, K.A., Suarez, C.E., Conley, P.G., Stich, R.W., Carson, K.H., and Rice-Ficht, A.C. 2001. A novel 20-kilodalton protein conserved in Babesia bovis and B. bigemina stimulates memory CD4(+) T lymphocyte responses in B. bovis-immune cattle. *Mol Biochem Parasitol* **118:** 97-109.

Broytman, O., and Malter, J.S. 2004. Anti-Abeta: The good, the bad, and the unforeseen. *J Neurosci Res* **75:** 301-306.

Bruey, J.M., Ducasse, C., Bonniaud, P., Ravagnan, L., Susin, S.A., Diaz-Latoud, C., Gurbuxani, S., Arrigo, A.P., Kroemer, G., Solary, E., et al. 2000. Hsp27 negatively regulates cell death by interacting with cytochrome c. *Nat Cell Biol* **2:** 645-652.

Butterfield, D.A., Griffin, S., Munch, G., and Pasinetti, G.M. 2002. Amyloid beta-peptide and amyloid pathology are central to the oxidative stress and inflammatory cascades under which Alzheimer's disease brain exists. *J Alzheimers Dis* **4:** 193-201.

Cairo, C.W., Strzelec, A., Murphy, R.M., and Kiessling, L.L. 2002. Affinity-based inhibition of beta-amyloid toxicity. *Biochemistry* **41:** 8620-8629.

Campion, D., Brice, A., Hannequin, D., Charbonnier, F., Dubois, B., Martin, C., Michon, A., Penet, C., Bellis, M., Calenda, A., et al. 1996. No founder effect in three novel Alzheimer's disease families with APP 717 Val-->Ile mutation. Clerget-darpoux. French Alzheimer's Disease Study Group. *J Med Genet* **33:** 661-664.

Carrell, R.W., and Gooptu, B. 1998. Conformational changes and disease--serpins, prions and Alzheimer's. *Curr Opin Struct Biol* **8:** 799-809.

Carrington, J.C., Jensen, P.E., and Schaad, M.C. 1998. Genetic evidence for an essential role for potyvirus CI protein in cell-to-cell movement. *Plant J* **14:** 393-400.

Carson, J.A., and Turner, A.J. 2002. Beta-amyloid catabolism: roles for neprilysin (NEP) and other metallopeptidases? *J Neurochem* **81:** 1-8.

Caspers, G.J., Leunissen, J.A., and de Jong, W.W. 1995. The expanding small heat-shock protein family, and structure predictions of the conserved "alpha-crystallin domain". *J Mol Evol* **40:** 238-248.

Choi, Y.T., Jung, C.H., Lee, S.R., Bae, J.H., Baek, W.K., Suh, M.H., Park, J., Park, C.W., and Suh, S.I. 2001. The green tea polyphenol (-)-epigallocatechin gallate attenuates beta-amyloid-induced neurotoxicity in cultured hippocampal neurons. *Life Sci* **70:** 603-614.

Chromy, B.A., Nowak, R.J., Lambert, M.P., Viola, K.L., Chang, L., Velasco, P.T., Jones, B.W., Fernandez, S.J., Lacor, P.N., Horowitz, P., et al. 2003. Self-assembly of Abeta(1-42) into globular neurotoxins. *Biochemistry* **42:** 12749-12760.

Clark, J.I., and Muchowski, P.J. 2000. Small heat-shock proteins and their potential role in human disease. *Curr Opin Struct Biol* **10:** 52-59.

Combarros, O., Alvarez-Arcaya, A., Sanchez-Guerra, M., Infante, J., and Berciano, J. 2002. Candidate gene association studies in sporadic Alzheimer's disease. *Dement Geriatr Cogn Disord* **14:** 41-54.

Creighton, T.E. 1993. *Proteins: structures and molecular properties*, 2nd ed. W. H. Freeman, New York, pp. xiii, 507 s.

Cross, D., Vial, C., and Maccioni, R.B. 1993. A tau-like protein interacts with stress fibers and microtubules in human and rodent cultured cell lines. *J Cell Sci* **105 (Pt 1):** 51-60.

Czech, C., Tremp, G., and Pradier, L. 2000. Presenilins and Alzheimer's disease: biological functions and pathogenic mechanisms. *Prog Neurobiol* **60:** 363-384.

Dahlgren, K.N., Manelli, A.M., Stine, W.B., Jr., Baker, L.K., Krafft, G.A., and LaDu, M.J. 2002. Oligomeric and fibrillar species of amyloid-beta peptides differentially affect neuronal viability. *J Biol Chem* **277:** 32046-32053.

Dandrea, M.R., Reiser, P.A., Gumula, N.A., Hertzog, B.M., and Andrade-Gordon, P. 2001. Application of triple immunohistochemistry to characterize amyloid

plaque-associated inflammation in brains with Alzheimer's disease. *Biotech Histochem* **76:** 97-106.

de Jong, W.W., Leunissen, J.A., and Voorter, C.E. 1993. Evolution of the alpha-crystallin/small heat-shock protein family. *Mol Biol Evol* **10:** 103-126.

Derham, B.K., van Boekel, M.A., Muchowski, P.J., Clark, J.I., Horwitz, J., Hepburne-Scott, H.W., de Jong, W.W., Crabbe, M.J., and Harding, J.J. 2001. Chaperone function of mutant versions of alpha A- and alpha B-crystallin prepared to pinpoint chaperone binding sites. *Eur J Biochem* **268:** 713-721.

Dobson, C.B., and Itzhaki, R.F. 1999. Herpes simplex virus type 1 and Alzheimer's disease. *Neurobiol Aging* **20:** 457-465.

Dobson, C.M. 2003. Protein folding and misfolding. *Nature* **426:** 884-890.

Doody, R.S. 2003. Current treatments for Alzheimer's disease: cholinesterase inhibitors. *J Clin Psychiatry* **64 Suppl 9:** 11-17.

Ege, C., and Lee, K.Y. 2004. Insertion of Alzheimer's A beta 40 peptide into lipid monolayers. *Biophys J* **87:** 1732-1740.

Ehrnsperger, M., Graber, S., Gaestel, M., and Buchner, J. 1997. Binding of non-native protein to Hsp25 during heat shock creates a reservoir of folding intermediates for reactivation. *Embo J* **16:** 221-229.

Esler, W.P., Stimson, E.R., Jennings, J.M., Vinters, H.V., Ghilardi, J.R., Lee, J.P., Mantyh, P.W., and Maggio, J.E. 2000. Alzheimer's disease amyloid propagation by a template-dependent dock-lock mechanism. *Biochemistry* **39:** 6288-6295.

Evans, D.A., Funkenstein, H.H., Albert, M.S., Scherr, P.A., Cook, N.R., Chown, M.J., Hebert, L.E., Hennekens, C.H., and Taylor, J.O. 1989. Prevalence of Alzheimer's disease in a community population of older persons. Higher than previously reported. *Jama* **262:** 2551-2556.

Farlow, M.R. 1998. Etiology and pathogenesis of Alzheimer's disease. *Am J Health Syst Pharm* **55 Suppl 2:** S5-10.

Farlow, M.R. 2003. Update on rivastigmine. *Neurologist* **9:** 230-234.

Farlow, M.R. 2004. NMDA receptor antagonists. A new therapeutic approach for Alzheimer's disease. *Geriatrics* **59:** 22-27.

Fersht, A.R., Matouschek, A., and Serrano, L. 1992. The folding of an enzyme. I. Theory of protein engineering analysis of stability and pathway of protein folding. *J Mol Biol* **224:** 771-782.

Festy, F., Lins, L., Peranzi, G., Octave, J.N., Brasseur, R., and Thomas, A. 2001. Is aggregation of beta-amyloid peptides a mis-functioning of a current interaction process? *Biochim Biophys Acta* **1546:** 356-364.

Fezoui, Y., and Teplow, D.B. 2002. Kinetic studies of amyloid beta-protein fibril assembly. Differential effects of alpha-helix stabilization. *J Biol Chem* **277:** 36948-36954.

Foguel, D., Suarez, M.C., Ferrao-Gonzales, A.D., Porto, T.C., Palmieri, L., Einsiedler, C.M., Andrade, L.R., Lashuel, H.A., Lansbury, P.T., Kelly, J.W., et al. 2003. Dissociation of amyloid fibrils of alpha-synuclein and transthyretin by pressure reveals their reversible nature and the formation of water-excluded cavities. *Proc Natl Acad Sci U S A* **100:** 9831-9836.

Fraser, P.E., Duffy, L.K., O'Malley, M.B., Nguyen, J., Inouye, H., and Kirschner, D.A. 1991. Morphology and antibody recognition of synthetic beta-amyloid peptides. *J Neurosci Res* **28:** 474-485.

Fraser, P.E., Yang, D.S., Yu, G., Levesque, L., Nishimura, M., Arawaka, S., Serpell, L.C., Rogaeva, E., and St George-Hyslop, P. 2000. Presenilin structure, function and role in Alzheimer disease. *Biochim Biophys Acta* **1502:** 1-15.

Friedhoff, P., von Bergen, M., Mandelkow, E.M., and Mandelkow, E. 2000. Structure of tau protein and assembly into paired helical filaments. *Biochim Biophys Acta* **1502:** 122-132.

Gabelli, C. 2003. Rivastigmine: an update on therapeutic efficacy in Alzheimer's disease

and other conditions. *Curr Med Res Opin* **19:** 69-82.

Ganea, E. 2001. Chaperone-like activity of alpha-crystallin and other small heat shock proteins. *Curr Protein Pept Sci* **2:** 205-225.

Gantier, R., Gilbert, D., Dumanchin, C., Campion, D., Davoust, D., Toma, F., and Frebourg, T. 2000. The pathogenic L392V mutation of presenilin 1 decreases the affinity to glycogen synthase kinase-3 beta. *Neurosci Lett* **283:** 217-220.

Garzon-Rodriguez, W., Sepulveda-Becerra, M., Milton, S., and Glabe, C.G. 1997. Soluble amyloid Abeta-(1-40) exists as a stable dimer at low concentrations. *J Biol Chem* **272:** 21037-21044.

Ghanta, J., Shen, C.L., Kiessling, L.L., and Murphy, R.M. 1996. A strategy for designing inhibitors of beta-amyloid toxicity. *J Biol Chem* **271:** 29525-29528.

Goate, A., Chartier-Harlin, M.C., Mullan, M., Brown, J., Crawford, F., Fidani, L., Giuffra, L., Haynes, A., Irving, N., James, L., et al. 1991. Segregation of a missense mutation in the amyloid precursor protein gene with familial Alzheimer's disease. *Nature* **349:** 704-706.

Goldberg, A.L. 2003. Protein degradation and protection against misfolded or damaged proteins. *Nature* **426:** 895-899.

Good, P.F., Werner, P., Hsu, A., Olanow, C.W., and Perl, D.P. 1996. Evidence of neuronal oxidative damage in Alzheimer's disease. *Am J Pathol* **149:** 21-28.

Gorman, P.M., and Chakrabartty, A. 2001. Alzheimer beta-amyloid peptides: structures of amyloid fibrils and alternate aggregation products. *Biopolymers* **60:** 381-394.

Gouras, G.K., and Beal, M.F. 2001. Metal chelator decreases Alzheimer beta-amyloid plaques. *Neuron* **30:** 641-642.

Greenberg, S.G., and Davies, P. 1990. A preparation of Alzheimer paired helical filaments that displays distinct tau proteins by polyacrylamide gel electrophoresis. *Proc Natl Acad Sci U S A* **87:** 5827-5831.

Gursky, O., and Aleshkov, S. 2000. Temperature-dependent beta-sheet formation in beta-

amyloid Abeta(1-40) peptide in water: uncoupling beta-structure folding from aggregation. *Biochim Biophys Acta* **1476:** 93-102.

Hammarstrom, P., Jiang, X., Deechongkit, S., and Kelly, J.W. 2001. Anion shielding of electrostatic repulsions in transthyretin modulates stability and amyloidosis: insight into the chaotrope unfolding dichotomy. *Biochemistry* **40:** 11453-11459.

Hardy, J. 1997. Amyloid, the presenilins and Alzheimer's disease. *Trends Neurosci* **20:** 154-159.

Harper, J.D., Lieber, C.M., and Lansbury, P.T., Jr. 1997. Atomic force microscopic imaging of seeded fibril formation and fibril branching by the Alzheimer's disease amyloid-beta protein. *Chem Biol* **4:** 951-959.

Harper, J.D., Wong, S.S., Lieber, C.M., and Lansbury, P.T., Jr. 1999. Assembly of A beta amyloid protofibrils: an *in vitro* model for a possible early event in Alzheimer's disease. *Biochemistry* **38:** 8972-8980.

Hartl, F.U., and Hayer-Hartl, M. 2002. Molecular chaperones in the cytosol: from nascent chain to folded protein. *Science* **295:** 1852-1858.

Hartmann, T. 2001. Cholesterol, A beta and Alzheimer's disease. *Trends Neurosci* **24:** S45-48.

Hatters, D.M., Lindner, R.A., Carver, J.A., and Howlett, G.J. 2001. The molecular chaperone, alpha-crystallin, inhibits amyloid formation by apolipoprotein C-II. *J Biol Chem* **276:** 33755-33761.

Head, E., and Lott, I.T. 2004. Down syndrome and beta-amyloid deposition. *Curr Opin Neurol* **17:** 95-100.

Hebert, L.E., Scherr, P.A., Bienias, J.L., Bennett, D.A., and Evans, D.A. 2003. Alzheimer disease in the US population: prevalence estimates using the 2000 census. *Arch Neurol* **60:** 1119-1122.

Hensley, K., Carney, J.M., Mattson, M.P., Aksenova, M., Harris, M., Wu, J.F., Floyd, R.A., and Butterfield, D.A. 1994. A model for beta-amyloid aggregation and

neurotoxicity based on free radical generation by the peptide: relevance to Alzheimer disease. *Proc Natl Acad Sci U S A* **91:** 3270-3274.

Hertel, C., Terzi, E., Hauser, N., Jakob-Rotne, R., Seelig, J., and Kemp, J.A. 1997. Inhibition of the electrostatic interaction between beta-amyloid peptide and membranes prevents beta-amyloid-induced toxicity. *Proc Natl Acad Sci U S A* **94:** 9412-9416.

Hetenyi, C., Szabo, Z., Klement, E., Datki, Z., Kortvelyesi, T., Zarandi, M., and Penke, B. 2002. Pentapeptide amides interfere with the aggregation of beta-amyloid peptide of Alzheimer's disease. *Biochem Biophys Res Commun* **292:** 931-936.

Hinkebein, J.H., Martin, T.A., Callahan, C.D., and Johnstone, B. 2003. Traumatic brain injury and Alzheimer's: deficit profile similarities and the impact of normal ageing. *Brain Inj* **17:** 1035-1042.

Holtzman, D.M., Fagan, A.M., Mackey, B., Tenkova, T., Sartorius, L., Paul, S.M., Bales, K., Ashe, K.H., Irizarry, M.C., and Hyman, B.T. 2000. Apolipoprotein E facilitates neuritic and cerebrovascular plaque formation in an Alzheimer's disease model. *Ann Neurol* **47:** 739-747.

Hoozemans, J.J., Veerhuis, R., Rozemuller, A.J., and Eikelenboom, P. 2003. Non-steroidal anti-inflammatory drugs and cyclooxygenase in Alzheimer's disease. *Curr Drug Targets* **4:** 461-468.

Horwitz, J. 1992. Alpha-crystallin can function as a molecular chaperone. *Proc Natl Acad Sci U S A* **89:** 10449-10453.

Horwitz, J. 2000. The function of alpha-crystallin in vision. *Semin Cell Dev Biol* **11:** 53-60.

Hoshi, M., Sato, M., Matsumoto, S., Noguchi, A., Yasutake, K., Yoshida, N., and Sato, K. 2003. Spherical aggregates of beta-amyloid (amylospheroid) show high neurotoxicity and activate tau protein kinase I/glycogen synthase kinase-3beta. *Proc Natl Acad Sci U S A* **100:** 6370-6375.

Howlett, D.R., Perry, A.E., Godfrey, F., Swatton, J.E., Jennings, K.H., Spitzfaden, C., Wadsworth, H., Wood, S.J., and Markwell, R.E. 1999. Inhibition of fibril formation in beta-amyloid peptide by a novel series of benzofurans. *Biochem J* **340 (Pt 1):** 283-289.

Huang, X., Atwood, C.S., Moir, R.D., Hartshorn, M.A., Tanzi, R.E., and Bush, A.I. 2004. Trace metal contamination initiates the apparent auto-aggregation, amyloidosis, and oligomerization of Alzheimer's Abeta peptides. *J Biol Inorg Chem* **9:** 954-960.

Hughes, S.R., Khorkova, O., Goyal, S., Knaeblein, J., Heroux, J., Riedel, N.G., and Sahasrabudhe, S. 1998. Alpha2-macroglobulin associates with beta-amyloid peptide and prevents fibril formation. *Proc Natl Acad Sci U S A* **95:** 3275-3280.

Hutton, M., Busfield, F., Wragg, M., Crook, R., Perez-Tur, J., Clark, R.F., Prihar, G., Talbot, C., Phillips, H., Wright, K., et al. 1996. Complete analysis of the presenilin 1 gene in early onset Alzheimer's disease. *Neuroreport* **7:** 801-805.

Hwang, W., Zhang, S., Kamm, R.D., and Karplus, M. 2004. Kinetic control of dimer structure formation in amyloid fibrillogenesis. *Proc Natl Acad Sci U S A* **101:** 12916-12921.

Imahori, K., and Uchida, T. 1997. Physiology and pathology of tau protein kinases in relation to Alzheimer's disease. *J Biochem (Tokyo)* **121:** 179-188.

Inouye, H., and Kirschner, D.A. 1998. Polypeptide chain folding in the hydrophobic core of hamster scrapie prion: analysis by X-ray diffraction. *J Struct Biol* **122:** 247-255.

Iqbal, K., Alonso Adel, C., El-Akkad, E., Gong, C.X., Haque, N., Khatoon, S., Pei, J.J., Tanimukai, H., Tsujio, I., Wang, J.Z., et al. 2003. Alzheimer neurofibrillary degeneration: therapeutic targets and high-throughput assays. *J Mol Neurosci* **20:** 425-429.

Iqbal, K., Braak, E., Braak, H., Zaidi, T., and Grundke-Iqbal, I. 1991. A silver

impregnation method for labeling both Alzheimer paired helical filaments and their polypeptides separated by sodium dodecyl sulfate-polyacrylamide gel electrophoresis. *Neurobiol Aging* **12:** 357-361.

Irving, N.G., and Miller, C.C. 1997. Tau phosphorylation in cells transfected with wild-type or an Alzheimer's disease mutant Presenilin 1. *Neurosci Lett* **222:** 71-74.

Ishiguro, K., Omori, A., Takamatsu, M., Sato, K., Arioka, M., Uchida, T., and Imahori, K. 1992. Phosphorylation sites on tau by tau protein kinase I, a bovine derived kinase generating an epitope of paired helical filaments. *Neurosci Lett* **148:** 202-206.

Iversen, L.L., Mortishire-Smith, R.J., Pollack, S.J., and Shearman, M.S. 1995. The toxicity *in vitro* of beta-amyloid protein. *Biochem J* **311 (Pt 1):** 1-16.

Iwaki, T., Kume-Iwaki, A., Liem, R.K., and Goldman, J.E. 1989. Alpha B-crystallin is expressed in non-lenticular tissues and accumulates in Alexander's disease brain. *Cell* **57:** 71-78.

Jacchieri, S.G. 1998. Study of alpha-helix to beta-strand to beta-sheet transitions in amyloid: the role of segregated hydrophobic beta-strands. *Biophys Chem* **74:** 23-34.

Jakob, U., Gaestel, M., Engel, K., and Buchner, J. 1993. Small heat shock proteins are molecular chaperones. *J Biol Chem* **268:** 1517-1520.

Jansen, R., Grudzielanek, S., Dzwolak, W., and Winter, R. 2004. High pressure promotes circularly shaped insulin amyloid. *J Mol Biol* **338:** 203-206.

Jarrett, J.T., Berger, E.P., and Lansbury, P.T., Jr. 1993. The carboxy terminus of the beta amyloid protein is critical for the seeding of amyloid formation: implications for the pathogenesis of Alzheimer's disease. *Biochemistry* **32:** 4693-4697.

Joachim, C.L., Mori, H., and Selkoe, D.J. 1989. Amyloid beta-protein deposition in tissues other than brain in Alzheimer's disease. *Nature* **341:** 226-230.

Jorm, A.F., Korten, A.E., and Henderson, A.S. 1987. The prevalence of dementia: a

quantitative integration of the literature. *Acta Psychiatr Scand* **76:** 465-479.

Kawooya, J.K., Emmons, T.L., Gonzalez-DeWhitt, P.A., Camp, M.C., and D'Andrea, S.C. 2003. Electrophoretic mobility of Alzheimer's amyloid-beta peptides in urea-sodium dodecyl sulfate-polyacrylamide gel electrophoresis. *Anal Biochem* **323:** 103-113.

Kayed, R., Head, E., Thompson, J.L., McIntire, T.M., Milton, S.C., Cotman, C.W., and Glabe, C.G. 2003. Common structure of soluble amyloid oligomers implies common mechanism of pathogenesis. *Science* **300:** 486-489.

Kelly, J.W. 1998. The alternative conformations of amyloidogenic proteins and their multi-step assembly pathways. *Curr Opin Struct Biol* **8:** 101-106.

Kim, J., and Lee, M. 2004. Observation of multi-step conformation switching in beta-amyloid peptide aggregation by fluorescence resonance energy transfer. *Biochem Biophys Res Commun* **316:** 393-397.

Kimberly, W.T., LaVoie, M.J., Ostaszewski, B.L., Ye, W., Wolfe, M.S., and Selkoe, D.J. 2003. Gamma-secretase is a membrane protein complex comprised of presenilin, nicastrin, Aph-1, and Pen-2. *Proc Natl Acad Sci U S A* **100:** 6382-6387.

Kisilevsky, R., Lemieux, L.J., Fraser, P.E., Kong, X., Hultin, P.G., and Szarek, W.A. 1995. Arresting amyloidosis *in vivo* using small-molecule anionic sulphonates or sulphates: implications for Alzheimer's disease. *Nat Med* **1:** 143-148.

Klein, W.L., Krafft, G.A., and Finch, C.E. 2001. Targeting small Abeta oligomers: the solution to an Alzheimer's disease conundrum? *Trends Neurosci* **24:** 219-224.

Klunk, W.E., Debnath, M.L., Koros, A.M., and Pettegrew, J.W. 1998. Chrysamine-G, a lipophilic analogue of Congo red, inhibits A beta-induced toxicity in PC12 cells. *Life Sci* **63:** 1807-1814.

Klunk, W.E., Jacob, R.F., and Mason, R.P. 1999. Quantifying amyloid beta-peptide (Abeta) aggregation using the Congo red-Abeta (CR-abeta) spectrophotometric assay. *Anal Biochem* **266:** 66-76.

Koh, J.Y., Yang, L.L., and Cotman, C.W. 1990. Beta-amyloid protein increases the vulnerability of cultured cortical neurons to excitotoxic damage. *Brain Res* **533:** 315-320.

Kojro, E., Gimpl, G., Lammich, S., Marz, W., and Fahrenholz, F. 2001. Low cholesterol stimulates the nonamyloidogenic pathway by its effect on the alpha -secretase ADAM 10. *Proc Natl Acad Sci U S A* **98:** 5815-5820.

Kosik, K.S., Joachim, C.L., and Selkoe, D.J. 1986. Microtubule-associated protein tau (tau) is a major antigenic component of paired helical filaments in Alzheimer disease. *Proc Natl Acad Sci U S A* **83:** 4044-4048.

Koteiche, H.A., and McHaourab, H.S. 1999. Folding pattern of the alpha-crystallin domain in alphaA-crystallin determined by site-directed spin labeling. *J Mol Biol* **294:** 561-577.

Kowalewski, T., and Holtzman, D.M. 1999. *In situ* atomic force microscopy study of Alzheimer's beta-amyloid peptide on different substrates: new insights into mechanism of beta-sheet formation. *Proc Natl Acad Sci U S A* **96:** 3688-3693.

Kudva, Y.C., Hiddinga, H.J., Butler, P.C., Mueske, C.S., and Eberhardt, N.L. 1997. Small heat shock proteins inhibit *in vitro* A beta(1-42) amyloidogenesis. *FEBS Lett* **416:** 117-121.

Kurz, A. 1998. The therapeutic potential of tacrine. *J Neural Transm Suppl* **54:** 295-299.

Lambert, M.P., Barlow, A.K., Chromy, B.A., Edwards, C., Freed, R., Liosatos, M., Morgan, T.E., Rozovsky, I., Trommer, B., Viola, K.L., et al. 1998. Diffusible, nonfibrillar ligands derived from Abeta1-42 are potent central nervous system neurotoxins. *Proc Natl Acad Sci U S A* **95:** 6448-6453.

Lansbury, P.T., Jr. 1997. Inhibition of amyloid formation: a strategy to delay the onset of Alzheimer's disease. *Curr Opin Chem Biol* **1:** 260-267.

Lansbury, P.T., Jr. 1999. Evolution of amyloid: what normal protein folding may tell us about fibrillogenesis and disease. *Proc Natl Acad Sci U S A* **96:** 3342-3344.

Lashuel, H.A., Hartley, D.M., Balakhaneh, D., Aggarwal, A., Teichberg, S., and Callaway, D.J. 2002. New class of inhibitors of amyloid-beta fibril formation. Implications for the mechanism of pathogenesis in Alzheimer's disease. *J Biol Chem* **277:** 42881-42890.

Lee, K.W., Lee, S.H., Kim, H., Song, J.S., Yang, S.D., Paik, S.G., and Han, P.L. 2004. Progressive cognitive impairment and anxiety induction in the absence of plaque deposition in C57BL/6 inbred mice expressing transgenic amyloid precursor protein. *J Neurosci Res* **76:** 572-580.

Lee, S., Carson, K., Rice-Ficht, A., and Good, T. 2005. Hsp20, a novel {alpha}-crystallin, prevents A{beta} fibril formation and toxicity. *Protein Sci* **14:** 593-601.

Levy-Lahad, E., Wasco, W., Poorkaj, P., Romano, D.M., Oshima, J., Pettingell, W.H., Yu, C.E., Jondro, P.D., Schmidt, S.D., Wang, K., et al. 1995. Candidate gene for the chromosome 1 familial Alzheimer's disease locus. *Science* **269:** 973-977.

Liang, J.J. 2000. Interaction between beta-amyloid and lens alphaB-crystallin. *FEBS Lett* **484:** 98-101.

Lippa, C.F. 1999. Familial Alzheimer's disease: genetic influences on the disease process (Review). *Int J Mol Med* **4:** 529-536.

Lomakin, A., Chung, D.S., Benedek, G.B., Kirschner, D.A., and Teplow, D.B. 1996. On the nucleation and growth of amyloid beta-protein fibrils: detection of nuclei and quantitation of rate constants. *Proc Natl Acad Sci U S A* **93:** 1125-1129.

Lomakin, A., Teplow, D.B., Kirschner, D.A., and Benedek, G.B. 1997. Kinetic theory of fibrillogenesis of amyloid beta-protein. *Proc Natl Acad Sci U S A* **94:** 7942-7947.

Lorenzo, A., and Yankner, B.A. 1994. Beta-amyloid neurotoxicity requires fibril formation and is inhibited by congo red. *Proc Natl Acad Sci U S A* **91:** 12243-12247.

Lott, I.T., and Head, E. 2001. Down syndrome and Alzheimer's disease: a link between development and aging. *Ment Retard Dev Disabil Res Rev* **7:** 172-178.

Loy, C., and Schneider, L. 2004. Galantamine for Alzheimer's disease. *Cochrane Database Syst Rev***:** CD001747.

Lynn, D.G., and Meredith, S.C. 2000. Review: model peptides and the physicochemical approach to beta-amyloids. *J Struct Biol* **130:** 153-173.

Maccioni, R.B., and Cambiazo, V. 1995. Role of microtubule-associated proteins in the control of microtubule assembly. *Physiol Rev* **75:** 835-864.

MacRae, T.H. 2000. Structure and function of small heat shock/alpha-crystallin proteins: established concepts and emerging ideas. *Cell Mol Life Sci* **57:** 899-913.

Malik, M.K., Slovin, J.P., Hwang, C.H., and Zimmerman, J.L. 1999. Modified expression of a carrot small heat shock protein gene, hsp17. 7, results in increased or decreased thermotolerancedouble dagger. *Plant J* **20:** 89-99.

Mandelkow, E.M., Biernat, J., Drewes, G., Gustke, N., Trinczek, B., and Mandelkow, E. 1995. Tau domains, phosphorylation, and interactions with microtubules. *Neurobiol Aging* **16:** 355-362; discussion 362-353.

Mandelkow, E.M., Biernat, J., Drewes, G., Steiner, B., Lichtenberg-Kraag, B., Wille, H., Gustke, N., and Mandelkow, E. 1993. Microtubule-associated protein tau, paired helical filaments, and phosphorylation. *Ann N Y Acad Sci* **695:** 209-216.

Manelli, A.M., Stine, W.B., Van Eldik, L.J., and LaDu, M.J. 2004. ApoE and Abeta1-42 interactions: effects of isoform and conformation on structure and function. *J Mol Neurosci* **23:** 235-246.

Manning, M., and Colon, W. 2004. Structural basis of protein kinetic stability: resistance to sodium dodecyl sulfate suggests a central role for rigidity and a bias toward beta-sheet structure. *Biochemistry* **43:** 11248-11254.

Mark, R.J., Blanc, E.M., and Mattson, M.P. 1996. Amyloid beta-peptide and oxidative cellular injury in Alzheimer's disease. *Mol Neurobiol* **12:** 211-224.

Marx, J. 2001. Alzheimer's disease. Bad for the heart, bad for the mind? *Science* **294:** 508-509.

Mathews, P.M., and Nixon, R.A. 2003. Setback for an Alzheimer's disease vaccine: lessons learned. *Neurology* **61:** 7-8.

McGeer, E.G., Yasojima, K., Schwab, C., and McGeer, P.L. 2001. The pentraxins: possible role in Alzheimer's disease and other innate inflammatory diseases. *Neurobiol Aging* **22:** 843-848.

McHaourab, H.S., Dodson, E.K., and Koteiche, H.A. 2002. Mechanism of chaperone function in small heat shock proteins. Two-mode binding of the excited states of T4 lysozyme mutants by alphaA-crystallin. *J Biol Chem* **277:** 40557-40566.

McLaurin, J., and Chakrabartty, A. 1997. Characterization of the interactions of Alzheimer beta-amyloid peptides with phospholipid membranes. *Eur J Biochem* **245:** 355-363.

Meek, P.D., McKeithan, K., and Schumock, G.T. 1998. Economic considerations in Alzheimer's disease. *Pharmacotherapy* **18:** 68-73; discussion 79-82.

Mehta, N.D., Refolo, L.M., Eckman, C., Sanders, S., Yager, D., Perez-Tur, J., Younkin, S., Duff, K., Hardy, J., and Hutton, M. 1998. Increased Abeta42(43) from cell lines expressing presenilin 1 mutations. *Ann Neurol* **43:** 256-258.

Michel, G., Mercken, M., Murayama, M., Noguchi, K., Ishiguro, K., Imahori, K., and Takashima, A. 1998. Characterization of tau phosphorylation in glycogen synthase kinase-3beta and cyclin dependent kinase-5 activator (p23) transfected cells. *Biochim Biophys Acta* **1380:** 177-182.

Minghetti, L. 2004. Cyclooxygenase-2 (COX-2) in inflammatory and degenerative brain diseases. *J Neuropathol Exp Neurol* **63:** 901-910.

Miranda, S., Opazo, C., Larrondo, L.F., Munoz, F.J., Ruiz, F., Leighton, F., and Inestrosa, N.C. 2000. The role of oxidative stress in the toxicity induced by amyloid beta-peptide in Alzheimer's disease. *Prog Neurobiol* **62:** 633-648.

Miura, T., Suzuki, K., Kohata, N., and Takeuchi, H. 2000. Metal binding modes of Alzheimer's amyloid beta-peptide in insoluble aggregates and soluble complexes.

Biochemistry **39:** 7024-7031.

Muchowski, P.J. 2002. Protein misfolding, amyloid formation, and neurodegeneration: a critical role for molecular chaperones? *Neuron* **35:** 9-12.

Munch, G., and Robinson, S.R. 2002. Alzheimer's vaccine: a cure as dangerous as the disease? *J Neural Transm* **109:** 537-539.

Murphy, R.M. 2002. Peptide aggregation in neurodegenerative disease. *Annu Rev Biomed Eng* **4:** 155-174.

Murphy, R.M., and Pallitto, M.M. 2000. Probing the kinetics of beta-amyloid self-association. *J Struct Biol* **130:** 109-122.

Murrell, J.R., Spillantini, M.G., Zolo, P., Guazzelli, M., Smith, M.J., Hasegawa, M., Redi, F., Crowther, R.A., Pietrini, P., Ghetti, B., et al. 1999. Tau gene mutation G389R causes a tauopathy with abundant pick body-like inclusions and axonal deposits. *J Neuropathol Exp Neurol* **58:** 1207-1226.

Myers, J.K., Pace, C.N., and Scholtz, J.M. 1995. Denaturant m values and heat capacity changes: relation to changes in accessible surface areas of protein unfolding. *Protein Sci* **4:** 2138-2148.

Nacharaju, P., Lewis, J., Easson, C., Yen, S., Hackett, J., Hutton, M., and Yen, S.H. 1999. Accelerated filament formation from tau protein with specific FTDP-17 missense mutations. *FEBS Lett* **447:** 195-199.

Narberhaus, F. 2002. Alpha-crystallin-type heat shock proteins: socializing minichaperones in the context of a multichaperone network. *Microbiol Mol Biol Rev* **66:** 64-93; table of contents.

Neve, R.L., McPhie, D.L., and Chen, Y. 2000. Alzheimer's disease: a dysfunction of the amyloid precursor protein(1). *Brain Res* **886:** 54-66.

Neve, R.L., McPhie, D.L., and Chen, Y. 2001. Alzheimer's disease: dysfunction of a signalling pathway mediated by the amyloid precursor protein? *Biochem Soc Symp***:** 37-50.

Olin, J., and Schneider, L. 2002. Galantamine for Alzheimer's disease. *Cochrane Database Syst Rev***:** CD001747.

Ono, K., Hasegawa, K., Naiki, H., and Yamada, M. 2004. Anti-amyloidogenic activity of tannic acid and its activity to destabilize Alzheimer's beta-amyloid fibrils *in vitro*. *Biochim Biophys Acta* **1690:** 193-202.

Orgogozo, J.M., Gilman, S., Dartigues, J.F., Laurent, B., Puel, M., Kirby, L.C., Jouanny, P., Dubois, B., Eisner, L., Flitman, S., et al. 2003. Subacute meningoencephalitis in a subset of patients with AD after Abeta42 immunization. *Neurology* **61:** 46-54.

Otvos, L., Jr., Szendrei, G.I., Lee, V.M., and Mantsch, H.H. 1993. Human and rodent Alzheimer beta-amyloid peptides acquire distinct conformations in membrane-mimicking solvents. *Eur J Biochem* **211:** 249-257.

Pace, C.N. 1990. Measuring and increasing protein stability. *Trends Biotechnol* **8:** 93-98.

Pace, C.N., and Shaw, K.L. 2000. Linear extrapolation method of analyzing solvent denaturation curves. *Proteins* **Suppl 4:** 1-7.

Pallitto, M.M., Ghanta, J., Heinzelman, P., Kiessling, L.L., and Murphy, R.M. 1999. Recognition sequence design for peptidyl modulators of beta-amyloid aggregation and toxicity. *Biochemistry* **38:** 3570-3578.

Pallitto, M.M., and Murphy, R.M. 2001. A mathematical model of the kinetics of beta-amyloid fibril growth from the denatured state. *Biophys J* **81:** 1805-1822.

Patrick, G.N., Zukerberg, L., Nikolic, M., de la Monte, S., Dikkes, P., and Tsai, L.H. 1999. Conversion of p35 to p25 deregulates Cdk5 activity and promotes neurodegeneration. *Nature* **402:** 615-622.

Petkova, A.T., Ishii, Y., Balbach, J.J., Antzutkin, O.N., Leapman, R.D., Delaglio, F., and Tycko, R. 2002. A structural model for Alzheimer's beta -amyloid fibrils based on experimental constraints from solid state NMR. *Proc Natl Acad Sci U S A* **99:** 16742-16747.

Petronis, A. 1999. Alzheimer's disease and down syndrome: from meiosis to dementia.

Exp Neurol **158:** 403-413.

Pike, C.J., Burdick, D., Walencewicz, A.J., Glabe, C.G., and Cotman, C.W. 1993. Neurodegeneration induced by beta-amyloid peptides *in vitro*: the role of peptide assembly state. *J Neurosci* **13:** 1676-1687.

Poirier, J. 2003. Apolipoprotein E and cholesterol metabolism in the pathogenesis and treatment of Alzheimer's disease. *Trends Mol Med* **9:** 94-101.

Price, D.L., Tanzi, R.E., Borchelt, D.R., and Sisodia, S.S. 1998. Alzheimer's disease: genetic studies and transgenic models. *Annu Rev Genet* **32:** 461-493.

Qizilbash, N., Birks, J., Lopez Arrieta, J., Lewington, S., and Szeto, S. 2000. Tacrine for Alzheimer's disease. *Cochrane Database Syst Rev***:** CD000202.

Rebeck, G.W., Moir, R.D., Mui, S., Strickland, D.K., Tanzi, R.E., and Hyman, B.T. 2001. Association of membrane-bound amyloid precursor protein APP with the apolipoprotein E receptor LRP. *Brain Res Mol Brain Res* **87:** 238-245.

Religa, D., and Winblad, B. 2003. Therapeutic strategies for Alzheimer's disease based on new molecular mechanisms. *Acta Neurobiol Exp (Wars)* **63:** 393-396.

Renkawek, K., Stege, G.J., and Bosman, G.J. 1999. Dementia, gliosis and expression of the small heat shock proteins hsp27 and alpha B-crystallin in Parkinson's disease. *Neuroreport* **10:** 2273-2276.

Robinson, S.R., Bishop, G.M., Lee, H.G., and Munch, G. 2004. Lessons from the AN 1792 Alzheimer vaccine: lest we forget. *Neurobiol Aging* **25:** 609-615.

Rogers, J., Cooper, N.R., Webster, S., Schultz, J., McGeer, P.L., Styren, S.D., Civin, W.H., Brachova, L., Bradt, B., Ward, P., et al. 1992. Complement activation by beta-amyloid in Alzheimer disease. *Proc Natl Acad Sci U S A* **89:** 10016-10020.

Rohan de Silva, H.A., and Patel, A.J. 1997. Presenilins and early-onset familial Alzheimer's disease. *Neuroreport* **8:** i-xii.

Roher, A.E., Baudry, J., Chaney, M.O., Kuo, Y.M., Stine, W.B., and Emmerling, M.R. 2000. Oligomerizaiton and fibril asssembly of the amyloid-beta protein. *Biochim*

Biophys Acta **1502:** 31-43.

Roman, G.C., and Rogers, S.J. 2004. Donepezil: a clinical review of current and emerging indications. *Expert Opin Pharmacother* **5:** 161-180.

Ross, C.A., and Poirier, M.A. 2004. Protein aggregation and neurodegenerative disease. *Nat Med* **10 Suppl:** S10-17.

Rosso, S.M., van Herpen, E., Deelen, W., Kamphorst, W., Severijnen, L.A., Willemsen, R., Ravid, R., Niermeijer, M.F., Dooijes, D., Smith, M.J., et al. 2002. A novel tau mutation, S320F, causes a tauopathy with inclusions similar to those in Pick's disease. *Ann Neurol* **51:** 373-376.

Sahara, N., Tomiyama, T., and Mori, H. 2000. Missense point mutations of tau to segregate with FTDP-17 exhibit site-specific effects on microtubule structure in COS cells: a novel action of R406W mutation. *J Neurosci Res* **60:** 380-387.

Saito, T., Takaki, Y., Iwata, N., Trojanowski, J., and Saido, T.C. 2003. Alzheimer's disease, neuropeptides, neuropeptidase, and amyloid-beta peptide metabolism. *Sci Aging Knowledge Environ* **2003:** PE1.

Salerno, J.C., Eifert, C.L., Salerno, K.M., and Koretz, J.F. 2003. Structural diversity in the small heat shock protein superfamily: control of aggregation by the N-terminal region. *Protein Eng* **16:** 847-851.

Saragoni, L., Hernandez, P., and Maccioni, R.B. 2000. Differential association of tau with subsets of microtubules containing posttranslationally-modified tubulin variants in neuroblastoma cells. *Neurochem Res* **25:** 59-70.

Saunders, A.M. 2001. Gene identification in Alzheimer's disease. *Pharmacogenomics* **2:** 239-249.

Schenk, D. 2002. Amyloid-beta immunotherapy for Alzheimer's disease: the end of the beginning. *Nat Rev Neurosci* **3:** 824-828.

Schubert, D., Behl, C., Lesley, R., Brack, A., Dargusch, R., Sagara, Y., and Kimura, H. 1995. Amyloid peptides are toxic via a common oxidative mechanism. *Proc Natl*

Acad Sci U S A **92:** 1989-1993.

Selkoe, D.J. 1999. Translating cell biology into therapeutic advances in Alzheimer's disease. *Nature* **399:** A23-31.

Selkoe, D.J. 2001. Alzheimer's disease: genes, proteins, and therapy. *Physiol Rev* **81:** 741-766.

Selkoe, D.J. 2003. Folding proteins in fatal ways. *Nature* **426:** 900-904.

Serio, T.R., Cashikar, A.G., Kowal, A.S., Sawicki, G.J., Moslehi, J.J., Serpell, L., Arnsdorf, M.F., and Lindquist, S.L. 2000. Nucleated conformational conversion and the replication of conformational information by a prion determinant. *Science* **289:** 1317-1321.

Serpell, L.C. 2000. Alzheimer's amyloid fibrils: structure and assembly. *Biochim Biophys Acta* **1502:** 16-30.

Serpell, L.C., Berriman, J., Jakes, R., Goedert, M., and Crowther, R.A. 2000. Fiber diffraction of synthetic alpha-synuclein filaments shows amyloid-like cross-beta conformation. *Proc Natl Acad Sci U S A* **97:** 4897-4902.

Seubert, P., Vigo-Pelfrey, C., Esch, F., Lee, M., Dovey, H., Davis, D., Sinha, S., Schlossmacher, M., Whaley, J., Swindlehurst, C., et al. 1992. Isolation and quantification of soluble Alzheimer's beta-peptide from biological fluids. *Nature* **359:** 325-327.

Sharma, K.K., Kaur, H., Kumar, G.S., and Kester, K. 1998. Interaction of 1,1'-bi(4-anilino)naphthalene-5,5'-disulfonic acid with alpha-crystallin. *J Biol Chem* **273:** 8965-8970.

Sheline, Y.I., Mittler, B.L., and Mintun, M.A. 2002. The hippocampus and depression. *Eur Psychiatry* **17 Suppl 3:** 300-305.

Shen, C.L., and Murphy, R.M. 1995. Solvent effects on self-assembly of beta-amyloid peptide. *Biophys J* **69:** 640-651.

Shoji, M., Golde, T.E., Ghiso, J., Cheung, T.T., Estus, S., Shaffer, L.M., Cai, X.D.,

McKay, D.M., Tintner, R., Frangione, B., et al. 1992. Production of the Alzheimer amyloid beta protein by normal proteolytic processing. *Science* **258:** 126-129.

Simons, K., and Ehehalt, R. 2002. Cholesterol, lipid rafts, and disease. *J Clin Invest* **110:** 597-603.

Simons, K., and Ikonen, E. 2000. How cells handle cholesterol. *Science* **290:** 1721-1726.

Simons, M., Keller, P., Dichgans, J., and Schulz, J.B. 2001. Cholesterol and Alzheimer's disease: is there a link? *Neurology* **57:** 1089-1093.

Sinha, S., and Lieberburg, I. 1999. Cellular mechanisms of beta-amyloid production and secretion. *Proc Natl Acad Sci U S A* **96:** 11049-11053.

Sipe, J.D. 1992. Amyloidosis. *Annu Rev Biochem* **61:** 947-975.

Sipe, J.D. 1994. Amyloidosis. *Crit Rev Clin Lab Sci* **31:** 325-354.

Sitia, R., and Braakman, I. 2003. Quality control in the endoplasmic reticulum protein factory. *Nature* **426:** 891-894.

Smith, D.P., Jones, S., Serpell, L.C., Sunde, M., and Radford, S.E. 2003. A systematic investigation into the effect of protein destabilisation on beta 2-microglobulin amyloid formation. *J Mol Biol* **330:** 943-954.

Smith Doody, R. 2003. Update on Alzheimer drugs (donepezil). *Neurologist* **9:** 225-229.

Snyder, S.W., Ladror, U.S., Wade, W.S., Wang, G.T., Barrett, L.W., Matayoshi, E.D., Huffaker, H.J., Krafft, G.A., and Holzman, T.F. 1994. Amyloid-beta aggregation: selective inhibition of aggregation in mixtures of amyloid with different chain lengths. *Biophys J* **67:** 1216-1228.

Sorbi, S., Forleo, P., Tedde, A., Cellini, E., Ciantelli, M., Bagnoli, S., and Nacmias, B. 2001. Genetic risk factors in familial Alzheimer's disease. *Mech Ageing Dev* **122:** 1951-1960.

Soreghan, B., Kosmoski, J., and Glabe, C. 1994. Surfactant properties of Alzheimer's A beta peptides and the mechanism of amyloid aggregation. *J Biol Chem* **269:**

28551-28554.

Soto, C., and Castano, E.M. 1996. The conformation of Alzheimer's beta peptide determines the rate of amyloid formation and its resistance to proteolysis. *Biochem J* **314 (Pt 2):** 701-707.

Soto, C., Sigurdsson, E.M., Morelli, L., Kumar, R.A., Castano, E.M., and Frangione, B. 1998. Beta-sheet breaker peptides inhibit fibrillogenesis in a rat brain model of amyloidosis: implications for Alzheimer's therapy. *Nat Med* **4:** 822-826.

Souillac, P.O., Uversky, V.N., Millett, I.S., Khurana, R., Doniach, S., and Fink, A.L. 2002. Elucidation of the molecular mechanism during the early events in immunoglobulin light chain amyloid fibrillation. Evidence for an off-pathway oligomer at acidic pH. *J Biol Chem* **277:** 12666-12679.

Spudich, G., and Marqusee, S. 2000. A change in the apparent m value reveals a populated intermediate under equilibrium conditions in Escherichia coli ribonuclease HI. *Biochemistry* **39:** 11677-11683.

Stege, G.J., Renkawek, K., Overkamp, P.S., Verschuure, P., van Rijk, A.F., Reijnen-Aalbers, A., Boelens, W.C., Bosman, G.J., and de Jong, W.W. 1999. The molecular chaperone alphaB-crystallin enhances amyloid beta neurotoxicity. *Biochem Biophys Res Commun* **262:** 152-156.

Stevens, A., and Augusteyn, R.C. 1997. Binding of 1-anilinonaphthalene-8-sulfonic acid to alpha-crystallin. *Eur J Biochem* **243:** 792-797.

Stine, W.B., Jr., Dahlgren, K.N., Krafft, G.A., and LaDu, M.J. 2003. *In vitro* characterization of conditions for amyloid-beta peptide oligomerization and fibrillogenesis. *J Biol Chem* **278:** 11612-11622.

Stine, W.B., Jr., Snyder, S.W., Ladror, U.S., Wade, W.S., Miller, M.F., Perun, T.J., Holzman, T.F., and Krafft, G.A. 1996. The nanometer-scale structure of amyloid-beta visualized by atomic force microscopy. *J Protein Chem* **15:** 193-203.

Szabo, Z., Klement, E., Jost, K., Zarandi, M., Soos, K., and Penke, B. 1999. An FT-IR

study of the beta-amyloid conformation: standardization of aggregation grade. *Biochem Biophys Res Commun* **265:** 297-300.

Takahashi, M., Ueno, A., and Mihara, H. 2000a. Peptide design based on an antibody complementarity-determining region (CDR): construction of porphyrin-binding peptides and their affinity maturation by a combinatorial method. *Chemistry* **6:** 3196-3203.

Takahashi, Y., Ueno, A., and Mihara, H. 2000b. Mutational analysis of designed peptides that undergo structural transition from alpha helix to beta sheet and amyloid fibril formation. *Structure Fold Des* **8:** 915-925.

Takashima, A., Noguchi, K., Sato, K., Hoshino, T., and Imahori, K. 1993. Tau protein kinase I is essential for amyloid beta-protein-induced neurotoxicity. *Proc Natl Acad Sci U S A* **90:** 7789-7793.

Tan, S.Y., and Pepys, M.B. 1994. Amyloidosis. *Histopathology* **25:** 403-414.

Tanford, C. 1970. Protein denaturation. C. Theoretical models for the mechanism of denaturation. *Adv Protein Chem* **24:** 1-95.

Tang, M.X., Maestre, G., Tsai, W.Y., Liu, X.H., Feng, L., Chung, W.Y., Chun, M., Schofield, P., Stern, Y., Tycko, B., et al. 1996. Effect of age, ethnicity, and head injury on the association between APOE genotypes and Alzheimer's disease. *Ann N Y Acad Sci* **802:** 6-15.

Tanzi, R.E. 1996. Neuropathology in the Down's syndrome brain. *Nat Med* **2:** 31-32.

Tanzi, R.E., Kovacs, D.M., Kim, T.W., Moir, R.D., Guenette, S.Y., and Wasco, W. 1996. The gene defects responsible for familial Alzheimer's disease. *Neurobiol Dis* **3:** 159-168.

Tanzi, R.E., Watkins, P.C., Stewart, G.D., Wexler, N.S., Gusella, J.F., and Haines, J.L. 1992. A genetic linkage map of human chromosome 21: analysis of recombination as a function of sex and age. *Am J Hum Genet* **50:** 551-558.

Taubes, G. 1996. Misfolding the way to disease. *Science* **271:** 1493-1495.

Taylor, J.P., Hardy, J., and Fischbeck, K.H. 2002. Toxic proteins in neurodegenerative disease. *Science* **296:** 1991-1995.

Terzi, E., Holzemann, G., and Seelig, J. 1995. Self-association of beta-amyloid peptide (1-40) in solution and binding to lipid membranes. *J Mol Biol* **252:** 633-642.

Terzi, E., Holzemann, G., and Seelig, J. 1997. Interaction of Alzheimer beta-amyloid peptide(1-40) with lipid membranes. *Biochemistry* **36:** 14845-14852.

Thompson, L.K. 2003. Unraveling the secrets of Alzheimer's beta-amyloid fibrils. *Proc Natl Acad Sci U S A* **100:** 383-385.

Tjernberg, L.O., Callaway, D.J., Tjernberg, A., Hahne, S., Lilliehook, C., Terenius, L., Thyberg, J., and Nordstedt, C. 1999. A molecular model of Alzheimer amyloid beta-peptide fibril formation. *J Biol Chem* **274:** 12619-12625.

Tjernberg, L.O., Naslund, J., Lindqvist, F., Johansson, J., Karlstrom, A.R., Thyberg, J., Terenius, L., and Nordstedt, C. 1996. Arrest of beta-amyloid fibril formation by a pentapeptide ligand. *J Biol Chem* **271:** 8545-8548.

Tomiyama, T., Shoji, A., Kataoka, K., Suwa, Y., Asano, S., Kaneko, H., and Endo, N. 1996. Inhibition of amyloid beta protein aggregation and neurotoxicity by rifampicin. Its possible function as a hydroxyl radical scavenger. *J Biol Chem* **271:** 6839-6844.

Tomski, S.J., and Murphy, R.M. 1992. Kinetics of aggregation of synthetic beta-amyloid peptide. *Arch Biochem Biophys* **294:** 630-638.

Tsai, L.H., Delalle, I., Caviness, V.S., Jr., Chae, T., and Harlow, E. 1994. p35 is a neural-specific regulatory subunit of cyclin-dependent kinase 5. *Nature* **371:** 419-423.

Tseng, B.P., Esler, W.P., Clish, C.B., Stimson, E.R., Ghilardi, J.R., Vinters, H.V., Mantyh, P.W., Lee, J.P., and Maggio, J.E. 1999. Deposition of monomeric, not oligomeric, Abeta mediates growth of Alzheimer's disease amyloid plaques in human brain preparations. *Biochemistry* **38:** 10424-10431.

Turner, A.J., Fisk, L., and Nalivaeva, N.N. 2004. Targeting amyloid-degrading enzymes

as therapeutic strategies in neurodegeneration. *Ann N Y Acad Sci* **1035:** 1-20.

Turner, P.R., O'Connor, K., Tate, W.P., and Abraham, W.C. 2003. Roles of amyloid precursor protein and its fragments in regulating neural activity, plasticity and memory. *Prog Neurobiol* **70:** 1-32.

van den, I.P., Norman, D.G., and Quinlan, R.A. 1999. Molecular chaperones: small heat shock proteins in the limelight. *Curr Biol* **9:** R103-105.

van Duijn, C.M., Clayton, D., Chandra, V., Fratiglioni, L., Graves, A.B., Heyman, A., Jorm, A.F., Kokmen, E., Kondo, K., Mortimer, J.A., et al. 1991. Familial aggregation of Alzheimer's disease and related disorders: a collaborative re-analysis of case-control studies. EURODEM Risk Factors Research Group. *Int J Epidemiol* **20 Suppl 2:** S13-20.

van Herpen, E., Rosso, S.M., Serverijnen, L.A., Yoshida, H., Breedveld, G., van de Graaf, R., Kamphorst, W., Ravid, R., Willemsen, R., Dooijes, D., et al. 2003. Variable phenotypic expression and extensive tau pathology in two families with the novel tau mutation L315R. *Ann Neurol* **54:** 573-581.

van Montfort, R.L., Basha, E., Friedrich, K.L., Slingsby, C., and Vierling, E. 2001. Crystal structure and assembly of a eukaryotic small heat shock protein. *Nat Struct Biol* **8:** 1025-1030.

Vassar, R. 2004. BACE1: the beta-secretase enzyme in Alzheimer's disease. *J Mol Neurosci* **23:** 105-114.

Walsh, D.M., Hartley, D.M., Kusumoto, Y., Fezoui, Y., Condron, M.M., Lomakin, A., Benedek, G.B., Selkoe, D.J., and Teplow, D.B. 1999. Amyloid beta-protein fibrillogenesis. Structure and biological activity of protofibrillar intermediates. *J Biol Chem* **274:** 25945-25952.

Walsh, D.M., Klyubin, I., Fadeeva, J.V., Cullen, W.K., Anwyl, R., Wolfe, M.S., Rowan, M.J., and Selkoe, D.J. 2002. Naturally secreted oligomers of amyloid beta protein potently inhibit hippocampal long-term potentiation *in vivo*. *Nature* **416:**

535-539.

Walsh, D.M., Lomakin, A., Benedek, G.B., Condron, M.M., and Teplow, D.B. 1997. Amyloid beta-protein fibrillogenesis. Detection of a protofibrillar intermediate. *J Biol Chem* **272:** 22364-22372.

Wang, S.S., Becerra-Arteaga, A., and Good, T.A. 2002. Development of a novel diffusion-based method to estimate the size of the aggregated Abeta species responsible for neurotoxicity. *Biotechnol Bioeng* **80:** 50-59.

Ward, R.V., Jennings, K.H., Jepras, R., Neville, W., Owen, D.E., Hawkins, J., Christie, G., Davis, J.B., George, A., Karran, E.H., et al. 2000. Fractionation and characterization of oligomeric, protofibrillar and fibrillar forms of beta-amyloid peptide. *Biochem J* **348 Pt 1:** 137-144.

Westlind-Danielsson, A., and Arnerup, G. 2001. Spontaneous *in vitro* formation of supramolecular beta-amyloid structures, "betaamy balls", by beta-amyloid 1-40 peptide. *Biochemistry* **40:** 14736-14743.

Wood, S.J., MacKenzie, L., Maleeff, B., Hurle, M.R., and Wetzel, R. 1996. Selective inhibition of Abeta fibril formation. *J Biol Chem* **271:** 4086-4092.

Yong, W., Lomakin, A., Kirkitadze, M.D., Teplow, D.B., Chen, S.H., and Benedek, G.B. 2002. Structure determination of micelle-like intermediates in amyloid beta -protein fibril assembly by using small angle neutron scattering. *Proc Natl Acad Sci U S A* **99:** 150-154.

Zhang, Q., Powers, E.T., Nieva, J., Huff, M.E., Dendle, M.A., Bieschke, J., Glabe, C.G., Eschenmoser, A., Wentworth, P., Jr., Lerner, R.A., et al. 2004. Metabolite-initiated protein misfolding may trigger Alzheimer's disease. *Proc Natl Acad Sci U S A* **101:** 4752-4757.

Zimmer, G. 2000. *Membrane structure in disease and drug therapy*. Marcel Dekker, New York, pp. XXI, 530 s.

VITA

SUNG MUN LEE
110-606 Usung Apt. Hagye-dong, Nowon-gu
Seoul, Korea

EDUCATION

Master of Science, *Chemical Engineering,* Seoul National University (1999), Korea
Bachelor of Science, *Chemical Engineering,* Korea University (1996), Korea

UNDERGRADUATE AND GRADUATE HONORS

1. Outstanding Chemical Engineering Graduate Student Award from Chemical Engineering Department, Texas A&M (Aug. 2003 - May 2005)
2. Outstanding Chemical Engineering Academic Scholarship from Chemical Engineering Department, Korea University (Mar. 1997)
3. Korea University Alumni Full Scholarship from Association of Korea University Alumni (Mar. 1991 - Sep. 1996)

SELECTED PUBLICATIONS

Sungmun Lee, Kenneth Carson, Allison Rice-Ficht, and Theresa Good, "Hsp20, a novel α-crystallin, prevents Aβ fibril formation and toxicity", *Protein Science*, **14**(3), 593-601 (2005)

Sungmun Lee, Joo Sang Yeo, Kyungmoon Park, and Young Je Yoo, "Synthesis of Lignin-phenol Copolymers Using Horseradish Peroxidase", *Korean Journal of Biotechnology and Bioengineering*, **15**(1), 22 - 26 (2000)

Under Preparation

Sungmun Lee, and Theresa Good, "Investigation of the Mechanism of Small Heat Shock Protein Aβ Fibril Formation and Toxicity Prevention"

Sungmun Lee, and Theresa Good, "Role of aggregation condition in structure and toxicity of intermediates in the Ab fibril formation pathway."

Sungmun Lee, and Theresa Good, "Kinetic modeling of Aβ fibril formation and Hsp interaction with Aβ"